

# The Role of the Proximal Segment in Peripheral Nerve Regeneration

Erik Taco Walbeehm

Walbeehm, Erik Taco  
The role of the proximal segment in peripheral nerve regeneration

ISBN: 90-8559-011-6

Cover: Danièle Huikeshoven en Gonneke Heerdink  
Layout: This document was prepared in  $\text{\LaTeX}$   
in samenwerking met Vincent Zee

Financial Support was given by: The Esser Foundation, Nederlandse Vereniging voor  
Plastische Chirurgie, Nederlandse Vereniging voor Handchirurgie, Johnson & John-  
son Medical BV  
Printed by Optima Grafische Communicatie, Rotterdam

The Role of the Proximal Segment in Peripheral Nerve Regeneration

De rol van het proximale segment in perifere zenuw regeneratie

Proefschrift

ter verkrijging van de graad van doctor aan de  
Erasmus Universiteit Rotterdam  
op gezag van de  
Rector Magnificus

Prof.dr. S.W.J. Lamberts

en volgens besluit van het College voor Promoties.  
De openbare verdediging zal plaatsvinden op

woensdag 24 november 2004 om 09:45 uur

door

Erik Taco Walbeehm  
geboren te 's-Gravenhage

Promotiecommissie:

Promotor: Prof. dr. S.E.R. Hovius

Overige leden: Prof. dr. P.A.E. Sillevius Smitt  
Prof. dr. ir. D.F. Stegeman  
Dr.ir. D.N. Meijer

Copromotor: Dr. G.H. Visser

“The Pure and simple truth is rarely pure and never  
simple.”

Oscar Wilde (the Importance of Being Earnest, 1895)

To Those That Helped....



## Contents

<b>1</b>	<b>Introduction</b>	<b>1</b>
1.1	Nerve Injury . . . . .	2
1.1.1	Classification of Nerve Injury . . . . .	3
1.1.2	Morphological Changes after Nerve Injury . . . . .	3
1.1.3	Cell Death . . . . .	5
1.1.4	The Axons . . . . .	7
1.1.5	Proximal Segment . . . . .	8
1.1.6	Distal Segment . . . . .	8
1.1.7	Restoration of Function . . . . .	11
1.2	Electrophysiological Changes . . . . .	11
1.2.1	Magnetoneurography (MNG) . . . . .	11
1.2.2	MNG versus ENG . . . . .	15
1.2.3	Relation between Axon and Signal . . . . .	16
1.3	Evaluation of Nerve Regeneration . . . . .	17
1.3.1	Forms of Evaluation . . . . .	17
1.4	Peripheral Nerve and Stretch . . . . .	21
1.4.1	Anatomy . . . . .	21
1.4.2	Stretch of Nerve . . . . .	22
1.4.3	Stretch and Nerve Function . . . . .	22
1.5	The Aims of This Thesis . . . . .	22
<b>2</b>	<b>CAC Amplitude, CV and Function</b>	<b>31</b>
<b>3</b>	<b>NCAC versus Myelinated Axon Counts</b>	<b>47</b>
<b>4</b>	<b>The Proximal Segment after Different Repairs</b>	<b>63</b>
<b>5</b>	<b>The D/P Peak-to-peak Amplitude Ratio</b>	<b>75</b>
<b>6</b>	<b>Primary vs Delayed Primary Nerve Repair</b>	<b>89</b>
<b>7</b>	<b>Mechanical Function of Peripheral Nerve</b>	<b>103</b>

<b>8</b>	<b>Shear-planes in Peripheral Nerves</b>	<b>117</b>
<b>9</b>	<b>General Discussion</b>	<b>131</b>
<b>10</b>	<b>Summary, Samenvatting &amp; Dankwoord</b>	<b>141</b>
10.1	Summary . . . . .	142
10.2	Samenvatting . . . . .	144
10.3	Dankwoord . . . . .	146
10.4	Curriculum vitae . . . . .	147

# Chapter 1

## **Introduction**

## Introduction

The peripheral nervous system is designed to connect the orchestrations of brain and spinal cord to the rest of the body. In addition, it connects the outside world and that same brain, gathering information from numerous sensory organs in our skin and from our other “senses”. Injury to a nerve subsequently results in impairment of function as well as impairment of that information gathering system.

In order to restore the damage, a series of complex changes is triggered in the cell body and the axon, all aimed at restoring motor and sensory function. However, different parts of the peripheral nervous system have different responses to injury. It is possible to distinguish three different parts: The cell body, the proximal segment and the distal segment. Proximal to the lesion, in the cell body and the proximal segment, the aim is to reconnect the axon to its effector organ as soon as possible. Distal to the lesion everything is aimed at creating an environment that allows reconnection of axons to happen.

In order to accomplish this, the nerve proceeds through a number of morphological and electrophysiological changes. Although maybe not directly obvious, those morphological transformations after injury are reflected in electrophysiological changes. Previous research demonstrated changes in peak-peak amplitude of compound nerve action signals in the proximal segment after nerve transection and reconstruction<sup>45–48</sup>. However, the mechanisms involved however, are still unclear.

The aim of this thesis is to explore the changes in the proximal segment and to clarify possible modifications to the proximal segment influencing repair.

## 1.1 Nerve Injury

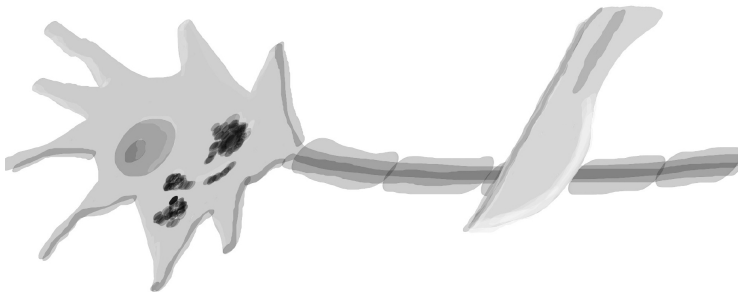


Figure 1.1: *Nerve Injury*

### 1.1.1 Classification of Nerve Injury

Peripheral nerve injury can be described using two classification systems. Seddon (1943) introduced a classification system that was modified later by Sunderland<sup>83</sup>. The clinically most useful system is the Seddon classification:

- Neurapraxia, in which the continuity of the axon is still intact. Function classically restores in 3-6 weeks.
- Axonotmesis, in which the continuity of the nerve is still intact, but the axon is severed. Function restores when the axon has regrown to its effector. As the basal lamina and collagen scaffolding of the nerve are still intact, 100% restoration of function is expected.
- Neurotmesis, is the type of injury where the continuity of the entire nerve is interrupted. Return of function depends on several circumstances but is never 100%.

Axonotmesis and neurotmesis experiments are the models used in this thesis.

### 1.1.2 Morphological Changes after Nerve Injury

Following nerve injury, a series of changes dramatically alters the morphological properties of the cell body, proximal segment and distal segment.

Changes in the cell body

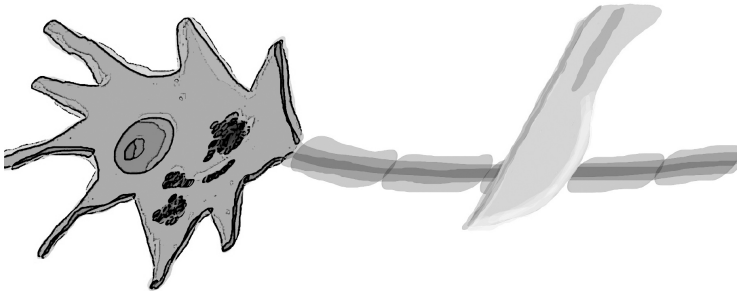


Figure 1.2: *Cellbody*

The cell body lies in the spinal cord (motor neuron) or just adjacent to it (in the dorsal root ganglion) and as such the peripheral nervous system has its origin in the

central nervous system. Each neuron has dendritic processes that contact surrounding neurons and form connections to axons arising from higher levels of the spinal cord. The axon is the connection between effector cells (f.i. muscle) and neurons, and between the information gathering sensory organs and neurons. Peripheral axotomy induces a series of events in the cell body. The typical response, first described by Nissl (1892), includes an increase of volume of the cell body, displacement of the nucleus to the periphery and disappearance of basophilic material from the cytoplasm (chromatolysis)<sup>58</sup>. Furthermore, changes occur in gene expression, leading to deafferentation and cell death in some cells.

#### Chromatolysis

The chromatolytic changes that occur in the cell body after peripheral nerve transection have been well documented in the literature. It basically involves a dis- or reorganization of the structure of the rough endoplasmic reticulum. The changes are most pronounced between 1 and 3 weeks after nerve transection and any peripheral neuron that is going to die and degenerate, will do so within the first 5 weeks after injury.<sup>51,70</sup> The neurons that have successfully regenerated axons subsequently recover from chromatolysis. The degree of chromatolytic change and cell loss that occurs following peripheral nerve transection is dependent on the species of animal, distance of the injury to the spinal cord, whether the nerve was reconstructed and the age at which the injury occurs.<sup>23</sup>

The cell body is the major site of synthesis of proteins and other materials required for growth of the axon. Most induced proteins are membrane proteins, and are transported rapidly into the axon. Those "growth associated proteins" (GAPs) are believed to be necessary for particular steps in axonal growth. A number of genes is involved in the reactive process following injury.

#### Changes in expression of genes

Recent studies using gene arrays have expanded the knowledge on the number of genes that change expression after nerve injury, exponentially. In an array testing 588 annotated genes in a response to a crush injury, 40% showed expression above background, 55 of these represented differential expression after nerve lesion. 30% of these genes were known to play a role in peripheral nerve regeneration. 70%, however, had not been detected in the peripheral nervous system before<sup>6,7</sup>.

#### Deafferentation

Another common consequence of axon transection is the apparent rejection of synapses by the cell body and dendrites. It is almost as if the cell body purposefully impairs information in- and output to and from other neurons, concentrating on the repair and regenerative processes and focus its energy expenditure<sup>87</sup>.

### 1.1.3 Cell Death

Following nerve injury, part of the cells of the dorsal root ganglion (DRG) and the motor neuron pool do not survive the impact, and die. It has been suggested that this is one of the reasons why functional outcome after peripheral nerve injury is disappointing.

#### Sensory Neuronal Cell Death

Extensive primary sensory neuronal death, between 30% and 50% of the dorsal root ganglion cells, is found after experimentally induced peripheral nerve lesions<sup>93,100–102</sup>. The onset of neuron loss was found between 4<sup>93</sup> to 10 days.<sup>31</sup>

However, Hart et al<sup>64</sup> demonstrated that neuronal death commences within 24h of sciatic nerve transection, but cell loss started at 7 days after sciatic nerve transection, in a rat model. The delay between the start of neuronal death and that of neuron loss can be explained by the time taken for individual neurons to progress from DNA fragmentation to complete involution, as well as the number of involuted cells to increase sufficiently to overcome normal biological variation in neuron numbers.

In vitro, neurons take a few hours to progress from DNA fragmentation to eventual cell death. In vivo, a delay in cell death of neonatal facial motoneurons of days is found after axotomy of the facial nerve in neonatal rats.<sup>64</sup> In the study by Hart et al<sup>64</sup>, at most 6 days passed between positive TUNEL (terminal deoxynucleotidyl transferase-mediated dUTP nick-end labeling, a technique that preferentially stains DNA strand breaks occurring in apoptosis.) staining and the occurrence of significant neuron loss. Although neuronal involution in the first few days may have occurred at such a slow rate that it did not translate into significant neuron loss, the full course of sensory neuronal death in vivo, from beginning (DNA fragmentation) to end (neuron loss), appears to last some days.

#### Motor Neuron Cell Death

The loss of motor neurons is particularly marked in neonatal and developing animals, because the immature cells do not have the same ability to resist trauma to their axons and separation from their muscle.<sup>23</sup> Brushart, et al.<sup>13</sup>, showed that the motoneuron population was 69% of its normal value 3 months after repair by direct epineurial suture, comparing very well with the result of Gilmour et al<sup>23</sup> of 68.5% at 100 days after the same repair. Other authors have reported that the number of functional motoneurons present in the spinal cord following peripheral nerve repair is significantly less than normal values.<sup>13,14</sup> However, the degree of cell loss is much less marked in cases in which the nerve has been repaired and allowed to regenerate<sup>23</sup>; however, even in such cases, muscle reinnervation is found to be abnormal not only in degree but also in specificity.<sup>13,14</sup>

## Mechanism of neuronal death

Several stimuli can initiate neuronal death, although loss of target-derived neurotrophic support appears to be most significant, This is demonstrated by the protective effect of exogenous neurotrophic factors such as nerve growth factor (NGF)<sup>54,69,73</sup>, NT3<sup>25,54</sup>, glial cell line-derived neurotrophic factor (GDNF)<sup>4</sup> and leukemia inhibitory factor (LIF)<sup>5</sup>. Surgical repair is also thought to restore that support. The number of TUNEL-positive neurons present 2 weeks after axotomy, was reduced by nerve repair<sup>64</sup>. The same trend was found for neuron loss, which was 21.3% of control (L4+L5) in the absence of a nerve repair, 12.4% when repair was delayed by 1 week and was minimal (4.8%) when the nerve was repaired immediately after transection. One week after transection virtually no further neuron loss occurred, providing further evidence of the beneficial effect upon neuron survival of contact with the distal stump (with accompanying neurotrophic support). These results give further support to the hypothesis that loss of distal-stump neurotrophic support is the major factor determining the magnitude of neuronal death after peripheral axotomy.<sup>64</sup>

## Effect of Type of Nerve Repair on Cell Death

Brushart, et al.,<sup>14</sup> compared two different methods of repair: direct epi-neurial suture and individual fascicular suture. The use of individual fascicular suture produced significantly better results than the direct epi-neurial suture in accuracy of reinnervation; however, there was no significant difference in numbers of, horseradish peroxidase labeled, motoneurons between the two methods of repair. Brushart explained his result by the fact that the epineurial suture allows the fascicles to change position within the epineurial sheath, which leads to subsequent misalignment.

In the study by Gilmour et al<sup>23</sup>, a larger number of motoneurons survived following a nerve crush, due to the fact that neural alignment was maintained. The direct epineurial suture consistently produced better results than either of the repair techniques that involved the use of a graft because the use of a graft results in the regenerating nerves having to negotiate two sets of suture lines.

The motoneuron population was 69% of its normal value 3 months to 100 days after repair by direct epineurial suture. Furthermore, a shift in the topographical position of the motoneuron population following the repair of a peripheral nerve by means of a direct epineurial suture was found, where the repaired groups recruited motoneurons from adjacent roots, compared to the control nerves.<sup>23</sup> Similar results were found for cell death in the DRG following repair, as described by Peyronnard et al<sup>70,71</sup> and Myles et al.<sup>68</sup>

### 1.1.4 The Axons

Following the 30-50% cell death of the neurons, it is confusing to find only a 5-7% decrease of myelinated axons in the proximal segment. In order to understand that mechanism, anatomical properties of the axons will be described first.

#### Axonal Anatomy

The axon extends from the neuron to the peripheral target organ and has a diameter in the range of 0.1 and 15-20  $\mu\text{m}$ .<sup>63,83</sup> They can be roughly divided in 2 groups: myelinated axons and unmyelinated axons.

Myelinated axons are surrounded by myelin sheaths. This is made up by a Schwann cell, "wrapped" around an axon, Each Schwann cell has a certain length, creating gaps between them: nodes of ranvier. The myelin insulates the axon. Conduction moves from node to node, i.e. saltatory conduction, and is not constrained by the conduction velocity of the axon itself. Axon diameter of the myelinated axons ranges from 2-20  $\mu\text{m}$ .<sup>58,63,83</sup>

Unmyelinated axons do not have the characteristic myelin sheath but lie in groups of fibers in contact with a schwann cell. Diameter ranges between 0.1 and 2  $\mu\text{m}$ . Following nerve injury, the number of smaller unmyelinated fibres appears to decrease significantly more than the larger myelinated fibres.<sup>58,63,83</sup>

#### Axonal Changes after Injury

Axonal morphology is mainly determined by the intracellular cytoskeleton. The integrity of the cytoskeleton is critical for the function and survival of neurons. After injury a number of changes occur in cytoskeleton synthesis, and to the cytoskeleton itself.<sup>8</sup>

Most prominent changes of the cytoskeleton are in neurofilament synthesis. The larger axons rely on neuronal neurofilament synthesis for sustaining their diameter. After transection of a nerve, neurofilament synthesis is downregulated. Neurofilaments are transported distally by slow axonal transport, and subsequently the axonal diameter decreases from the neuron in distal direction, a process called somatofugal atrophy.

The moment distal reconnections with target organs have been established, neurofilament synthesis is upregulated and axonal diameter is restored to almost normal diameters.<sup>33-38</sup> In contrast to axonal diameter decrease after injury, fibre diameter (axon + myelin sheath) does not seem to change after injury. Gillespie and Stein<sup>22</sup> describe in a mathematical model how axon diameter can decrease without changing fibre diameter. A consequence of this is the decrease of roundness of the axon.

### 1.1.5 Proximal Segment

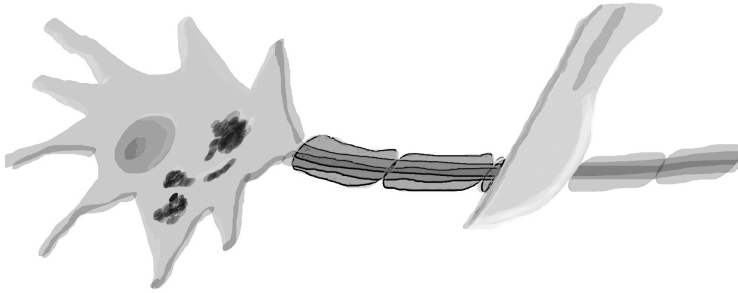


Figure 1.3: *Proximal Segment*

Contrary to the cell loss in the DRG and motor neuron pool, the number of axons decreases less than the number of DRG- or motor-neurons, after axotomy. Literature states that the number of myelinated fibres decreases by 5-7% in the proximal segment.<sup>71</sup> There is also a tendency for a left shift in the axon diameter distribution towards smaller axons.<sup>26</sup>

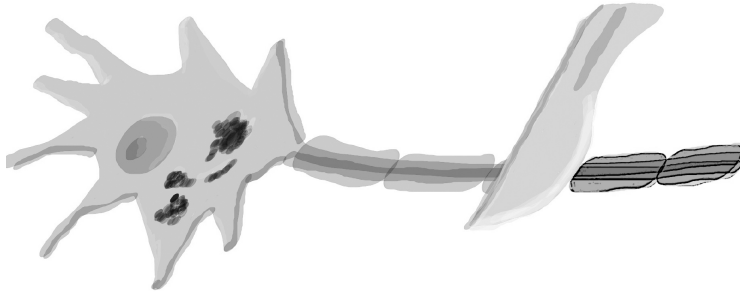
Fugleholm et al found that proximal to the lesion after crushing, sectioning and section and freeze, the number of myelinated fibers, and their diameter distributions were similar to those in normal and control nerves examined at corresponding levels, at 200-300 days post-injury.<sup>19,20</sup> However, Mackinnon et al<sup>62</sup> showed that 1 cm proximal to a lesion in a rat sciatic nerve, axon diameters declined and remained smaller up to 24 months post-repair. Also, an increase in numbers of axons 1 cm proximal to the repair was found, and explained as retrograde growth of sprouts.

The discrepancy between decrease in numbers of cells and only moderate decrease in numbers of fibres, can be explained in part on the level of the DRG. Most of the DRG neurons have unmyelinated axons, and their numbers decrease dramatically, following transection. However, It is not yet clear how approximately 30% of motor neurons disappear where myelinated fibres only diminish by 7%. Furthermore, considering that the type of nerve repair influences the number of surviving motorneurons, not much is known about the effect of the type of nerve repair on the properties of the proximal segment.

Following injury, sprouts occur from the axons in the proximal segment within hours, and are either guided or drawn to the distal segment.<sup>87-89</sup>

### 1.1.6 Distal Segment

From 2 - 3 days after injury, the axons in the distal segment start to breakdown. A massive influx of T-cells and macrophages follows. Debris, including myelin is

Figure 1.4: *Distal Segment*

removed by macrophages and by schwann cells. This process is called Wallerian degeneration. The basal lamina remains intact in the distal segment and forms the scaffolding for the schwann cells to proliferate along, forming the bands of Bugner.

The signal for induction of proliferation of the Schwann cells are probably chemotactic clues from the invading macrophages, as suggested by experiments using the C57BL/Ola (C57BL/Wld) mouse. This mutant mouse does not recruit macrophages and consequently the distal segment does not undergo Wallerian degeneration.<sup>11</sup>

Fibroblast response is most prominent following transection, and is maximal at 2-5 days following injury, lasting up to months.

The distal segment secretes three known neurotrophic factors. Nerve growth factor (NGF), first described by Levi-Montalcini and Hamburger<sup>50</sup>, is the best characterized factor of importance for survival of embryonic dorsal root ganglion neurons and the vast majority of sympathetic and sensory, but not parasympathetic, neurons during the critical stage of development.<sup>17</sup> Normally, NGF mRNA is present at low concentration in healthy nerves; however, following nerve injury it is upregulated in the distal nerve segment.<sup>1,30</sup> NGF is released by the schwann cells and perineurial fibroblasts, directly after trauma. A second increase in NGF is seen weeks after trauma and is released by the macrophages. NGF plays an important role in the survival of the sensory neurons as well as outgrowth of their neurites, while the substance has little or no influence on motor neurons and their neurite outgrowth.<sup>73</sup> Only neurons with that express the high-affinity NGF receptor (trkA) can respond to NGF.

Brain derived neurotrophic factor (BDNF) is also released by the schwann cells, starting 3-4 days post-trauma, with its maximum 3-4 weeks post-injury. BDNF is released in 10 fold higher concentrations compared to NGF. BDNF acts as a trophic factor for motor neurons and supports the survival of motor neurons in culture, rescues developing motor neurons from natural cell death, and has a role in preventing the cell death following axotomy of motor neurons in anterior spinal horns.<sup>40,55</sup>

Ciliary neurotrophic factor (CNTF)<sup>2,40,76</sup> is present in mature schwann cells and released in the extracellular space, but its synthesis appears to be reduced, following transection. BDNF and NGF both enhance neurite outgrowth and CNTF prevents degeneration of motor neurons. Neurotrophin-3 (NT3), NT4/5 and NT6 play a role in survival and differentiation of sensory as well as motor neurons.<sup>9,77,79-81</sup>

Clinically, the use of these factors has been limited, mostly due to the different timing at which different factors have their beneficial effects. Currently, the use of conduits from different (bio-)materials are under investigation, as carriers for neurotrophic factors.<sup>32,43,79,96,98,99</sup> Timed release, for instance, is a material property that can now be engineered. Also, schwann cells infected with adenoviruses, producing specific factors implanted on conduits are tested in animal models.<sup>10,24,52,53,67</sup>

### Sprouting

Following cell sealing by the damaged axons, sprouting starts from the proximal segment 3-4 hrs post-injury, usually from the first internode proximal to the injury. Terminally in each sprout there is a growth cone, a swelling from which several microspikes or filopodia arise. These microspikes are constantly moving, exploring the local microenvironment. The activity of the growth cones plays an essential role.

There are various explanations for determination of the growth direction of the sprouts. The molecular composition of the microenvironment may be either permissive or repellent in nature. The adhesiveness and the molecular composition of the growth substrate is of importance in this respect, especially with reference to the presence of so-called "neurite-promoting factors" promoting the extension of axons.<sup>55,59</sup>

Substances of special interest, possessing neurite-promoting effects, are the glycoproteins laminin and fibronectin.<sup>43,75,79,85,90,96,97</sup> The axons will be guided to the distal segment through neurotrophic factors. Once the axons have found the distal segment, contact with basal lamina molecules like laminin and fibronectin will guide axon growth in the right direction. Remyelination occurs during this process. Myelin is present 7-15 days following injury and is derived from de novo synthesis and from the reutilization from cholesterol from myelin debris, by the Schwann cells. Some cholesterol is derived from the blood stream. Remyelination proceeds down the nerve fibre, following the growth cones, without unduly delay.

Multiple sprouts come from the proximal axons. Mackinnon et al<sup>62</sup> demonstrated in a rat sciatic nerve model, that numbers of fibres increased in the distal segment up to 9 months post-repair, (from  $\pm 7100$  fibres in the normal sciatic nerve to  $\pm 11.700$  in the distal segment at 9 months) and then started declining. At this point distal reconnections have been made and superfluous sprouts die-back in a process called pruning. At 24 months fibres had reached normal numbers again.<sup>58,62,63</sup> This explains why histology of the distal segment does not correlate with functional outcome, and that functional outcome needs to be assessed separately.

### 1.1.7 Restoration of Function

Reconnections with the target organs are the last step in the growth process. Motor neurons will try and find motor endplates on muscle. One axon may innervate more fibres, and the normal ratio of muscle fibres per axon increases. This explains the giant motor unit potentials found on EMG after reinnervation. IGF and LIF influence formation of the connections.

Sensory neurons make connections with pacinian- and meisner corpuscles. The sensory axon endings regrow into skin but exactly how reinnervation of touch, pain and temperature are restored is still unclear. Recently, TRP channels have been discovered in the membranes of the so-called free nerve endings, as transducers for mechanical stimuli, However, their behaviour after nerve injury is still unclear.

## 1.2 Electro-physiological Changes after Nerve Transection and Reconstruction

The electrophysiological changes after nerve transection and reconstruction are a reflection of the morphological changes described above. For the purpose of this thesis only changes in conductive properties in the axonal component of the nerve and loss of axons will be discussed. However, before the conductive properties can be discussed the electrophysiological tests magnetoneurography and electroneurography have to be explained.

### 1.2.1 Magnetoneurography (MNG)

Magnetic Neurography (MNG) is a technique used to evaluate currents in single axons as well as in nerves during physiological and regenerative processes. It is based on the recording of intra-axonal currents producing nerve compound action currents (NCAC's) by means of induction in two magnetic sensor coils (toroids) (see fig. 1.5). This technique was developed by Wikswo and co-workers, and adapted by Kuypers and van Egeraat for use in an animal experimental model of regeneration using the common peroneal nerve in rabbits. MNG has been evaluated in healthy frog sciatic nerve and rabbit common peroneal nerve. Furthermore it has been correlated to functional recovery, nerve conduction velocity after nerve transection and reconstruction in a rabbit model.

The set-up used involved complete dissection of the common peroneal nerve from where the nerve enters the tibialis anterior muscle to the lumbar plexus, proximal to the femoral head. The nerve is transected and ligated as far proximally as possible, and subsequently passed through two toroidal sensor coils, together with a calibration wire. Two sensor coils are used in order to measure conduction velocity in the proximal segment. A bipolar stimulator is placed around the nerve, 4 cm

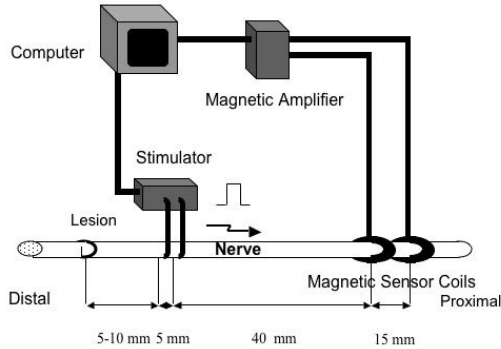


Figure 1.5: Schematic representation of the MNG set-up. The nerve is stimulated, and the response compound nerve action current is recorded by two magnetic sensor coils. The signal is amplified by a magnetic amplifier, and recorded and stored on a computer for analysis. The stimulator also sends a  $1 \mu\text{A}$  calibration signal prior to the nerve stimulus, through a wire which is also threaded through the two sensors.

distal to the distal toroid.

An important finding, when using MNG to evaluate nerve regeneration after transection and microsurgical reconstruction of the common peroneal in rabbits, was a consistent decrease of 50-60% in peak-peak amplitude in the stump proximal to the lesion, compared to the healthy contralateral control nerve (see fig. 1.6). Changes in conduction velocity (CV) were also observed during the first 8 weeks post-operatively, but returned to normal after 12 weeks. Supporting this idea, a 40-50% decrease in compound action potential, as opposed to current, was described in separate studies using electroneurography (ENG). Initially the conclusion was that the decrease in peak-peak amplitude involved an approximate 50% decrease in number of functional fibres.

However, correlations between electrophysiological evaluations and morphometrical data have been the subject of previous studies with different degrees of success. It has been demonstrated that Single Fibre Action Current (SFAC) is strongly related to axon and fibre diameter, although these are not the only factors. Therefore, because of its reproducibility and the relation between the SFAC and axon di-

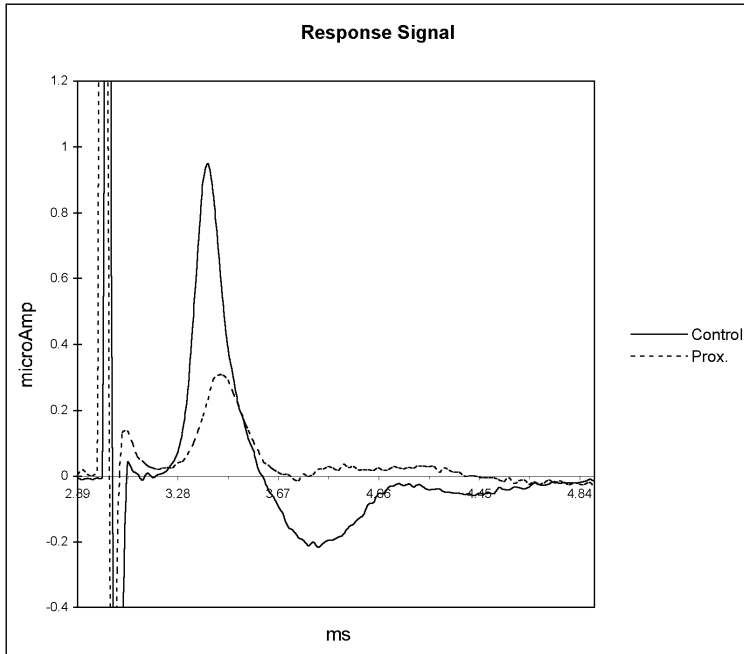


Figure 1.6: Representation of the response signal, recorded in the toroid nearest to the stimulator (40 mm). Signal is from a transected and immediately reconstructed nerve and its contralateral control nerve and the decrease in peak-peak amplitude is apparent. Stimulation artefact is visible, but calibration signal is not.

ameter, a strong correlation between the NCAC's and morphometric characteristics can be expected. Consequently, accurate quantification of functional nerve fibres in regenerating nerves by MNG should be possible.

#### Technical Aspects of MNG: Recording Operation

The animals in the subsequent experimental groups were re-anaesthetized 12 weeks following their nerve reconstruction of the left common peroneal nerve. The nerve was then dissected between the biceps femoris- and vastus lateralis muscles, freed from the sciatic nerve and mobilised from the knee to the lumbar plexus. It was transected and ligated proximal to the femoral head. The nerve was guided through two toroidal sensor coils, consisting of a ferrite core surrounded by an insulated 50 (m copper wire. The sensors were 15 mm apart. A bipolar stimulator was adjusted around the nerve, more distally, subsequently distal and proximal to the

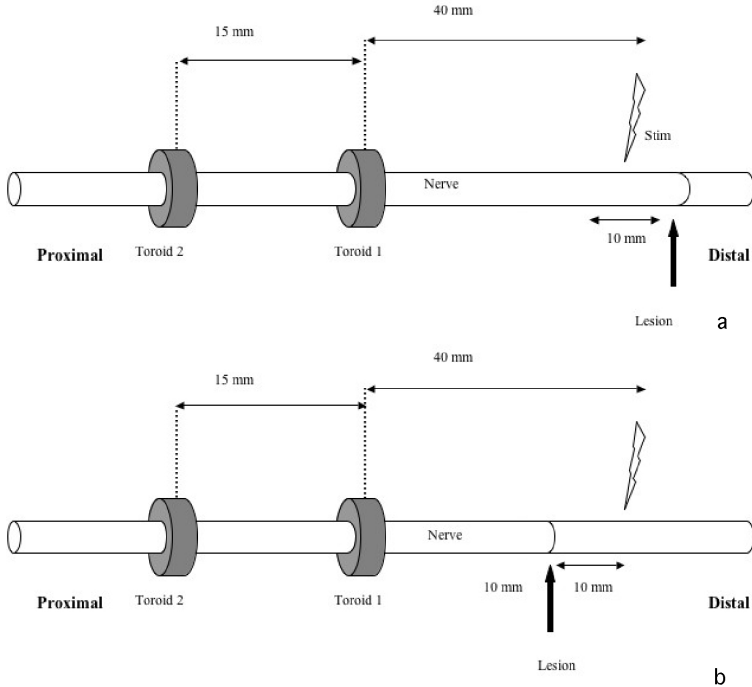


Figure 1.7: *a* shows the proximal measurement set-up. Stimulation is performed 10 mm proximal to the lesion. Recording at 40 and 55 mm proximal to the stimulator. *b* is the distal measurement set-up. Stimulation is performed 10 mm distal to the lesion. Recording at 40 and 55 mm proximal to the stimulator. Therefore, to measure both positions, approximately 7 cm of nerve is needed.

nerve lesion. The distance between the distal toroid and the stimulator was kept at 40 mm.

Then the wound area was flushed with heated ( $36\text{ }^{\circ}\text{C} \pm 0.5\text{ }^{\circ}\text{C}$ ), normal saline (0.9% NaCl), in order to submerge the nerve. The effect was two-fold: to keep the nerve from drying out, and to disperse the return of the magnetic signal, which influences the measurement. Simply put, the magnetic field had to return outside the sensor coils. Supramaximal stimulation (i.e. 3 times maximal stimulation in order to stimulate all nerve fibres) using a  $50\text{ }\mu\text{s}$ , rectangular, monophasic pulse (see fig. 1.7a&b). The moving NCAC produces a moving magnetic field, that passes through the sensors, inducing a current. This was then boosted by a magnetic amplifier (see fig. 1.5 on p. 12) and recorded.

Together with the nerve an insulated wire was threaded through the sensors,

through which a  $1 \mu\text{A}$  calibration signal was fed. This signal was sent just prior to the actual stimulus to the nerve, and recorded simultaneously. This entire procedure was repeated on the right side; the unoperated nerve served as control value. All procedures were conducted according to the regulations of the Animal Experimental Committee.

#### Technical Aspects of MNG: Signal evaluation

All data were recorded using NDA and averaged with Datacorr 3.0, which are a custom-written data acquisition and correction programmes, respectively. Each signal was calibrated by means of an accompanying  $1 \mu\text{A}$  calibration signal, which was recorded prior to every stimulus. The final signal is an average of 1024 measurements (consisting of 4 batches of 256 measurements). Further analyses were performed using MatLab<sup>®</sup> (The MathWorks, Inc. Natick, Mass. USA).

First, the baseline drift in a 1.6 ms window containing the MNG response was estimated using a piecewise cubic Hermite interpolation, based on the signal samples immediately preceding and following this window. After correction for this drift, the NCAC peak-to-peak amplitude could be easily determined as the difference between NCAC maximum and minimum. Onset latency was determined semi-automatically, as the value at 5% increase of the first peak, outside the noise to signal ratio. This was visually checked for each signal.

The NCV was estimated by cross-correlating the signal of the second toroidal sensor coil with that of the first. If the maximum value of the cross-correlation function exceeded 0.75, the signals were assumed to be sufficiently similar to allow a reliable calculation of the NCV. The position of the maximum was used as indication of the time shift  $\Delta t$  between the two signals. The NCV was then calculated as  $\Delta x / \Delta t$ , with  $\Delta x$  the intertoroidal distance of 15 mm. Finally, the area below the signal was determined between the signal onset (determined semi-automatically) and the end of the second phase of the MNG signal (as marked by the first zero-crossing of the signal after its minimum). The results were stored and statistically analysed in Excel X<sup>®</sup> (Microsoft Corp, Redmond, Wash., USA). Unless otherwise indicated, a two-sample Student t-test was used to test for significance (p values) of intergroup differences.

#### 1.2.2 MNG versus ENG

The main advantage of MNG over more conventional electro-neurography (ENG) is that the magnetic field is less influenced by the impedances of the surrounding tissues (i.e. the epineurium and mesoneurium) and by the position of the nerve in relation to the toroid sensor. This allows excellent reproducibility. However, in order to adjust for the conversion of magnetic field to current a calibration signal needs to be added. This calibration signal is fed through a wire, which is guided through

both toroidal sensor coils. A rectangular 1 msec, 1  $\mu$ A pulse is run through the wire just preceding the nerve compound signal. (see fig. 1.6) This enables quantification and diminishes bias because of toroid differences.

One of the drawbacks of MNG is that the nerve needs to be transected to accommodate the sensors. Transecting more proximally excludes evaluation of F-waves, which allows for motor unit estimation. However, this can be circumvented by using other types of stimulation. This is subject to testing at this moment.

Comparing MNG to ENG demonstrated that MNG had superior reproducibility. One shortcoming of this study was that ENG measurements were performed submerged in saline, similar to the MNG measurements. In MNG, this is essential to allow the return of the magnetic field outside the sensors, because of the conductive properties of the saline. This vector has the opposite direction to the current in the nerve and would decrease the signal. In ENG this disperses the signal. Normal ENG is performed dry or in oil, which changes the properties of the surrounding electric field considerably, and increases the signal reproducibility.

### 1.2.3 Relation between Axon and Signal

The nerve compound action potentials (NCAP's) and nerve compound action currents (NCAC's) are dependent on superposition of single fibre action potentials or -currents. Following the mathematical principles of superposition of waves, the peak-peak amplitude is not only a summation of all peak-peak amplitudes, but also subject to phase cancellation, which in turn decreases peak-peak amplitude.

There is a relation between fibre diameter, peak-peak amplitude and conduction velocity. Smaller fibres have smaller peak-peak amplitude and lower conduction velocity. Hursh<sup>39</sup> demonstrated the difference in maximum conduction velocity in different nerves in cats. The common peroneal demonstrated fast conduction velocities ranging from 108-111 m/s. In contrast, the conduction velocity of the hypogastric nerve ranged from 11-41 m/s. Hursh<sup>39</sup> correlated the conduction velocities to fibre diameters, taking into account an average axon shrinkage of  $10.1 \pm 0.2\%$  due to the histological fixation and dehydration. He found a linear relationship between fibre diameter and conduction velocity.

When comparing axon diameter and MNG signals, there is a direct relation (almost linear, sigmoidal shape, M. Dudok van Heel et al, unpublished results) between fibre diameter and conduction velocity and a square relationship between diameter and peak-peak amplitude. For example, a 5  $\mu$ m fibre would have half the conduction velocity of a 10  $\mu$ m fibre, and only 20% of its amplitude. Phase cancellation can then be explained as a reduction in amplitude of a large, high velocity signal by the slower, and smaller signal. This means that the smaller, unmyelinated axons, although large in numbers, are an insignificant, un-investigable part of the compound signal. Therefore, in techniques that measure compound signals, only the larger axons (between 10 and 15  $\mu$ m) are evaluated. After transection, the rules change

slightly, because of the differences in axon diameter.

#### Peak-peak amplitude and Axon diameter

In the proximal segment, a decrease in peak-peak amplitude has been described for conventional ENG as well as for MNG. It has been subject of discussion whether this decrease was directly proportional to a decrease in the total number of fibres, a decrease in functioning fibres or a decrease in larger fibres. Deconvolution of the signal, based on the Hodgkin-Huxley model (M. Dudok van Heel, unpublished results), demonstrated that a 5% decrease of the largest (10-18  $\mu\text{m}$ ) axons would cause an approximate 0% decrease in peak-peak amplitude. However, a similar result could be found if the number of functioning fibres of all diameters decreased. This will be tested empirically in this thesis.

#### NCV and Axon Diameter

Sensory nerves react differently to transection than motor nerves. Several studies have shown that conduction velocity of large diameter sensory fibres are more severely altered than motor fibers after transection of a mixed nerve. Extracellular *in vitro* recordings of the CNAP's in the proximal stump in transected cat hindlimb nerves indicate that action potentials are propagated slightly slower in dorsal roots than in the ventral roots, which is the reversal of the normal condition. Additionally, the fastest peak of the dorsal root CNAP showed the greatest decline.

Another difference is that after axotomy without reconstruction in cat hindlimbs, after 6 weeks the motor nerves were still electrically active and remained so almost indefinitely, whereas the sensory nerves fell silent. Also initially the rate of axonal atrophy was similar, but after 6 weeks, the axonal atrophy stabilized for the motor fibres, but continued to decline for the sensory neurons.<sup>87</sup>

## 1.3 Evaluation of Nerve Regeneration

There is no golden standard for the evaluation of nerve regeneration. Papers evaluating correlations between different evaluation types cannot elucidate positive correlations.<sup>41</sup> Therefore it is widely accepted to perform a number of different, non-related tests to evaluate nerve regeneration, before conclusions are drawn.

### 1.3.1 Forms of Evaluation

Other than the electrophysiological tests, that are discussed in the previous paragraphs, the evaluation of peripheral nerve regeneration encompasses function tests, histology and immunohistology,

## Function Tests

Different function tests have been described for different animals, but only function tests evaluating peripheral nerve repair in animals are discussed.

In rats the sciatic function index (SFI) is a widely used functional test. Several measurements are taken from the footprints (i) distance from the heel to the third toe, the print length (PL); (ii) distance from the first to the fifth toe, the toe spread (TS); and (iii) distance from the second to the fourth toe, the intermediary toe spread (ITS).

The SFI was originally developed by De Medinaceli et al. in 1982<sup>16</sup>, and modified by Bain et al. in 1989<sup>3</sup>, as reviewed by Varejao et al.<sup>92</sup>. They reported a new modification of the SFI, calculating the factors as follows: (i) print length factor (PLF) = (EPL-NPL)/NPL; (ii) toe spread factor (TSF) = (ETS-NTS)/NTS; (iii) intermediary toe spread factor (ITF) = (EIT-NIT)/NIT. These factors were then incorporated into the Bain-Mackinnon-Hunter (BMH) sciatic function index-formula:  $SFI = -38.3 \cdot PLF + 109.5 \cdot TSF + 13.3 \cdot ITF - 8.8$ . An SFI of 0 is normal. An SFI of -100 indicates total impairment, such as would result from a complete transection of the sciatic nerve<sup>42,86</sup>. Proponents of the walking track analysis advocate that there is a direct relationship between individual hind limb muscle function and print measurements.<sup>72</sup>

A similar function assay of peroneal and posterior tibial nerve lesions was developed by Bain et al.<sup>3</sup> Since its development by De Medinaceli's group in 1982, the validity of the SFI has been questioned by several investigators because of bias (taking the most representative prints for analysis<sup>3,27,78</sup>, false, untypically long print lengths because of standing, changes in gait velocity and the influence of contractions).

In rabbits the Toe-spread reflex is used.<sup>57</sup> This simple test can be used semi-quantitatively but should be used just to proof regeneration because of the bias involved in the assessment of this test. The rabbit is held by the skin of its neck and dropped over a distance of 40 cm. In a reflex to minimize impact on the ground, the rabbit spreads his legs and toes, dorsiflexes his ankle. This response can be graded from 0 to 2.

Indicators of function are muscle weight and muscle strength. In the rabbit for instance, the anterior tibial muscle can be used for evaluation of peroneal nerve lesions, since this muscle is specifically innervated by that nerve. The muscle can be attached to a spring and contraction force on stimulation measured.<sup>15,28</sup> Subsequently muscle weight can be recorded, dry or wet. Dry has the advantage of eliminating edema, whereas wet muscle weight can be performed more easily.<sup>18,29,44</sup>

Sensory function tests include different ways of subjecting the experimental animal to pain, heat or current and recording when the animal withdraws its injured limb.<sup>66</sup> Age and thickness of skin, however, influence these parameters.

## Histology

Histological evaluation is also widely used for evaluation of peripheral nerve regeneration. The main advantage is that specific markers can be used to evaluate specific subsets of cells. For instance protein product 9.5 (PGP) is a pan neuronal marker. Calcitonin gene-related peptide (CGRP) and Substance P (SP) are sensory neuropeptides. Vasoactive intestinal peptide (VIP) is present in cholinergic fibres. Neuropeptide Y (NpY), its C-flanking peptide C-PON and the enzyme tyrosine hydroxylase (TH) are present in sympathetic fibres. Markers like von Willebrand factor (vWF) and vasoconstrictor peptide endothelin 1 (ET 1) are present in endothelial cells, marking vascularisation.<sup>85</sup>

Another advantage is that evaluation can be done early because reinnervation is not essential, since the markers will be present in the subsets at any given time.

Myelinated axon counts evaluate myelin thickness, axon diameter and numbers of myelinated axons ranging from 1 - 20  $\mu\text{m}$ . (See fig. 1.8 on page 20) This can be done semi automated and fully automated by custom made or ready available soft- and hardware. The advantage is that the relation between diameter and electrophysiological parameters has been described in detail. The main drawback is misinterpretation of data due to artifacts. Non-roundness, detachment of myelin from the axon, the Schwann cell nucleus and blood vessels are known problems. Also, this method is still quite labourious, since most of the myelinated axon counts still need considerable manual input for separation of fibres and exclusion of artefacts. The main comment on histological evaluation is that function is not tested.

## Evaluation of a nerve repair

Most function tests evaluate the final function of part of the peripheral nervous system. As described above, sensory tests evaluate the subjects response to touch, pain or temperature and muscle tests evaluate strength or fatiguability. A major drawback is that an organism can rely on back-up systems or bypass specific function. Sensory recovery might partly rely on overlap of adjacent, intact nerves and motor recovery is enhanced by connections of a single sprout with multiple muscle fibres.

For surgeons, it is essential to have an indication of the result of their procedure. Therefore, it would be of interest to develop a testing method of the quality of regeneration across a nerve repair.

MNG has the ability to separate the stimulation artefact and the signal on short conduction distances (4 cm). Hence it is possible to stimulate distal as well as proximal to the lesion. When recording is always performed proximal to the lesion, theoretically only the axons that are stimulated that are crossing the repair.

Another advantage is that the number of sprouts has no influence on the signal since recording is performed proximal to the area where the sprouts form. It is difficult however to test this hypothesis, since none of the other evaluation tests provide similar functional information. Therefore, it can only be assessed by testing

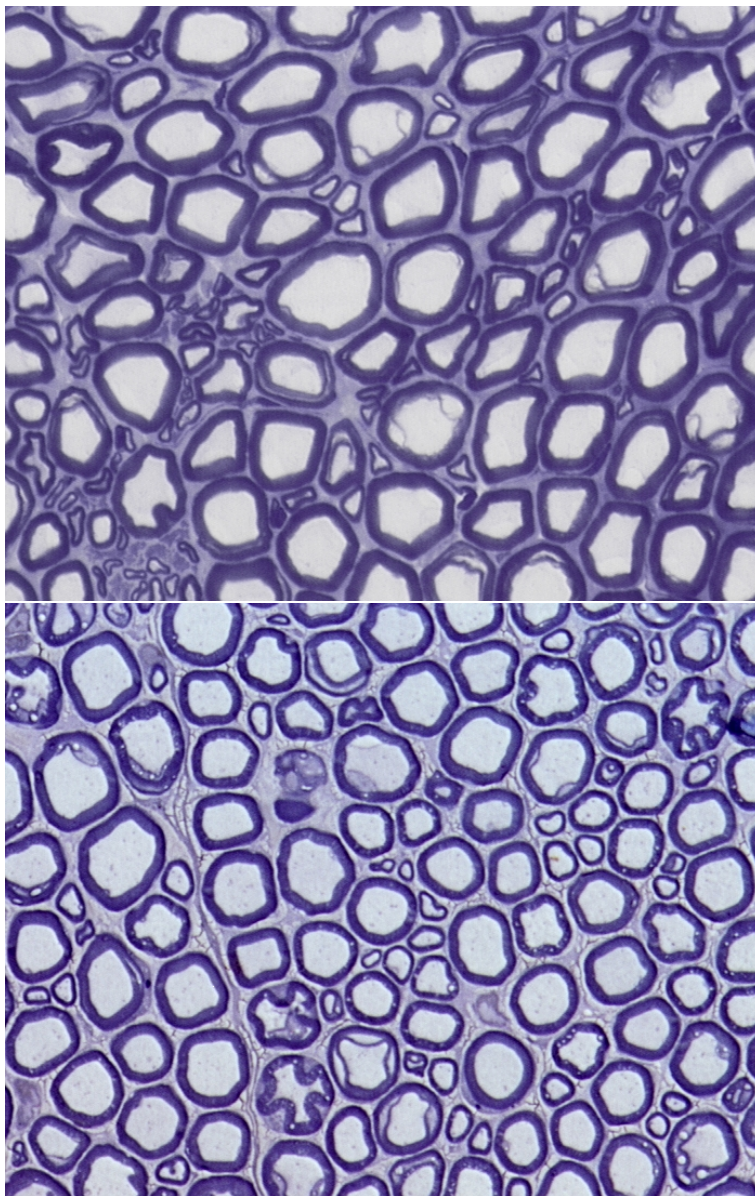


Figure 1.8: Sections of a control nerve (top picture) and a proximal segment (bottom picture) of a transected and reconstructed nerve. Myelin is stained by 1% osmium tetroxide.  $1\mu\text{m}$  transverse sections were stained with thionine blue and acridine orange to enhance myelin contrast for semi-automated myelinated axon counts.

two modes of injury with a known, different, outcome. In this thesis transection and reconstruction are compared with a crush lesion.

## 1.4 Peripheral Nerve and Stretch

The central dogma in peripheral nerve surgery is not to suture nerves under tension. The reason stated is that this will produce scarring. Therefore, if any tension is suspected a nerve graft or a conduit needs to be used. However, it is well known that outcomes after a graft are less than the results of a primary repair. After transection of a peripheral nerve, the proximal and distal segments retract, and it remains a question to the surgeon at what gap, between the two nerve ends, to insert a nerve graft or choose for direct suture. Interestingly, for smaller gaps, up to 3-4 cm, although opinions vary between 2 and 15 cm, the conduits from different (bio-)materials, have now been used clinically with varying degrees of success.<sup>65</sup>

But before the question at what tension to insert a graft or to suture primarily, can be resolved, certain basic problems need to be answered first. It is essential to define what structure of the nerve is the main load-bearing component and all extracellular matrix structures have been implied until recently. Furthermore, it is still unclear how a nerve deals with tension and what tension can be subjected to the different structures.

### 1.4.1 Anatomy

Biomechanical properties of the whole nerve have been described in detailed studies.<sup>12,49,61,74,94,95</sup> In these studies, all the matrix elements of the nerve, epineurium, perineurium, and endoneurium, have in turn been reported to be the main load-bearing component. There is a consensus, however, that the conductive tissues have little capacity to withstand any longitudinal forces.

Ultrastructural studies of the collagen scaffolding of rat sciatic nerve have shown that the epineurium consists of interwoven, thick, flat, tape-like collagen bundles. The perineurium comprises a lacework of smaller collagen fibres orientated longitudinally and obliquely spiralling, also containing the perineurial cell layer and basement membrane.<sup>82,91</sup> Based on this ultrastructure it has been suggested that the architecture of the epineurium might allow some degree of extensibility of the nerve, and that the perineurium is set up to withstand the positive endoneurial pressure.<sup>56,60,82,91</sup>

Clinically, after transection of a nerve, both ends retract, seemingly due to tension. Elastin fibres have been identified in all three layers of the peripheral nerve, but in small quantities, not sufficient to explain the retraction.

### 1.4.2 Stretch of Nerve

The mechanical properties of whole nerves have been described. Most important properties of tension are stiffness and creep. Stiffness can be defined as the tension required to increase a nerve over a certain length, and creep as the relaxation of that tension of the nerve at constant length. Strain can subsequently be defined as stiffness related to cross-sectional area of a nerve (in order to compare different size nerves). A key element in stiffness behaviour of nerve is a 'toe-region'.<sup>49,74,84</sup> This region is marked by an increase in length, on stretching of a nerve (or any material) with only a very slow build-up of force. Rydevik et al<sup>74</sup> reported, in a rabbit model using the tibial nerve, a toe-region up to approximately 15% strain, and linear stiffness was reached around 27%. It is unclear whether this toe-region is a physiological phenomenon or an artefact.

### 1.4.3 Stretch and Nerve Function

Nerve function in relation to stretch was ultimately investigated in the squid giant axon. This is a single, unmyelinated fibre, with a diameter between 400 - 600 nm, and very little extracellular matrix. This axon has shown a load deflection curve, or toe-region, with a turning point at approximately 10% stretch.<sup>21</sup> Functional irreversible impairment started from 19% stretch, where the axon could not be stimulated anymore. This implies that the intact neural tissue is able to cope with elongation. Kwan et al and Rydevik et al found that around 12% stretch in rabbit tibial nerve, conduction remained impaired for longer than an hour after release of stretch.

## 1.5 The Aims of This Thesis

In respect of the previous paragraphs the following aims for this thesis are postulated:

- to investigate the relation between parameters of nerve regeneration in the proximal segment: i.e. the relation between the decrease in peak-peak amplitude and the conduction velocity and the relation between the decrease in peak-peak amplitude and myelinated axon counts to further clarify the role of the proximal segment
- to examine the influence of the type of repair on electrophysiological properties in the proximal segment
- to develop a measure for evaluation of nerve repair techniques in a rabbit model
- to assess the effects of longitudinal tension on a peripheral nerve

## References

1. Anand P, Terenghi G, Warner G, Kopelman P, Williams-Chestnut R, Sinicropi D. The role of endogenous nerve growth factor in human diabetic neuropathy. *Nat Med* 1996;2:703-707.
2. Arakawa Y, Sendtner M, Thoenen H. Survival effect of ciliary neurotrophic factor (CNTF) on chick embryonic motoneurons in culture: comparison with other neurotrophic factors and cytokines. *J Neurosci* 1990;10:3507-3515.
3. Bain J, Mackinnon S, Hunter D. Functional evaluation of complete sciatic, peroneal, and posterior tibial nerve lesions in the rat. *Plast Reconstr Surg* 1989;83:129-138.
4. Bennett DL, Michael GJ, Ramachandran N, Munson JB, Averill S, Yan Q, McMahon SB, Priestley JV. A distinct subgroup of small DRG cells express GDNF receptor components and GDNF is protective for these neurons after nerve injury. *J Neurosci* 1998;18:3059-3072.
5. Bennett TM, Dowsing BJ, Austin L, Messina A, Nicola NA, Morrison WA. Anterograde transport of leukemia inhibitory factor within transected sciatic nerves. *Muscle Nerve* 1999;22:78-87.
6. Boeshore KL, Schreiber RC, Vaccariello SA, Sachs HH, Salazar R, Lee J, Ratan RR, Leahy P, Zigmond RE. Novel changes in gene expression following axotomy of a sympathetic ganglion: a microarray analysis. *J Neurobiol* 2004;59:216-235.
7. Bosse F, Kury P, Muller HW. Gene expression profiling and molecular aspects in peripheral nerve regeneration. *Restor Neurol Neurosci* 2001;19:5-18.
8. Brandt R. Cytoskeletal mechanisms of neuronal degeneration. *Cell Tissue Res* 2001;305:255-265.
9. Braun S, Croizat B, Lagrange MC, Warter JM, Poindron P. Neurotrophins increase motoneurons' ability to innervate skeletal muscle fibers in rat spinal cord-human muscle cocultures. *J Neurol Sci* 1996;136:17-23.
10. Brecknell JE, Du JS, Muir E, Fidler PS, Hlavin ML, Dunnett SB, Fawcett JW. Bridge grafts of fibroblast growth factor-4-secreting schwannoma cells promote functional axonal regeneration in the nigrostriatal pathway of the adult rat. *Neuroscience* 1996;74:775-784.
11. Brecknell JE, Fawcett JW. Axonal regeneration. *Biol Rev Camb Philos Soc* 1996;71:227-255.
12. Brown R, Padowitz R, Rydevik B, Woo S, Hargens A, Massie J, Kwan M, Garfin SR. Effects of acute graded strain on efferent conduction properties in the rabbit tibial nerve. *Clin Orthop* 1993:288-294.
13. Brushart TM, Mesulam MM. Alteration in connections between muscle and anterior horn motoneurons after peripheral nerve repair. *Science* 1980;208:603-605.
14. Brushart TM, Tarlov EC, Mesulam MM. Specificity of muscle reinnervation after epineurial and individual fascicular suture of the rat sciatic nerve. *J Hand Surg [Am]* 1983;8:248-253.
15. Davis L, Gordon T, Hoffer J, Jhamandas J, Stein R. Compound action poten-

tials recorded from mammalian peripheral nerves following ligation or resuturing. *J Physiol (Lond)* 1978;285:543-559.

16. de Medinaceli L, Freed WJ, Wyatt RJ. An index of the functional condition of rat sciatic nerve based on measurements made from walking tracks. *Exp Neurol* 1982;77:634-643.

17. Deckwerth TL, Johnson EM, Jr. Temporal analysis of events associated with programmed cell death (apoptosis) of sympathetic neurons deprived of nerve growth factor. *J Cell Biol* 1993;123:1207-1222.

18. Frykman GK, McMillan PJ, Yegge S. A review of experimental methods measuring peripheral nerve regeneration in animals. *Orthop Clin North Am* 1988;19:209-219.

19. Fugleholm K, Schmalbruch H, Krarup C. Early peripheral nerve regeneration after crushing, sectioning, and freeze studied by implanted electrodes in the cat. *J Neurosci* 1994;14:2659-2673.

20. Fugleholm K, Schmalbruch H, Krarup C. Post reinnervation maturation of myelinated nerve fibers in the cat tibial nerve: chronic electrophysiological and morphometric studies. *J Peripher Nerv Syst* 2000;5:82-95.

21. Galbraith JA, Thibault LE, Matteson DR. Mechanical and electrical responses of the squid giant axon to simple elongation. *J Biomech Eng* 1993;115:13-22.

22. Gillespie M, Stein R. The relationship between axon diameter, myelin thickness and conduction velocity during atrophy of mammalian peripheral nerves. *Brain Res* 1983;259:41-56.

23. Gilmour J, Myles L, Glasby M. The fate of motoneurons in the spinal cord after peripheral nerve repair: a quantitative study using the neural tracer horseradish peroxidase. *J Neurosurg* 1995;82:623-629.

24. Gravel C, Gotz R, Lorrain A, Sendtner M. Adenoviral gene transfer of ciliary neurotrophic factor and brain-derived neurotrophic factor leads to long-term survival of axotomized motor neurons. *Nat Med* 1997;3:765-770.

25. Groves MJ, An SF, Giometto B, Scaravilli F. Inhibition of sensory neuron apoptosis and prevention of loss by NT-3 administration following axotomy. *Exp Neurol* 1999;155:284-294.

26. Gutman E, Sanders F. Recovery of fibre numbers and diameters in the regeneration of peripheral nerves. *J Physiol* 1943;101:489-518.

27. Hare G, Evans P, Mackinnon S, Best T, Bain J, Szalai J, Hunter D. Walking track analysis: a long-term assessment of peripheral nerve recovery. *Plast Reconstr Surg* 1992;89:251-258.

28. Hatcher D, Luff A, Westerman R, Finkelstein D. Contractile properties of cat motor units enlarged by motoneurone sprouting. *Exp Brain Res* 1985;60:590-593.

29. Herbison GJ, Jaweed MM, Scott CM, Ditunno JF, Jr. Muscle weight and protein content of rat skeletal muscle following sciatic nerve crush. *Arch Phys Med Rehabil* 1974;55:241-246.

30. Heumann R. Regulation of the synthesis of nerve growth factor. *J Exp Biol*

1987;132:133-150.

31. Himes BT, Tessler A. Death of some dorsal root ganglion neurons and plasticity of others following sciatic nerve section in adult and neonatal rats. *J Comp Neurol* 1989;284:215-230.

32. Hobson MI, Green CJ, Terenghi G. VEGF enhances intraneural angiogenesis and improves nerve regeneration after axotomy. *J Anat* 2000;197 Pt 4:591-605.

33. Hoffman P. Distinct roles of neurofilament and tubulin gene expression in axonal growth. *Ciba Found Symp* 1988;138:192-204.

34. Hoffman P, Cleveland D. Neurofilament and tubulin expression recapitulates the developmental program during axonal regeneration: induction of a specific beta-tubulin isotype. *Proc Natl Acad Sci U S A* 1988;85:4530-4533.

35. Hoffman P, Cleveland D, Griffin J, Landes P, Cowan N, Price D. Neurofilament gene expression: a major determinant of axonal caliber. *Proc Natl Acad Sci U S A* 1987;84:3472-3476.

36. Hoffman P, Griffin J, Gold B, Price D. Slowing of neurofilament transport and the radial growth of developing nerve fibers. *J Neurosci* 1985;5:2920-2929.

37. Hoffman P, Griffin J, Price D. Control of axonal caliber by neurofilament transport. *J Cell Biol* 1984;99:705-714.

38. Hoffman P, Lasek R. Axonal transport of the cytoskeleton in regenerating motor neurons: constancy and change. *Brain Res* 1980;202:317-333.

39. Hursh J. Conduction Velocity and Diameter of Nerve Fibres. *Amer J Physiol* 1939;127:131-139.

40. Ide C. Peripheral nerve regeneration. *Neurosci Res* 1996;25:101-121.

41. Kanaya F, Firrell J, Breidenbach W. Sciatic function index, nerve conduction tests, muscle contraction, and axon morphometry as indicators of regeneration. *Plast Reconstr Surg* 1996;98:1264-1271, discussion 1272-1264.

42. Kanaya F, Firrell J, Tsai T, Breidenbach W. Functional results of vascularized versus nonvascularized nerve grafting. *Plast Reconstr Surg* 1992;89:924-930.

43. Kauppila T, Jyvasjarvi E, Huopaniemi T, Hujanen E, Liesi P. A laminin graft replaces neurorrhaphy in the restorative surgery of the rat sciatic nerve. *Exp Neurol* 1993;123:181-191.

44. Kobayashi J, Mackinnon S, Watanabe O, Ball D, Gu X, Hunter D, Kuzon WM J. The effect of duration of muscle denervation on functional recovery in the rat model. *Muscle Nerve* 1997;20:858-866.

45. Kuypers PD, Gielen FL, Wai RT, Hovius SE, Godschalk M, van Egeraat JM. A comparison of electric and magnetic compound action signals as quantitative assays of peripheral nerve regeneration. *Muscle Nerve* 1993;16:634-641.

46. Kuypers PD, van Egeraat JM, Dudok v Heel M, van Briemen LJ, Godschalk M, Hovius SE. A magnetic evaluation of peripheral nerve regeneration: I. The discrepancy between magnetic and histologic data from the proximal segment. *Muscle Nerve* 1998;21:739-749.

47. Kuypers PD, van Egeraat JM, Godschalk M, Hovius SE. Loss of viable neuronal

- units in the proximal stump as possible cause for poor function recovery following nerve reconstructions. *Exp Neurol* 1995;132:77-81.
48. Kuypers PD, Walbeehm ET, Heel MD, Godschalk M, Hovius SE. Changes in the compound action current amplitudes in relation to the conduction velocity and functional recovery in the reconstructed peripheral nerve. *Muscle Nerve* 1999;22:1087-1093.
49. Kwan MK, Wall EJ, Massie J, Garfin SR. Strain, stress and stretch of peripheral nerve. Rabbit experiments in vitro and in vivo. *Acta Orthopaedica Scandinavica* 1992;63:267-272.
50. Levi-Montalcini R, Hamburger V. A diffusible agent of mouse sarcoma producing hyperplasia of sympathetic ganglia and hypernematization of viscera in the chick embryo. *J Exp Zool* 1953;123:233-278.
51. Lieberman AR. The axon reaction: a review of the principal features of perikaryal responses to axon injury. *Int Rev Neurobiol* 1971;14:49-124.
52. Liu Y, Himes BT, Murray M, Tessler A, Fischer I. Grafts of BDNF-producing fibroblasts rescue axotomized rubrospinal neurons and prevent their atrophy. *Exp Neurol* 2002;178:150-164.
53. Liu Y, Kim D, Himes BT, Chow SY, Schallert T, Murray M, Tessler A, Fischer I. Transplants of fibroblasts genetically modified to express BDNF promote regeneration of adult rat rubrospinal axons and recovery of forelimb function. *J Neurosci* 1999;19:4370-4387.
54. Ljungberg C, Novikov L, Kellerth JO, Ebendal T, Wiberg M. The neurotrophins NGF and NT-3 reduce sensory neuronal loss in adult rat after peripheral nerve lesion. *Neurosci Lett* 1999;262:29-32.
55. Lundborg G. A 25-year perspective of peripheral nerve surgery: evolving neuroscientific concepts and clinical significance. *J Hand Surg [Am]* 2000;25:391-414.
56. Lundborg G. Intraneural microcirculation. *Orthop Clin North Am* 1988;19:1-12.
57. Lundborg G. Ischemic nerve injury. Experimental studies on intraneural microvascular pathophysiology and nerve function in a limb subjected to temporary circulatory arrest. *Scand J Plast Reconstr Surg Suppl* 1970;6:3-113.
58. Lundborg G. *Nerve Injury and Repair*. Edinburgh London Melbourne and New York: Churchill Livingstone; 1988.
59. Lundborg G, Dahlin L, Danielsen N, Zhao Q. Trophism, tropism, and specificity in nerve regeneration. *J Reconstr Microsurg* 1994;10:345-354.
60. Lundborg G, Myers R, Powell H. Nerve compression injury and increased endoneurial fluid pressure: a "miniature compartment syndrome". *J Neurol Neurosurg Psychiatry* 1983;46:1119-1124.
61. Lundborg G, Rydevik B. Effects of stretching the tibial nerve of the rabbit. A preliminary study of the intraneural circulation and the barrier function of the perineurium. *J Bone Joint Surg [Br]* 1973;55:390-401.
62. Mackinnon S, Dellon A, OqBrien J. Changes in nerve fiber numbers distal to a

- nerve repair in the rat sciatic nerve model. *Muscle Nerve* 1991;14:1116-1122.
63. Mackinnon SE, Dellon AL. *Surgery of the Peripheral Nerve*. New York: Thieme; 1988.
64. McKay Hart A, Brannstrom T, Wiberg M, Terenghi G. Primary sensory neurons and satellite cells after peripheral axotomy in the adult rat: timecourse of cell death and elimination. *Exp Brain Res* 2002;142:308-318.
65. Meek MF, Coert JH. Clinical use of nerve conduits in peripheral-nerve repair: review of the literature. *J Reconstr Microsurg* 2002;18:97-109.
66. Moller KA, Johansson B, Berge OG. Assessing mechanical allodynia in the rat paw with a new electronic algometer. *J Neurosci Methods* 1998;84:41-47.
67. Mosahebi A, Woodward B, Wiberg M, Martin R, Terenghi G. Retroviral labeling of Schwann cells: in vitro characterization and in vivo transplantation to improve peripheral nerve regeneration. *Glia* 2001;34:8-17.
68. Myles L, Gilmour J, Glasby M. Effects of different methods of peripheral nerve repair on the number and distribution of muscle afferent neurons in rat dorsal root ganglion. *J Neurosurg* 1992;77:457-462.
69. Otto D, Unsicker K, Grothe C. Pharmacological effects of nerve growth factor and fibroblast growth factor applied to the transected sciatic nerve on neuron death in adult rat dorsal root ganglia. *Neurosci Lett* 1987;83:156-160.
70. Peyronnard J, Charron L, Lavoie J, Messier J. Differences in horseradish peroxidase labeling of sensory, motor and sympathetic neurons following chronic axotomy of the rat sural nerve. *Brain Res* 1986;364:137-150.
71. Peyronnard J, Charron L, Lavoie J, Messier J, Bergouignan F. A comparative study of the effects of chronic axotomy, crush lesion and re-anastomosis of the rat sural nerve on horseradish peroxidase labelling of primary sensory neurons. *Brain Res* 1988;443:295-309.
72. Reynolds JL, Urbanek MS, Asato H, Kuzon WM, Jr. Deletion of individual muscles alters rat walking-track parameters. *J Reconstr Microsurg* 1996;12:461-466.
73. Rich KM, Luszczyński JR, Osborne PA, Johnson EM, Jr. Nerve growth factor protects adult sensory neurons from cell death and atrophy caused by nerve injury. *J Neurocytol* 1987;16:261-268.
74. Rydevik BL, Kwan MK, Myers RR, Brown RA, Triggs KJ, Woo SL, Garfin SR. An in vitro mechanical and histological study of acute stretching on rabbit tibial nerve. *Journal Of Orthopaedic Research* 1990;8:694-701.
75. Salonen V, Peltonen J, Roytta M, Virtanen I. Laminin in traumatized peripheral nerve: basement membrane changes during degeneration and regeneration. *J Neurocytol* 1987;16:713-720.
76. Sendtner M, Arakawa Y, Stockli KA, Kreutzberg GW, Thoenen H. Effect of ciliary neurotrophic factor (CNTF) on motoneuron survival. *J Cell Sci Suppl* 1991;15:103-109.
77. Sendtner M, Holtmann B, Hughes RA. The response of motoneurons to neu-

- rotrophins. *Neurochem Res* 1996;21:831-841.
78. Shenaq JM, Shenaq SM, Spira M. Reliability of sciatic function index in assessing nerve regeneration across a 1 cm gap. *Microsurgery* 1989;10:214-219.
79. Sterne G, Brown R, Green C, Terenghi G. Neurotrophin-3 delivered locally via fibronectin mats enhances peripheral nerve regeneration. *Eur J Neurosci* 1997;9:1388-1396.
80. Sterne G, Coulton G, Brown R, Green C, Terenghi G. Neurotrophin-3-enhanced nerve regeneration selectively improves recovery of muscle fibers expressing myosin heavy chains 2b. *J Cell Biol* 1997;139:709-715.
81. Sterne GD, Brown RA, Green CJ, Terenghi G. NT-3 modulates NPY expression in primary sensory neurons following peripheral nerve injury. *Journal Of Anatomy* 1998;193 ( Pt 2):273-281.
82. Stolinski C. Structure and composition of the outer connective tissue sheaths of peripheral nerve. *Journal Of Anatomy* 1995;186 ( Pt 1):123-130.
83. Sunderland S. *Nerve Injuries and their Repair. A Critical Appraisal*. Melbourne: Churchill Livingstone; 1991. 418-420 p.
84. Sunderland S. Stretch-compression neuropathy. *Clin Exp Neurol* 1981;18:1-13.
85. Terenghi G. Peripheral nerve injury and regeneration. *Histol Histopathol* 1995;-10:709-718.
86. Terris DJ, Cheng ET, Utley DS, Tarn DM, Ho PR, Verity AN. Functional recovery following nerve injury and repair by silicon tubulization: comparison of laminin-fibronectin, dialyzed plasma, collagen gel, and phosphate buffered solution. *Auris Nasus Larynx* 1999;26:117-122.
87. Titmus MJ, Faber DS. Axotomy-induced alterations in the electrophysiological characteristics of neurons. *Prog Neurobiol* 1990;35:1-51.
88. Toby E, Meyer B, Schwappach J, Alvine G. Changes in the structural properties of peripheral nerves after transection. *J Hand Surg [Am]* 1996;21A:1086-1090.
89. Toft P, Fugleholm K, Schmalbruch H. Axonal branching following crush lesions of peripheral nerves of rat. *Muscle Nerve* 1988;11:880-889.
90. Tohyama K, Ide C. The localization of laminin and fibronectin on the Schwann cell basal lamina. *Arch Histol Jpn* 1984;47:519-532.
91. Ushiki T, Ide C. Three-dimensional organization of the collagen fibrils in the rat sciatic nerve as revealed by transmission- and scanning electron microscopy. *Cell Tissue Res* 1990;260:175-184.
92. Varejao AS, Meek MF, Ferreira AJ, Patricio JA, Cabrita AM. Functional evaluation of peripheral nerve regeneration in the rat: walking track analysis. *J Neurosci Methods* 2001;108:1-9.
93. Vestergaard S, Tandrup T, Jakobsen J. Effect of permanent axotomy on number and volume of dorsal root ganglion cell bodies. *J Comp Neurol* 1997;388:307-312.
94. Wall EJ, Kwan MK, Rydevik BL, Woo SL, Garfin SR. Stress relaxation of a peripheral nerve. *Journal Of Hand Surgery American Volume* 1991;16:859-863.
95. Wall EJ, Massie JB, Kwan MK, Rydevik BL, Myers RR, Garfin SR. Experimental

stretch neuropathy. Changes in nerve conduction under tension. *J Bone Joint Surg [Br]* 1992;74:126-129.

96. Whitworth I, Brown R, Dore C, Anand P, Green C, Terenghi G. Nerve growth factor enhances nerve regeneration through fibronectin grafts. *J Hand Surg [Br]* 1996;21:514-522.

97. Whitworth I, Brown R, Dore C, Green C, Terenghi G. Orientated mats of fibronectin as a conduit material for use in peripheral nerve repair. *J Hand Surg [Br]* 1995;20:429-436.

98. Whitworth IH, Terenghi G, Green CJ, Brown RA, Stevens E, Tomlinson DR. Targeted delivery of nerve growth factor via fibronectin conduits assists nerve regeneration in control and diabetic rats. *European Journal Of Neuroscience* 1995;7:2220-2225.

99. Young RC, Wiberg M, Terenghi G. Poly-3-hydroxybutyrate (PHB): a resorbable conduit for long-gap repair in peripheral nerves. *Br J Plast Surg* 2002;55:235-240.

100. Liss A, Ekenstam F, Wiberg M. Cell loss in sensory ganglia after peripheral nerve injury. An anatomical tracer study using lectin-coupled horseradish peroxidase in cats. *Scand J Plast Reconstr Surg Hand Surg* 1994;28:177-188.

101. Liss A, Ekenstam F, Wiberg M. Loss of neurons in the dorsal root ganglia after transection of a peripheral sensory nerve. An anatomical study in monkeys. *Scand J Plast Reconstr Surg Hand Surg* 1996;30:1-6.

102. Terenghi G. Peripheral nerve regeneration and neurotrophic factors. *Journal Of Anatomy* 1999;194 ( Pt 1):1-14.



# Chapter 2

## **Changes in the Compound Action Current Amplitudes in Relation to the Conduction Velocity and Functional Recovery in the Reconstructed Peripheral Nerve**

*(Muscle and Nerve 1999;22:8:1087-93)*

Paul D.L. Kuypers  
Erik T Walbeehm  
Michiel Dudok van Heel  
Moshe Godschalk  
Steven E.R. Hovius

## Abstract

The average axon diameter in the proximal segment of a transected and reconstructed peripheral nerve will decrease shortly after the transection and increase again when the ating axons make contact with their targets. The magnetically recorded nerve compound action current (NCAC) amplitude and the conduction velocity (CV) are directly related to the xon diameters. In this experiment, the peroneal nerve was unilaterally transected and reconstructed in 42 rabbits. After 3, 4.5, 6, 8, 12, 20, and 36 weeks of regeneration time, hind leg motor function recovery, NCAC amplitude, and CV 1st peak were studied. Our results demonstrate a significant decrease in signal amplitude and CV in the first 8 weeks after econstruction. These decreases are related ( $P < 0.05$ ). After 8 weeks of regeneration time, motor function and the CV of the recorded signals start to recover, but the signal udes do not. Based on the correlation of the CV and signal amplitude with axon diameter, they would both be expected to increase with recovering function. As an explanation for s lack of increase of signal amplitude, we suggest that, at the same time as some axons reach their target organs and start to mature, a number of the axons which have not reached a proper target organ will lose their signal-conducting capability. This will cause a decrease in compound signal amplitude, which cancels out the expected increase in NCAC de, due to axonal maturation.

## Introduction

Magnetoneurography (MNG) has been developed to measure nerve compound action currents (NCACs) from peripheral nerves.<sup>13-16</sup> The signals are highly reproducible and can be used to quantify the number of functional neuronal units, i.e., an axon and all sprouts growing from it, which will conduct a signal after being stimulated<sup>16</sup> in a nerve.<sup>6,15,27,28,30</sup>

Former studies concerning the evaluation of transected and reconstructed peripheral nerves in the rabbit with MNG have demonstrated the following: (1) 8 weeks after reconstruction, the amplitudes of the signals recorded from the proximal segment had decreased by approximately 60% compared with the signals recorded from the healthy contralateral control nerves<sup>16</sup>; (2) there was no function during the first 6 weeks after the nerve reconstructions.

After 6 weeks of regeneration time, function started to recover and reached a maximum at 20 weeks of regeneration time<sup>14</sup>; (3) the decrease in signal amplitude measured from the proximal segment of the reconstructed nerves at 8 weeks postreconstruction persisted after 20 weeks of regeneration time.<sup>13</sup> Thus, the signal amplitude recorded from the proximal segment did not alter during functional recovery. This is in contrast to what would be expected, because the single fibre action current (SFAC) amplitude is related to axon diameter.<sup>31</sup> Histological studies have demonstrated that the average axon diameter in the proximal segment of a transected and reconstructed nerve decreases shortly after the reconstruction<sup>2,4,9</sup>; after long regeneration times, the axon diameters regain their normal values.<sup>4,20</sup>

In theory, such a recovery of axon diameters should also result in a recovery of signal amplitudes.<sup>31</sup> The goal of this experiment was to study short and long-term changes in the NCAC amplitudes recorded from the proximal segment of transected and reconstructed peripheral nerves in the rabbit using MNG and to relate these values to the conduction velocity (CV 1st peak) and the recovery of motor function in the hind leg.

## Methods

**Reconstruction Operation.** Forty-two New Zealand White rabbits, 12-14 weeks of age (3-4 kg body weight), were used. The common peroneal nerve was unilaterally transected and microsurgically reconstructed. To this end a lateral incision at the thigh was made, and the nerve partially mobilized. The nerve was transected at 15 mm proximal to where it enters the long peroneal muscle and reconstructed tension-free, with 4-5 10-0 ethilon perineurial sutures.

These reconstructions were performed with the aid of an operating microscope and according to a standardized protocol.<sup>13</sup> After the reconstruction, the wound was closed. Following this operation the animals were divided into seven groups of six animals each. The survival times were 3, 4.5, 6, 8, 12, 20 and 36 weeks, respectively, after which the signals were recorded from the reconstructed and the

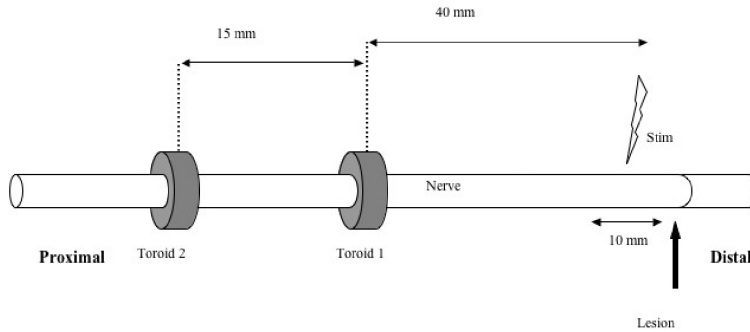


Figure 2.1: A schematic overview of the recording setup for measuring the magnetic signals from the proximal segment of the reconstructed nerves. The nerves were stimulated at a site 10 mm proximal to the lesion and recordings were obtained simultaneously at 40 and 56 mm proximal to the stimulation site.

healthy contralateral nerve. In the 4.5 weeks regeneration-time group, the signals could not be measured due to technical problems.

**Recording Operation.** After the respective regeneration times, the reconstructed nerves were again mobilized through a similar incision and transected as far proximal as possible. The nerve was threaded through two toroidal sensor coils placed 16 mm apart. A double metal hook served as a bipolar stimulation electrode. During the procedure, the tissues were kept moist by creating a bath with the skin flaps. The bath was continuously perfused with 0.9% NaCl solution (20 mL/min), which was maintained at  $37 \pm 0.50$  C.<sup>15</sup>

**Recording Technique.** The MNG technique measures the changes in magnetic fields caused by the intra-axonal electric currents that occur when a signal is propagated through a stimulated peripheral nerve.<sup>29,39</sup> The changes in magnetic fields caused by the stimulated nerves are recorded through induction currents (NCACs) in the toroidal coils placed around the nerves.<sup>7,29,30</sup> Each coil consisted of a ferrite core that was wound with insulated copper wire (diameter  $50\mu\text{m}$ ). The coil was 4.8 mm in diameter and 1.5 mm thick.<sup>15</sup> Figure 1 demonstrates typical examples of such magnetically recorded NCACs measured from the healthy and reconstructed peroneal nerves of a rabbit after 20 weeks of regeneration time.

The nerves were stimulated at a site 10 mm proximal to the lesion (see fig. 2.1);  $50\mu\text{s}$ , monophasic, rectangular pulses were delivered. The pulse amplitude was supramaximal (three times the specific threshold amplitude for each nerve) in order to stimulate all viable axons in the bundle. This was confirmed by the fact

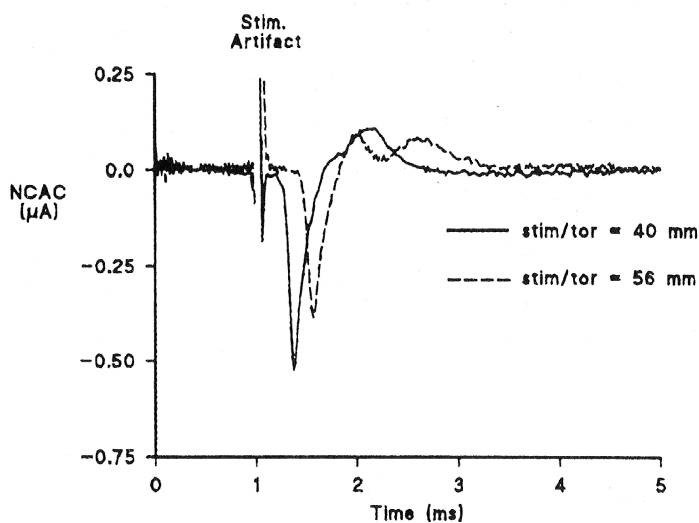


Figure 2.2: Typical examples of magnetic signals recorded from a reconstructed nerve (dashed line) and from the contralateral control nerve (solid line) measured after 20 weeks of regeneration time.

that a further increase in stimulus amplitude did not influence the recorded signal amplitude.

For each measurement, 1024 NCACs were averaged to increase the signal/noise ratio. The signals were simultaneously recorded at 40 and  $56 \pm 0.5$  mm proximal to the stimulation site<sup>15</sup> (see figs. 2.2 & 2.3). For control purposes, NCACs were also recorded from the intact contralateral nerve, following the same procedures as on the reconstructed side. All operations were executed under general inhalation anesthesia ( $O_2$ ,  $N_2O$ , and Enflurane). After the recording operation, the animals were euthanized. All procedures were performed in accordance with the Erasmus University guidelines for animal experiments.

**Functional Recovery.** Prior to the recording operation, functional recovery was evaluated by using the toe-spread test.<sup>17</sup> This test evaluates the reflex dorsiflexion of the ankle and the spreading of the toes induced by dropping the rabbit over a distance of approximately 20 cm while holding the animal by the skin of the neck. These reflexes are predominantly controlled through the peroneal nerve.<sup>17,26</sup>

The functional recovery is presented as the percentage of animals in a regeneration-time group in which the reflex was either absent (no reflex), good (maximal

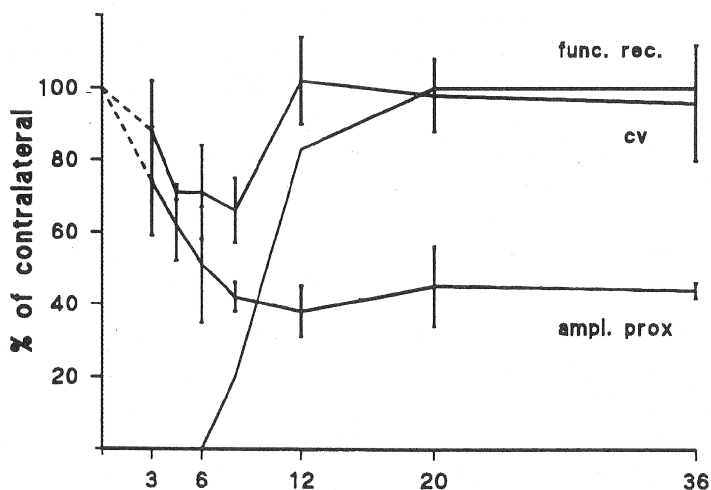


Figure 2.3: Typical examples of NCAC's measured at 40 mm (black line) and at 56 mm (dashed line) proximal to the stimulation site in the proximal segment of a reconstructed nerve after 36 weeks of regeneration time.

dorsiflexion of the ankle and spreading of the toes), or poor (all remaining results).  
14

## Results

For each animal, the signal amplitudes and CVs were normalized with the signals measured from the contralateral control nerves. The signal amplitudes measured from the proximal segment of the transected nerves after 3 weeks of regeneration time were on average 74% of those measured from the control nerves (see table 2.1 and fig. 2.4). This decrease is statistically significant ( $p < 0.02$ ; one-tailed t test). In the 4.5-weeks group, the amplitudes further decreased to an average of 62% and subsequently to 50% and 40% after 6 and 8 weeks of regeneration time, respectively. The amplitudes did not change significantly after more prolonged periods (see table 2.1 and fig. 2.4).

The CV of the first peak (CV 1st peak) of the signals measured from the proximal segment of the operated nerves was calculated by dividing the distance between the two sensors by the time difference between in the first-peak latency times measured by the two sensors. The CV 1st peak in the control nerves was on average 95 m/s. The CV 1st peak in the operated nerves 3 weeks after the reconstruction had

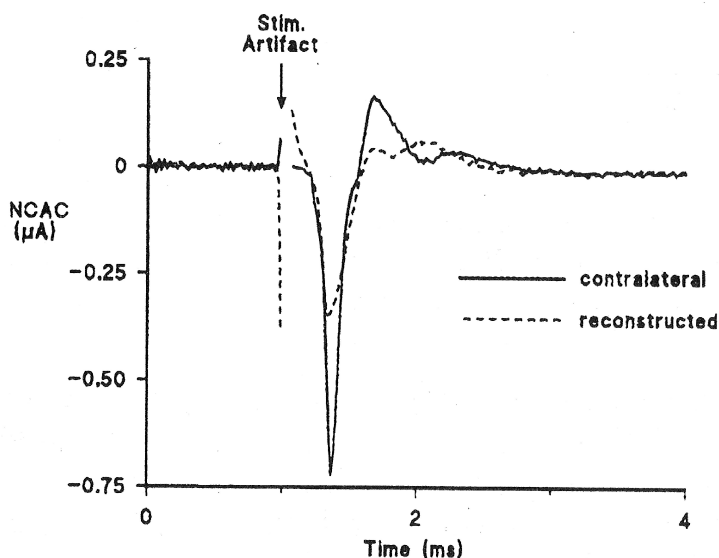


Figure 2.4: The functional recovery, CV and NCAC amplitude as measured 3, 4.5, 6, 8, 12, 20 and 36 weeks after a peripheral nerve transection and reconstruction. Functional recovery is presented as the percentage of animals in the corresponding regeneration time group that reached "good" function. Conduction velocity and signal amplitude in the reconstructed nerve are presented as a percentage of the signal from the contralateral control nerve, averaged per group.

decreased to  $88\% \pm 14$  of the value measured from the contralateral control nerves (see table 2.1 and fig. 2.4). The CV 1st peak after 4.5 weeks had decreased to  $71\% \pm 2$ . This difference of 1% between the two groups is statistically significant ( $P < 0.05$ ; two-tailed t test). After 8 weeks of regeneration time, the CV 1st peak in the reconstructed nerves had further decreased to  $66\% \pm$  of the value measured from the contralateral nerve. At 12 weeks, the CV 1st peak had again returned to control level and remained so for the following 24 weeks, which was the end of the experiment (see table 2.1). The increase between 8 and 12 weeks of regeneration time is statistically significant ( $P < 0.002$ ; two-tailed t test).

A statistically significant correlation ( $P = 0.05$ ; Spearman correlation test) was found between the signal amplitude and the CV 1st peak per animal over the first 8 weeks after the reconstruction. The signal duration time was measured for the signals from the 20- and the 36-weeks survival-time groups. The duration time was calculated from the moment the signal reached one third of the height of its first peak until it reached two thirds of the height of the second peak. The average

Table 2.1. The functional recovery, CV, and NCAC amplitude as measured 3,4.5, 6, 8, 12, 20 and 36 weeks after a peripheral nerve transection and reconstruction. \*

Reg. time (wk)	n	NCAC ampl. (% of Control $\pm$ SD)	CV 1st peak (non/poor/good)	Functional recovery
3	6	74 $\pm$ 15	88 $\pm$ 14	100/0/0
4.5	5	62 $\pm$ 10	71 $\pm$ 2	100/0/0
6	6	51 $\pm$ 16	71 $\pm$ 13	100/0/0
8	6	42 $\pm$ 4	66 $\pm$ 9	40/40/20
12	6	38 $\pm$ 7	102 $\pm$ 12	0/20/80
20	6	45 $\pm$ 11	98 $\pm$ 10	0/0/100
36	6	44 $\pm$ 2	96 $\pm$ 16	0/0/100

Table 2.1: \* *The NCAC amplitude measured from the reconstructed nerves is presented as a percentage of the signal amplitude measured from their contralateral control nerve. The CV 1st peak is given as a percentage of the CV 1st peak measured from the contralateral control nerve. The data are calculated per animal and given as an average per regeneration-time group. The recovery of function as tested with the toe-spread test is presented as the percentage of the regeneration-time group with absent, poor and good function.*

duration of the signals measured from the proximal segment of reconstructed nerves in the 20-weeks survival-time group was on average 108% of those measured in the control nerves, with a standard deviation of 14. This increase in signal duration is not statistically significant ( $P = 0.274$ ; paired t test).

The fact that no significance can be demonstrated could be due to the small number of samples. But even when the change in signal duration time was calculated for the 20- and 36-weeks regeneration-time groups taken together, no statistical significance was found. Motor function recovery as measured in our experiment was found to be absent after the transection and reconstruction. The function started to recover after 6 weeks of regeneration time and was maximal after 20 weeks (see table 2.1 and fig. 2.4).<sup>14</sup> When correlating the changes in CV 1st peak with the functional recovery per animal over the period from 8 to 36 weeks after the reconstruction, a statistically significant correlation ( $P < 0.01$ ; Mann-Whitney correlation analysis) was also found.

## Discussion

The MNG recording technique measures the changes in magnetic fields caused by action currents in a nerve. Because the magnetic fields are not significantly influenced by the biological tissues between the axons and the sensor, the MNG signals are highly reproducible and thus can be used for quantitative analysis.<sup>13,15,29,30</sup>

Furthermore, a correlation between the NCAC amplitude and the number of motor neurons in the healthy nerve has been demonstrated.<sup>6,15,16,28</sup> Possible variables which could cause a decrease in signal amplitude in the proximal segment of a reconstructed nerve have been discussed previously.<sup>14</sup>

Based on these findings, we have used the NCAC amplitude as an indicator for the neuronal number of functional units in the nerve bundle. In previous experiments, we have measured the signal amplitude from the proximal segment of reconstructed nerves at 8 and 20 weeks after the reconstruction. At 8 weeks, the amplitudes had decreased to approximately half those measured from the contralateral control nerves.<sup>16</sup> This decrease still persisted at 20 weeks after the reconstruction.<sup>13</sup> It was also demonstrated that the number of histologically counted myelinated axons at 10 and 50 mm proximal to the lesion site had decreased by only 5%.<sup>13</sup> This decrease is approximately equal to the decreases reported in the literature.<sup>10,22,32</sup> Because the signal amplitude is related to the number of functional neuronal units in a nerve, the 5% loss due to degeneration cannot explain a 50% decrease in signal amplitude. In the present experiment, the signal amplitudes were studied after 3, 4.5, 6, 8, 12, 20, and 36 weeks of nerve regeneration.

The amplitude measured from the proximal segment of the reconstructed nerves decreased significantly during the first 8 weeks after the reconstruction, as did the CV 1st peak (see table 2.1 and fig. 2.4). The reductions in CV 1st peak and signal amplitude during these 8 weeks are found to be correlated ( $P = 0.05$ ; Spearman correlation analysis). A reduction in CV proximal to a peripheral nerve lesion shortly after the reconstruction has also been demonstrated by other authors.<sup>2,10</sup> Conduction velocity is strongly related to axon diameter.<sup>1</sup> The loss of CV shortly after the reconstruction has therefore been explained by a histologically confirmed reduction in the average axon diameter proximal to the lesion.<sup>2,3,8</sup> The amplitude of SFAC has also been demonstrated to be related to the axon diameter.<sup>31</sup> Therefore, the decrease in axon diameter, as described for the proximal segment of the reconstructed nerves, would also be expected to result in a decrease of NCAC amplitude. Such a decrease indeed occurred in our experiment.

The notion that CV and signal amplitude are related by means of their relation to axon diameter seems to be supported by the correlation between the CV 1st peak and the NCAC amplitude in the first 8 weeks after the reconstruction, as found in our experiment. Regenerating axons in a transected and reconstructed peripheral nerve are known to first form thin sprouts that will regenerate into the distal segment and try to find a target organ. During this regeneration phase, the diameter of the axons proximal to the lesion is reduced.<sup>2,9</sup> Once a sprout has made contact with a proper target organ, it will start to mature. An important aspect of this maturation is the increase in diameter of the regenerated sprout.<sup>21</sup> After long regeneration times, the maturation phase will have been completed. This corresponds with the changes in axon diameters in the proximal segment, which return to normal values.<sup>2,4,20</sup>

In our experiment, the CV 1st peak increased from 66% to normal (100%) in

the period from 8 to 12 weeks after the reconstruction. This change was correlated in time ( $P < 0.01$ ) to the recovery of motor function, which increased from absent to good between 6 and 20 weeks after the reconstruction (see table 2.1 and fig. 2.4). It is tempting to explain this correlation in recovery of function and CV by the increase in axon diameter after the axon reaches its target and matures. Besides recovery of function and increase in CV, an increase in the NCAC amplitude would be expected at the same time, because both amplitude and CV are related to axon diameter.<sup>31</sup>

However, this was not the case in our experiment. The NCAC amplitude remained at approximately 45% of the signal amplitude measured from the contralateral nerve (see table 2.1 and fig. 2.4), whereas the CV 1st peak returned to normal. Other authors<sup>3</sup> have tried to explain this lack of recovery of signal amplitude while the CV 1st peak regains normal values, hypothesizing that only a small number of thick axons reach their target organs and therefore mature. This will result in an increased CV 1st peak. One would also expect the signal amplitude to increase. But because the other axons, which are unsuccessful in reinnervating a distal target organ, continue to conduct signals slowly, this will result in an increase in dispersion of the compound signal. An increase in dispersion will cause a decrease in the compound signal amplitudes. This would compensate for the increase in signal amplitude due to the maturation. Thus, although the peak latency may recover, the signal amplitude will not.<sup>3</sup>

This theory, however, does not seem a plausible explanation for the lack of recovery of the signal amplitudes as found in our experiment. The amplitude of signals measured from single nerve fibers varies approximately as the square of the CV.<sup>3,23</sup> A change in the axon diameters would therefore have a much higher impact on the NCAC amplitude than on the CV 1st peak. In our experiment, an increase in signal amplitude would thus be expected even when a major increase in dispersion occurs. This was not the case. Furthermore, such an increase in dispersion would also result in an increase in duration of the first and second peak. In the signals measured in this experiment, however, no increase in signal duration was observed (see Results and figs. 2.2 & 2.3).

In previous experiments, we suggested that after 8 weeks of regeneration time, a considerable number of the neuronal units in the proximal segment of the transected and reconstructed nerves lose their signal-conducting capability.<sup>14,15</sup> Similar conclusions have been drawn in histological studies.<sup>20</sup> In longterm experiments, the number of peripheral nerve cells labeled with horseradish peroxidase (HRP), after applying the dye to the proximal segment of a transected and reconstructed peripheral nerve, decreased to approximately 60% of the number found in the contralateral control nerves. No decrease was found when applying the dye to the nerve segment proximal to a crush lesion.<sup>20</sup> Based on the earlier finding that the amount of HRP absorbed by peripheral nerves is influenced by the electrical activity of the nerve,<sup>18,19</sup> this suggests a decrease in electrical activity of approximately 40% of

the neuronal units in the proximal segment of a reconstructed peripheral nerve after a transection and reconstruction. Because the decrease is not found in the crushed nerves, it cannot be due to a decrease of input from the regenerating sensory axons.

Furthermore, Friede and Bischhausen,<sup>5</sup> Ramon y Cajal,<sup>21</sup> and Stroebe<sup>24</sup> noticed a great number of so-called “sterile axons” in the proximal segment of a transected and reconstructed peripheral nerve between 1 and 28 days of regeneration time. These sterile axons do not form functional growth cones and are therefore unable to regenerate. They become varicose, and the axonoplasm contains many vacuoles. It might be that these axons also do not transport HRP and may have lost their signal-conducting capability. These results support our conclusion that a great number of functional neuronal units lose their signalconducting capability while remaining histologically viable.<sup>14</sup> Such a loss of functional neuronal units could explain the lack of recovery of the signal amplitudes in the proximal segment after 8 weeks of regeneration time, as found in the present experiment. At about this time, an increasing number of neuronal units start to lose their signal-conducting capability<sup>16</sup> for instance, due to a lack of target organs produced neurotrophic factor transported to the nerve cell body. A decrease in signal amplitude would be caused by this. But, at the same time, other regenerating axons reach their target organs and will contribute to functional recovery. Due to subsequent maturation, their axon diameter will increase, which in turn will result in an increase in their signal amplitude (and CV 1st peak). The decrease of signal amplitude due to the loss of functional neuronal units will thus be compensated by the gain in signal amplitude due to axon maturation.

In conclusion, the loss of signal amplitude measured from the proximal segment of a nerve shortly after transection and reconstruction is related to the decrease in the CV 1st peak. These two phenomena are both caused by a decrease in axon diameter, which is due to axon regeneration. The CV 1st peak will regain normal values after the regenerating neuronal units have reached their target organs and start to mature. The persisting low NCAC amplitude after more than 12 weeks of regeneration time, while the CV 1st peak has normalized, may be explained by a significant number of functional neuronal units losing their signal-conducting capabilities. This may be due to lack of target organ-produced neurotrophic factors transported to the nerve cell bodies. If such a loss of the conductivity could be reversed, the number of functional neuronal units regenerating across the lesion into the distal segment may also increase. Because theoretically the number of functional neuronal units that grow into the distal segment relates to functional recovery,<sup>11,12,25</sup> an increase in the number of functional units in the proximal segment may well be of clinical importance.

#### Acknowledgements

The authors thank R. Hawkins for preparing the histological sections, the technicians of the Animal Experimental Center of the Erasmus University Rotterdam for

taking care of the operated animals, L.J. v Briemen for his technical support, and Dr. K. Mechelse for his advice. This work was funded by the departments of Plastic & Reconstructive Surgery, Neurology and Anatomy of the Erasmus University Rotterdam.

## References

1. Boyd I.A., Kalu K.U. Scaling factor relating conduction velocity and diameter for myelinated afferent nerve fibres in the cat hind limb. *J Physiol* 1978;289:277-297.
2. Cragg B.G., Thomas P.K. Changes in conduction velocity and fibre size proximal to peripheral nerve lesions. *J Physiol* 1961; 157:559-573.
3. Davis L.A., Gordon T., Hoffer J.A., Jhamandas J., Stein R.B. Compound action potentials recorded from mammalian peripheral nerves following ligation or resuturing. *J Physiol* 1978; 285:543-559.
4. Fawcett J.W., Keynes R.J. Peripheral nerve regeneration. *Ann Rev Neurosci* 1990;13:43-60.
5. Friede R.L., Bischhausen R. The fine structure of stump of transected nerve fibers in subserial sections. *J Neurol Sci* 1980;44:181-203.
6. Gielen F.L., Friedman R.N., Wikswo J.P.J. In vivo magnetic and electric recordings from nerve bundles and single motor units in mammalian skeletal muscle. Correlations with muscle force. *J Gen Physiol* 1991;98:1043-1061.
7. Gielen F.L., Roth B.R., Wikswo J.P.J. Capabilities of a toroid amplifier system for magnetic measurement of current in biological tissue. *IEEE Trans Biomed Eng* 1986;BME-33:910-921.
8. Gillespie M.J., Stein R.B. The relationship between axon diameter, myelin thickness and conduction velocity during atrophy of mammalian peripheral nerves. *Brain Res* 1983;259:41-56.
9. Hoffman P.N., Lasek R.J. Axonal transport of the cytoskeleton in regenerating motor neurons: constancy and change. *Brain Res* 1980;202:317-333.
10. Horch K.W., Lisney S.J. On the number and nature of regenerating myelinated axons after lesions of cutaneous nerves in the cat. *J Physiol* 1981;313:275-286.
11. Johansson R.S., Vallbo A.B. Spatial properties of the population of mechanoreceptive units in the glabrous skin of the human hand. *Brain Res* 1980;184:353-366.
12. Johansson R.S., Vallbo A.B., Westling G. Thresholds of mechanosensitive afferents in the human hand as measured with von Frey hairs. *Brain Res* 1980;184:343-351.
13. Kuypers P.D., Egeraat v J.M., Dudok v Heel M., Briemen van L., Godschalk M., Hovius S.E. A magnetic evaluation of peripheral nerve regeneration: I. The discrepancy between magnetic and histologic data from the proximal segment. *Muscle Nerve* 1998;21:739-749.
14. Kuypers P.D., Egeraat van J.M., Briemen van L., Godschalk M., Hovius S.E. A magnetic evaluation of peripheral nerve regeneration: II. The signal amplitude in the distal segment in relation to functional recovery. *Muscle Nerve* 1998;21: 750-755.
15. Kuypers P.D., Gielen F.L., Wai R.T., Hovius S.E., Godschalk M., van Egeraat J.M. A comparison of electric and magnetic compound action signals as quantitative assays of peripheral nerve regeneration. *Muscle Nerve* 1993;16:634-641.
16. Kuypers P.D., van Egeraat J.M., Godschalk M., Hovius S.E. Loss of viable neuronal units in the proximal stump as possible cause for poor function recovery following nerve reconstructions. *Exp Neurol* 1995;132:77-81.

17. Lundborg G. Ischemic nerv injury: experimental studies on microvascular pathophysiology and nerve function in a limb subject to temporary circulation arrest. *Scand J Plast Reconstruct Surg Suppl* 1970;6:3-113.
18. Peyronnard JM, Charron L. Decreased horseradish peroxidase labeling in deafferented spinal motoneurons of the rat. *Brain Res* 1983;275:203-214.
19. Peyronnard JM, Charron L, Lavoie J, Messier JP. Differences in horseradish peroxidase labeling of sensory, motor and sympathetic neurons following chronic axotomy of the rat sural nerve. *Brain Res* 1986;364:137-150.
20. Peyronnard JM, Charron L, Lavoie J, Messier JP, Bergouignan FX. A comparative study of the effects of chronic axotomy, crush lesion and re-anastomosis of the rat sural nerve on horseradish-peroxidase labelling of primary sensory neurons. *Brain Res* 1988;443:295-309.
21. Ramon y Cajal S. Degeneration and regeneration of the nervous system. New York: Oxford University Press; 1991.
22. Shawe G. On the numbers of branches formed by regenerating nerve fibres. *Br J Surg* 1954;42:474-488.
23. Stein RB, Nichols TR, Jhamandas J, Davis LA, Charles D. Stable long-term recordings from cat peripheral nerves. *Brain Res* 1977;128:21-38.
24. Stroebe: Experimentelle untersuchungen uber degeneration und regeneration peripherer nerven nach verletzungen. *Beitrage zur pathol.Anat.und zur allgem.Pathol von E.Ziegler* 1893; Bd 13.
25. Vallbo AB, Johansson RS. Properties of cutaneous mechanoreceptors in the human hand related to touch sensation. *Hum Neurobiol* 1984;3:3-14.
26. van der Wey LP, Polder TW, Merks MH, Stegeman DF, Vingerhoets DH, Gabreels-Festen AA, Spauwen PH, Gabreels FJ. Peripheral nerve elongation by laser Doppler flowmetry controlled expansion: functional and neurophysiological aspects. *J Neurol Sci* 1994;124:149-155.
27. Wijesinghe RS, Gielen FL, Wikswow JPJ. A model for compound action potentials and currents in a nerve bundle. III: A comparison of the conduction velocity distributions calculated from compound action currents and potentials. *Ann Biomed Eng* 1991;19:97-121.
28. Wijesinghe RS, Wikswow JPJ. A model for compound action potentials and currents in a nerve bundle. II: A sensitivity analysis of model parameters for the forward and inverse calculations. *Ann Biomed Eng* 1991;19:73-96.
29. Wikswow JPJ, Barach JP, Freeman JA. Magnetic field of a nerve impulse: first measurements. *Science* 1980;208:53-55.
30. Wikswow JPJ, van Egeraat JM. Cellular magnetic fields: fundamental and applied measurements on nerve axons, peripheral nerve bundles, and skeletal muscle. *J Clin Neurophysiol* 1991;8:170-188.
31. Woosley JK, Roth BJ, Wikswow JPJ. The magnetic field of a single axon: a volume conductor model. *Math Biosci* 1985; 76:1-36.
32. Ygge J. Neuronal loss in lumbar dorsal root ganglia after proximal compared to

distal sciatic nerve resection: a quantitative study in the rat. *Brain Res* 1989;478:193-195.



# Chapter 3

## **Nerve Compound Action Current (NCAC) Measurements and Morphometric Analysis in the Proximal Stump after Nerve Transection and Repair in a Rabbit Model**

*(J. Peripheral Nervous System 2003;8:108-115)*

Erik T. Walbeehm  
Michiel Dudok van Heel  
Paul D.L. Kuypers  
Giorgio Terenghi  
Steven E.R. Hovius

Part of these results were presented as a poster at the Peripheral Nerve Society Meeting, 21 - 24 July 1999, University of California, San Diego, USA

## Abstract

In the evaluation of nerve regeneration using Magneto-Neurography (MNG), the proximal segment showed a reproducible decrease in peak-peak amplitude of the Nerve Compound Action Currents (NCAC) of 60%. In order to explain these changes, morphometry of myelinated axons in the proximal segment is compared to the MNG signals. A standardised nerve transection and reconstruction was performed in rabbits. NCACs were measured approximately 5 cm proximal to the lesion from operated and control nerves after 12 weeks. Histological samples were taken from the same area of the nerve where the NCACs were obtained.

Results showed a decrease of the peak-peak amplitude of the NCAC of 57% compared to the control. Conduction Velocity decreased 15% (not significant). Morphometry elicited a decrease in larger (10 - 15  $\mu\text{m}$ ) axons ( $284 \pm 134$  versus  $82 \pm 55$ ) and an increase in smaller (2-5  $\mu\text{m}$ ) axons ( $1445 \pm 360$  versus  $1921 \pm 393$ ). A strong correlation existed between the decrease in amplitude and the decrease in larger axons ( $p=0.85$ ).

Peak-peak amplitude varies approximately with the square of the diameter axon. Therefore, because peak-peak amplitude is mainly dependent on the larger diameter axons, the decrease in peak-peak amplitude of the NCACs may be explained by a decrease in numbers of 10 - 15  $\mu\text{m}$  axons.

## Introduction

Magnetic Neurography (MNG) is a technique used to evaluate currents in single axons as well as in nerves during physiological and regenerative processes. It is based on the recording of intra-axonal currents producing nerve compound action currents (NCACs) by means of induction in two magnetic sensor coils (toroids). This technique was developed by Wikswo and co-workers<sup>24–29</sup>, and adapted by Kuypers and van Egeraat<sup>14–18</sup> for use in an animal experimental model of regeneration using the common peroneal nerve in rabbits.

The main advantage of MNG over more conventional electro-neurography (ENG) is the addition of a calibration signal with each measurement, which enables more accurate quantification. Furthermore, MNG is less influenced by the conductive properties of the surrounding tissues, increasing its reproducibility<sup>21–23</sup>.

MNG has been evaluated in healthy frog sciatic nerve<sup>21–23</sup>. Furthermore it has been correlated to functional recovery<sup>18</sup> and to histological and morphometric data after nerve transection and reconstruction in a rabbit model<sup>15,17</sup>. A striking feature when using MNG to evaluate nerve regeneration after transection and microsurgical reconstruction of the common peroneal in rabbits, was a consistent decrease of 50–60% in peak-peak amplitude in the stump proximal to the lesion, compared to the healthy contralateral control nerve.

Changes in conduction velocity (CV) were also present during the first 8 weeks post-operatively, but returned to normal after 12 weeks. This led to the conclusion that the 60% decrease in Peak-peak amplitude involved an approximate 50% decrease in number of functional fibres<sup>14–18</sup>.

Supporting this idea, a 40–50% decrease in compound action potential, as opposed to current, was described in separate studies using electro-neurography (ENG)<sup>2</sup>. Histological changes in the proximal stump after crush- and transection and reconstruction experiments consisted of a decrease in axon- and fibre diameter, with a more marked decrease of the former in both crush and neurotomy experiments. Also, changes in myelin sheath thickness have been reported<sup>1,4,6,12</sup>.

Correlations between electrophysiological evaluations and morphometrical data have been the subject of previous studies with different degrees of success<sup>13</sup>. It has been demonstrated that Single Fibre Action Current (SFAC) is, amongst other factors, related to axon and fibre diameter<sup>19,21–23</sup>.

Therefore, because of its reproducibility and the relation between the SFAC and axon diameter, a strong correlation between the NCACs and morphometric characteristics can be expected. Consequently, accurate quantification of functional nerve fibres in regenerating nerves by MNG should be possible. The aim of our study was to investigate the morphological changes in the proximal segment in a reconstructed nerve and to correlate these with MNG responses in the regenerating nerve.

## Materials and Methods

Five New Zealand White rabbits (2.5-3.0 kg) were anaesthetised (Hypnorm, 0.8ml IM for induction, Ethrane, 3% maximally, as anaesthetic). Fentanyl IV as pre-medication and analgesic; 0.5ml before operation, and 0.8ml before nerve transection, no muscle relaxants). A 3 or 3.5mm tube was used for ventilation.

A standardised microsurgical transection of the left common peroneal nerve was performed, approximately 1.5 cm proximal to where the nerve passes underneath the tibialis anterior muscle. The ventral surface of the nerve was marked with two 11-0 epineurial sutures and the nerve transected. For reconstruction two epineurial 10/0 nylon microsutures and two drops of Human Fibrin glue, on the dorsal- and ventral surface, were used. All procedures were performed by the same surgeon. The operated limbs were not immobilised and no antibiotics were given. Nerves were left to regenerate for 12 weeks.

## Toe-Spread Reflex (TSR)

After a regeneration time of 12 weeks the Toe-Spread-Reflex (TSR) test was performed, prior to the anaesthesia for the evaluation. The rabbit (held by the skin of its neck) was dropped over a distance of 40 cm. Reflexively, the rabbit spreads its toes and dorsiflexes its foot. The response was graded 0 to ++, with 0 for no response and ++ for a normal TSR response.

Magnetic Neurography (MNG)-measurements (modified from Kuypers et al <sup>14,16</sup>) After 12 weeks regeneration, the animals were anaesthetized (as above) the nerve was approached through an extended incision via the intramuscular septum between the biceps femoris- and vastus lateralis muscles. It was mobilised from the knee to the lumbar plexus, and transected as far proximally as possible. A bipolar stimulator was adjusted around the transected nerve 8-10 mm proximal to the regenerated lesion site. The nerve was guided through two toroidal sensor coils consisting of a ferrite core surrounded by an insulated copper wire (50  $\mu$ m diameter) with a known number of windings.

The moving NCAC passes through the sensors inducing a current, which is then boosted by a magnetic amplifier (see fig. 3.1 & 3.2). Stimulation was performed using a 50  $\mu$ sec, rectangular, monophasic pulse. Supramaximal stimulation was used in order to be certain that all fibres would be stimulated.

During the recording procedure the nerve was kept submerged in a continuously flushing normal saline bath (0.9% NaCl), created by retracted muscle- and skinflaps, actively kept at 36 oC ( $\pm$  0.5 oC). The signals were averaged 1024 times to improve the signal-noise ratio. This entire procedure was repeated on the right side, the unoperated nerve served as control value. All procedures were conducted according to the regulations of the Animal Experimental Committee.

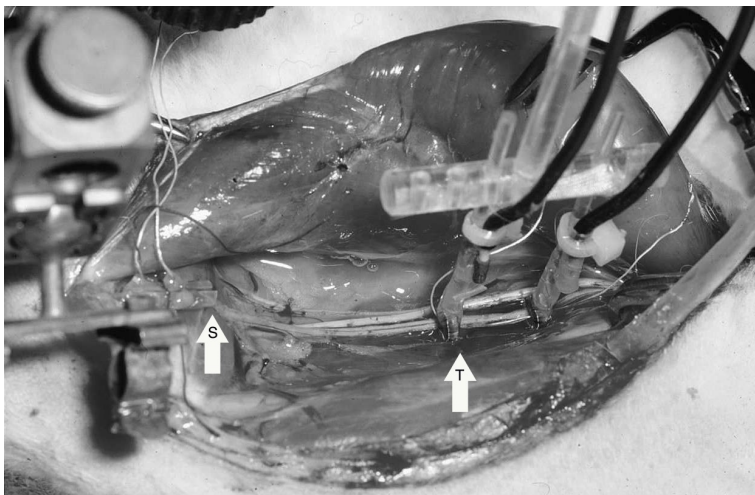


Figure 3.1: A picture of the MNG setup as used in the rabbit. *t*) are the toroidal sensors, near the sciatic notch (near the femoral head), *s*) is the stimulator overlying the peroneal muscle group. The peroneal nerve is dissected from the sciatic nerve, and guided through both sensors.

**Signal evaluation** All data were recorded in D-scope, a custom written acquisition programme. All signals were then further corrected, using the  $1\mu\text{A}$  calibration signal which was sent before every stimulus, using Datacorr. Subsequently, every signal was compared to the calibration signal to measure the parameters.

The final signal is an average of 1024 measurements (consisting of four batches of 256 measurements). NCAC peak-peak amplitudes were calculated, using Datacorr, from the maximum of the first peak to the minimum of the second peak. Onset latencies were calculated from the intersection between a linear fit through the baseline and a linear fit through the slope of the first peak. Conduction velocity was calculated by dividing the inter-toroidal distance (15 mm) by the difference in time between the onset latencies of the signals of the toroids. Conduction distance between the stimulator and the first toroid was calculated from the conduction velocity, and the peak-peak amplitude was normalised for a conduction distance of 50 mm by using a linear interpolation of both NCAC amplitudes.

**Histology** (modified from Sterne et al <sup>20</sup>) A nerve tissue sample (4-5 mm) was taken between the two toroidal sensors, directly after the MNG measurements. The epineurium was scored to give proper fixation (2.5% Glutaraldehyde in 0.1 M Phosphate buffer, pH 7.4, at 4 °C overnight). After 3 washes with buffer nerve segments

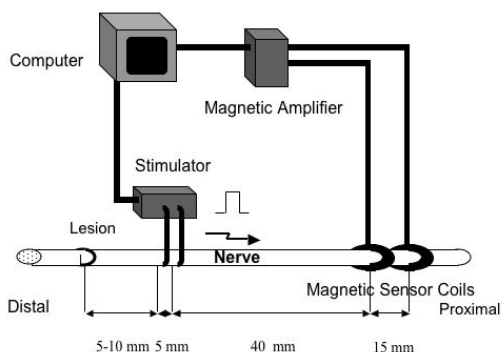


Figure 3.2: A diagrammatic representation of the MNG set-up. The measurements are performed retrogradely i.e. stimulation is done distally and recording of the changes in magnetic field is performed proximally. Also, in this experiment the stimulator is proximal to the lesion.

were post-fixed with 1% osmium tetra-oxide (Agar Scientific, Stansted, UK) in 0.1 M phosphate buffer for 1 hour at room temperature, washed with phosphate buffer and dehydrated serially through increasing concentrations of acetone. Infiltration of the specimen was initially carried out overnight with 1:1 acetone: araldite CY212 resin (Agar Scientific, Stansted, UK), followed by two changes of fresh resin and finally embedded in araldite CY212 resin. The blocks were polymerised at 60 °C for 18 hours. Semithin (1  $\mu\text{m}$ ) transverse sections were cut and stained with thionine blue and acridine orange to enhance myelin contrast. Tissue analysis and all subsequent morphometric assessment were performed on coded sections without knowledge of the source.

Histological Quantification (modified from Sterne et al)<sup>20</sup> Each specimen was assessed by using a computerised image analysis system (Seescan Analytical Services, Cambridge, UK). One section per nerve was assessed. Following automatic background subtraction, image editing and automatic thresholding, the number of myelinated fibres was measured in five fields (x 40 objective) per section. The first field was taken in the centre of the section, and the remaining four were placed around

Table 3.1.MNG results summarised

NCAC	P-P 50 ( $\mu\text{A}$ )	O. Lat. 50 (msec)	NCV OL( m/s)
Prox. Segm.	$0.30 \pm 0.08$	$0.59 \pm 0.05$	$85.1 \pm 6.3$
Controls	$0.68 \pm 0.19$	$0.50 \pm 0.06$	$101.2 \pm 12.3$
% of Control	$42.30\% \pm 9.1\%$	$119\% \pm 20.4\%$	$85\% \pm 14.2\%$
Significance	( $p < 0.01$ )	n.s.	n.s.

Table 3.1: summarises the MNG results. Peak-peak amplitude (P-P) in  $\mu\text{A}$ , onset latency (O.Lat) in msec and the nerve conduction velocity, measured at the onset latency (NCV OL) in m/sec

the centre field, one in each direction, making sure not to let the fields overlap. The mean internal and external areas of each myelinated fibre were automatically measured. The axon- and fibre diameters, myelin thickness and g-ratio were calculated from these data, and the outer perimeter of the nerve section was used to derive the cross-sectional area. Results were subsequently corrected by means of the Total Field Area/Nerve Crosssectional Area ratio. On average 20% of the nerve was analysed.

Software D-scope is a custom written signal-acquisition programme. Datacorr was developed by A. Viddeleer. The results were stored in Excel'97 (Microsoft<sup>®</sup>). Statistical analysis was performed with SPSS v8.0 (SPSS, Inc.).

## Results

MNG results. Peak-peak amplitude significantly decreased  $57.70\% \pm 9.1\%$  ( $p < 0.01$ , paired Student t-test) in the proximal stump of the reconstructed nerve compared to the contralateral control nerve. Onset latency, conduction velocity and the TSR were not statistically significantly changed, though onset latency showed a non-significant trend towards an increase ( $0.50 \pm 0.06$  msec to  $0.59 \pm 0.05$  msec), conduction velocity revealed a trend towards a decrease ( $101.2 \pm 12.3$  m/sec to  $85.1 \pm 6.3$  m/sec) (table 3.1) and TSR exhibited a decrease (table 3.2).

Histology In order to compare MNG results with morphometrical data, the axon diameter classes were arbitrarily subdivided into 2-5  $\mu\text{m}$ , 5-10  $\mu\text{m}$  and 10-15  $\mu\text{m}$  groups. Similarly, fibre (axon + myelin) diameter classes were set at 5-10  $\mu\text{m}$ , 10-15  $\mu\text{m}$  and 15-20  $\mu\text{m}$ , which corresponds roughly with the axon diameter classes based on the assumption that the average g-ratio (axon diameter/fibre diameter) is approximately 0.5<sup>3</sup>.

Table 3.2 Toe-Spread-Reflex (TSR)

Rabbit	Control	Proximal
1	++	+
2	++	+
3	++	++
4	++	++
5	++	+

Table 3.2: shows the toe-spread-reflex results. It is only used as an indication of regeneration. 0 is no reaction, + is an intermediate reaction and ++ is (almost) normal reaction.

**Axon Diameter Distribution.** The average number of large axons in the 10-15  $\mu\text{m}$  group has significantly decreased in the regenerating nerve compared to the uninjured control from  $284 \pm 134$  to  $82 \pm 55$  ( $p=0.02$ , paired Student t-test). Furthermore, the number of axons in the 2-5  $\mu\text{m}$  group has significantly increased in the proximal stump from  $1445 \pm 360$  to  $1921 \pm 393$  ( $p=0.04$ , paired Student t-test) (see fig. 3.3). The maximal measured axon diameter decreased significantly ( $p=0.05$ , paired Student t-test) by 6% from  $12.85 \mu\text{m} \pm 0.60 \mu\text{m}$  to  $12.02 \mu\text{m} \pm 0.65 \mu\text{m}$ .

**Fibre (Axon + Myelin Sheath) Diameter Distribution.** The number of fibres has not decreased significantly in the largest group (15 - 20  $\mu\text{m}$ ), but the changes in fibre diameter distribution seem to follow the axonal diameter distribution; no change in the 10-15  $\mu\text{m}$  group and an increase in numbers in the smaller fibres. Myelin thickness, the overall g-ratio and the total number of fibres are not significantly changed (Paired Student t-test, table 3.3).

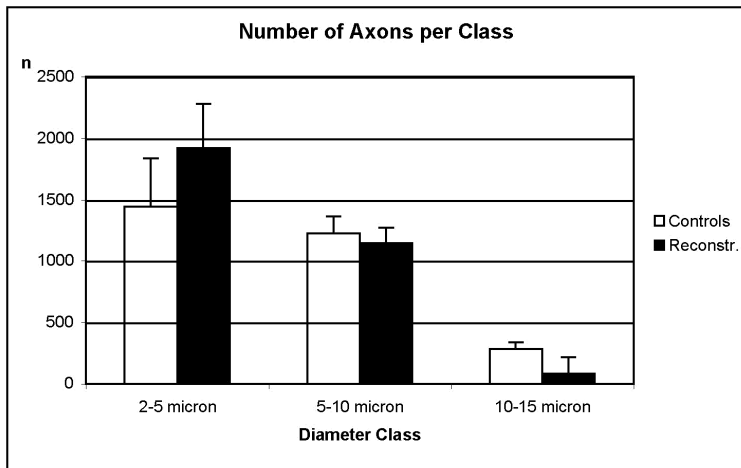


Figure 3.3: The white areas represent the numbers of axons per diameter class of the control nerves, and the black areas the number of axons per diameter class of the regenerated nerves.

Table 3.3 Myelin Thickness, G-ratio and total number of fibres

Myelin Thickness ( $\mu\text{m}$ )	G-ratio		Total Nr of Fibres
	05-10 $\mu\text{m}$	15-20 $\mu\text{m}$	
Class	10-15 $\mu\text{m}$	G-All	
Proximal Stump	$2.01 \pm 0.12$	$3.67 \pm 0.42$	$5296 \pm 1445$
Controls	$1.81 \pm 0.20$	$3.25 \pm 0.37$	$4249 \pm 783$

Table 3.3: summarises the results for myelin thickness per fibre diameter class, overall g-ratio and the total number of fibres in the control nerves and proximal segment, 12 weeks post-reconstruction. No significant changes could be elicited using a paired Student t-test.

**Correlations.** In order to answer the questions of the changes in the proximal stump correlations between morphometrical and electrophysiological data were calculated. Peak-peak amplitude correlated very well with the number of axons in the 10-15  $\mu\text{m}$  group (correlation coefficient=0.85,  $p < 0.01$ ) (see fig 3.3). Also, peak-peak amplitude correlated well with the maximal axonal diameter measured (correlation coefficient = 0.77,  $p < 0.05$ ).

## Discussion

**Magneto-Neurographic Changes in the proximal stump after 12 weeks regeneration**  
MNG measures the changes in the magnetic field around a nerve, caused by moving intra-axonal electric currents, which occur when a signal is conducted through the nerve. These changes are recorded by two toroidal sensor coils.

Peak-peak amplitude measured in the proximal stump, 12 weeks after reconstruction, shows a significant decrease of 57% compared to the contralateral nerve. Conduction velocity and onset latency did not elicit statistically significant changes, but the conduction velocity demonstrated a trend for a decrease (101.2 m/sec vs. 85.1 m/sec) and onset latency showed a consequent trend for an increase (0.50 msec vs. 0.59 msec), after injury. These MNG results are consistent with previous studies. All these studies, using the same experimental model, show this decrease in compound action current amplitude of approximately 60% in the proximal stump at 12 weeks post-reconstruction<sup>14-17</sup>.

Other authors, using similar ENG experiments, found that compound action potential amplitudes, did not reach control values over 150 days after resuturing the nerve but remained at 50-60% of the control. A conclusion in early experiments was that the changes in latency produced further changes in amplitude through the dispersion of impulses from fibres of different diameters and partial cancellation of positive and negative phases by changes in conduction velocity<sup>2</sup>. Later experiments showed that conduction velocity decreases in the first weeks after injury, which is consistent with early amplitude decreases. After longer regeneration periods conduction velocities are reported to return to normal<sup>15-17</sup> or remain slightly lowered<sup>1</sup>.

However, the most important change recorded with MNG, the statistically significant decrease in peak-peak amplitude, remains consistent with previous experiments, implying a role in the regenerative process.

**Histological changes in the proximal segment after 12 weeks regeneration**  
Histological changes in the regenerative process of the proximal stump of a transected and reconstructed nerve have been reported as early as 1943 by Gutman and Sanders<sup>6</sup>. They found a significant decrease of fibre (axon + myelin) diameter, approximately 15 mm proximal to the lesion, as well as a decrease of the average axon diameter. These results had not normalised up to one year of transection and recon-

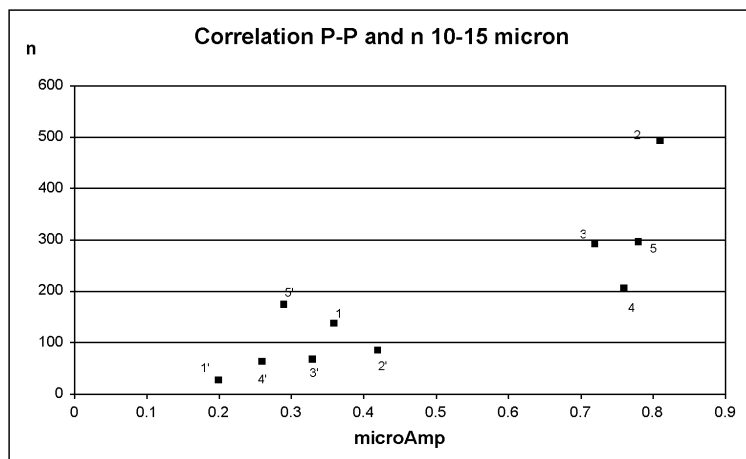


Figure 3.4: Correlation between peak-peak amplitude and number of axons in the larger axon diameter class of the reconstructed and control nerves. Pairs are shown. The accented numbers are the reconstructed nerves. Pair 1-1' is interesting in that it has very low peak-peak amplitude in the control nerve, but this is matched with a very low peak-peak amplitude in the reconstructed nerve, compared to the other animals. Also, it has a lower number of larger axons in the control nerve, consistent with the lower signal.

struction. Similar results have been published subsequently. Up to 1.5 years most authors found a decrease in axon diameter concurring with a smaller decrease in fibre diameter<sup>1,4,12</sup>.

The histological results of our control nerves are consistent with the literature<sup>3</sup>. Also, the results of the injured nerves are similar to the earlier descriptions. In this experiment the most prominent histological changes, at 12 weeks after neurotomy, are the decrease in number of axons in the larger myelinated axon group (10-15  $\mu\text{m}$ ) from  $284 \pm 134$  to  $82 \pm 55$ , and the decrease in diameter of the largest myelinated axon measured per nerve section from  $12.87 \mu\text{m} \pm 0.60 \mu\text{m}$  to  $12.02 \mu\text{m} \pm 0.65 \mu\text{m}$ . The positive TSR provided proof of reinnervation.

An explanation for the decrease in axonal diameter can be found in how this diameter is controlled. Axonal diameter of large myelinated axons depends mainly on the amount of neurofilaments (NF) present in the nerve fibre and the degree of phosphorylation of the filaments. During growth and regeneration the changes in axonal diameter in the proximal stump are dependent on the amount of NF in the axon, although there is no change in density (dependent on the degree of phosphorylation of neurofilaments). After injury, downregulation of NF-gene expres-

sion decreases the synthesis of neurofilaments resulting in loss of axonal diameter. This reduction originates near the cell body and proceeds anterogradely at the rate of slow axonal transport (0.1-30 mm/day). Hence the name somatofugal atrophy<sup>7-11</sup>. The changes in neurofilament content coincided temporally with alterations in axon calibre in regenerating motor fibres. Eight weeks after axotomy the delivery of neurofilament proteins returned to pre-axotomy levels and axon calibre was restored to almost normal. This restoration is probably due to reinnervation and neuron-target cell interactions<sup>5,7-11</sup>.

An explanation for the changes in axonal diameter with lesser significant changes in fibre diameter is provided by Gillespie and Stein<sup>4</sup>. By means of a mathematical model they showed that as the diameter of the axons decreases, the myelin sheath collapses and axon diameter can theoretically decrease to zero while the myelin sheath does not change resulting in a dramatic decrease in axon diameter and a significantly lesser decrease of fibre diameter (see fig 3.2 & 3.3) Summarising, the most prominent morphological changes in the proximal segment of a reconstructed nerve are a decrease in number of larger axons (10-15  $\mu\text{m}$ ) and a decrease in maximal axonal diameter measured per nerve.

**Relation between Histology and Electrophysiology** The amplitude of the action potential and the action current of a single axon are described by complex mathematical equations which are outside the scope of this paper. Simply summarised the amplitude varies approximately with the square of the diameter<sup>22</sup>. The relation becomes progressively complex when studying compound signals. In earlier experiments using MNG the 55% decrease in peak-peak amplitude is compared with a quantification of the number of myelinated fibres present. In these experiments a small but measurable 5-7% decrease in numbers of fibres was found, which was consistent with literature, but quantitative morphometry was not performed<sup>14-18</sup>. Together with the recurrence of conduction velocity to normal values at 20 weeks and return to a normal TSR, it is tempting to speculate that approximately 40% of the fibres were present but not functioning, accounting for the loss of amplitude.

In our experiment, a close correlation was demonstrated between the decrease in peak-peak amplitude and the decrease in number of axons in the 10-15  $\mu\text{m}$  diameter class and between peak-peak amplitude and the largest axonal diameter measured per nerve section (correlation coefficients 0.85 and 0.77 respectively). Since it has been established that larger axons account for larger action currents it seems logical, when comparing the presented morphometric data with the changes measured by MNG after neurotomy as described during this experiment, that the loss of amplitude can also largely be explained by the decrease of diameter of the larger axons and not so much by impairment of excitability of nerve fibres. Also, for a single fibre, the relationship between axonal diameter and conduction velocity is less strong than the relationship between the diameter and amplitude, as amplitude is approximately the square of the diameter<sup>22</sup>. This means for a single fibre,

that a 6% decrease in diameter as measured in this experiment will already cause a subsequent 12% decrease in amplitude. However, data from this experiment cannot exclude the possibility of non-excitabile fibres because those fibres can not be demonstrated by current histological techniques, and therefore, both phenomena might exist simultaneously.

The small decrease in conduction velocity (or increase of onset latency) could not be correlated with the decrease in axonal diameter nor with fibre diameter. It is possible, based on the histological changes described above, that the lack of correlation between peak-peak amplitude and conduction velocity is due to the fact that the regenerative process has already produced a number of larger axons. The onset of the signal depends on the fastest conducting axons, only small numbers of the largest axons are needed to set the signal off. In the unreconstructed, atrophied nerves,<sup>4</sup> such regenerating axons are not present and the conduction velocity decreases with the continuous decrease of axonal diameter. After 12 weeks regeneration in the reconstructed nerve, a small number of axons will have reached their distal target organs, and will have matured to almost normal diameters. They will determine conduction velocity and onset latency rather than the axons that still have decreased diameters.

On conclusion, a histological argument for the decrease in peak-peak amplitude of the NCAC in the proximal stump after nerve transection and reconstruction, appears to be the decrease in number of larger axons (10-15  $\mu\text{m}$ ). Further research is warranted to investigate whether this is an irrevocable reaction to the trauma inflicted by the transection, and if influencing this process has consequences to the quality of the clinical end result.

#### Acknowledgements

The authors are indebted to Ineke Hekking. Also to Enno Collij, Rob Meijer and Henk Dronk for the anaesthesia. To Alain Viddeleer for writing Datacorr. Furthermore to Prof. Robert Brown, Dr. M. Godschalk and Lourens van Briemen for their invaluable comments and the technicians at Blond-McIndoe and the EUR who made histology possible.

Sadly, Michiel Dudok van Heel passed away during the writing of this manuscript. His kind personality and company are missed every day.

## References

1. Cragg B, Thomas P. Changes in conduction velocity and fibre size proximal to nerve lesions. *J Physiol* 1961;157:315-327.
2. Davis L, Gordon T, Hoffer J, Jhamandas J, Stein R. Compound action potentials recorded from mammalian peripheral nerves following ligation or resuturing. *J Physiol (Lond)* 1978;285:543-559.
3. Germana G, Muglia U, Santoro M, Abbate F, Laura R, Gugliotta M, Vita G, Ciriaco E. Morphometric analysis of sciatic nerve and its main branches in the rabbit. *Biol Struct Morphog* 1992;4:11-15.
4. Gillespie M, Stein R. The relationship between axon diameter, myelin thickness and conduction velocity during atrophy of mammalian peripheral nerves. *Brain Res* 1983;259:41-56.
5. Goldstein M, Cooper H, Bruce J, Carden M, Lee V, Schlaepfer W. Phosphorylation of neurofilament proteins and chromatolysis following transection of rat sciatic nerve. *J Neurosci* 1987;7:1586-1594.
6. Gutman E, Sanders F. Recovery of fibre numbers and diameters in the regeneration of peripheral nerves. *J Physiol* 1943;101:489-518.
7. Hoffman P. Distinct roles of neurofilament and tubulin gene expression in axonal growth. *Ciba Found Symp* 1988;138:192-204.
8. Hoffman P, Cleveland D. Neurofilament and tubulin expression recapitulates the developmental program during axonal regeneration: induction of a specific beta-tubulin isotype. *Proc Natl Acad Sci U S A* 1988;85:4530-4533.
9. Hoffman P, Cleveland D, Griffin J, Landes P, Cowan N, Price D. Neurofilament gene expression: a major determinant of axonal caliber. *Proc Natl Acad Sci U S A* 1987;84:3472-3476.
10. Hoffman P, Griffin J, Gold B, Price D. Slowing of neurofilament transport and the radial growth of developing nerve fibers. *J Neurosci* 1985;5:2920-2929.
11. Hoffman P, Thompson G, Griffin J, Price D. Changes in neurofilament transport coincide temporally with alterations in the caliber of axons in regenerating motor fibers. *J Cell Biol* 1985;101:1332-1340.
12. Horch K, Lisney S. On the number and nature of regenerating myelinated axons after lesions of cutaneous nerves in the cat. *J Physiol (Lond)* 1981;313:275-286.
13. Kanaya F, Firrell J, Breidenbach W. Sciatic function index, nerve conduction tests, muscle contraction, and axon morphometry as indicators of regeneration. *Plast Reconstr Surg* 1996;98:1264-1271, discussion 1272-1264.
14. Kuypers PD, Gielen FL, Wai RT, Hovius SE, Godschalk M, van Egeraat JM. A comparison of electric and magnetic compound action signals as quantitative assays of peripheral nerve regeneration. *Muscle Nerve* 1993;16:634-641.
15. Kuypers PD, van Egeraat JM, Dudok v Heel M, van Briemen LJ, Godschalk M, Hovius SE. A magnetic evaluation of peripheral nerve regeneration: I. The discrepancy between magnetic and histologic data from the proximal segment. *Muscle Nerve* 1998;21:739-749.

16. Kuypers PD, van Egeraat JM, Godschalk M, Hovius SE. Loss of viable neuronal units in the proximal stump as possible cause for poor function recovery following nerve reconstructions. *Exp Neurol* 1995;132:77-81.
17. Kuypers PD, van Egeraat JM, van Briemen LJ, Godschalk M, Hovius SE. A magnetic evaluation of peripheral nerve regeneration: II. The signal amplitude in the distal segment in relation to functional recovery. *Muscle Nerve* 1998;21:750-755.
18. Kuypers PD, Walbeehm ET, Heel MD, Godschalk M, Hovius SE. Changes in the compound action current amplitudes in relation to the conduction velocity and functional recovery in the reconstructed peripheral nerve. *Muscle Nerve* 1999;22:1087-1093.
19. Roth B, Wikswo JP J. The magnetic field of a single axon. A comparison of theory and experiment. *Biophys J* 1985;48:93-109.
20. Sterne G, Brown R, Green C, Terenghi G. Neurotrophin-3 delivered locally via fibronectin mats enhances peripheral nerve regeneration. *Eur J Neurosci* 1997;9:1388-1396.
21. Wijesinghe R, Gielen F, Wikswo JP J. A model for compound action potentials and currents in a nerve bundle. I: The forward calculation. *Ann Biomed Eng* 1991;19:43-72.
22. Wijesinghe R, Gielen F, Wikswo JP J. A model for compound action potentials and currents in a nerve bundle. III: A comparison of the conduction velocity distributions calculated from compound action currents and potentials. *Ann Biomed Eng* 1991;19:97-121.
23. Wijesinghe R, Wikswo JP J. A model for compound action potentials and currents in a nerve bundle. II: A sensitivity analysis of model parameters for the forward and inverse calculations [published erratum appears in *Ann Biomed Eng* 1991;19(3):339]. *Ann Biomed Eng* 1991;19:73-96.
24. Wikswo J, Barach J. An estimate of the steady magnetic field strength required to influence nerve conduction. *IEEE Trans Biomed Eng* 1980;27:722-723.
25. Wikswo J, Barach J, Freeman J. Magnetic field of a nerve impulse: first measurements. *Science* 1980;208:53-55.
26. Wikswo JP J. Improved instrumentation for measuring the magnetic field of cellular action currents. *Rev Sci Instrum* 1982;53:1846-1850.
27. Wikswo JP J, Roth B. Magnetic determination of the spatial extent of a single cortical current source: a theoretical analysis. *Electroencephalogr Clin Neurophysiol* 1988;69:266-276.
28. Wikswo JP J, Samson P, Giffard R. A low-noise low input impedance amplifier for magnetic measurements of nerve action currents. *IEEE Trans Biomed Eng* 1983;30:215-221.
29. Wikswo JP J, van Egeraat J. Cellular magnetic fields: fundamental and applied measurements on nerve axons, peripheral nerve bundles, and skeletal muscle. *J Clin Neurophysiol* 1991;8:170-188.

# Chapter 4

## **Magnetoneurographic Evaluation of the Proximal Segment after Different Types of Repair**

*(Submitted to Muscle and Nerve)*

Erik T. Walbeehm  
Joleen H. Blok  
B. Stefan de Kool  
Johan W. van Neck  
Steven E.R. Hovius

Part of these results have been presented at the VIth Congress of the European Federation of Societies for Surgery of the Hand, 21 - 24 June 2000, Barcelona, Spain.

## Abstract

The role of the proximal segment following nerve repair is still unclear. Therefore, the electrophysiological properties of the proximal segment of the nerve following different types of reconstruction after transection were evaluated. The types of reconstruction were: immediate reconstruction using microsutures, 24 hour delayed reconstruction using microsutures, 14 days delayed reconstruction using microsutures, immediate reconstruction using fibrin glue and immediate reconstruction using fibrin glue and 2 microsutures were evaluated. One group was transected and not reconstructed. The electrophysiological properties were evaluated by magnetoneurography (MNG). The reconstruction after 24 hours did statistically significantly better than the immediate reconstruction and the other groups for peak-peak amplitude ( $43.01\% \pm 8.8\%$  vs  $36.33\% \pm 6.4\%$ ,  $p < 0.05$ ) in the proximal segment, compared to the contralateral control. The onset latency and conduction velocity did not reach a statistically significant difference. Peak-peak amplitude in the non-reconstruction group was significantly lower than the immediate reconstruction ( $24.65\% \pm 7.9\%$  vs  $36.33\% \pm 6.4\%$ ,  $p < 0.001$ )

On conclusion, it is possible to modify the changes in the proximal segment by the repair. However, it appears that timing is more important than the type of repair used. Delaying a repair for 24 hrs is beneficial for the electrophysiological properties of the proximal stump.

## Introduction

Changes in the proximal nerve segment following nerve injury have been described<sup>18</sup>, but it remains unclear what the influence of the proximal segment is in peripheral nerve regeneration. Histological changes described in the proximal stump after crush- or transection and reconstruction experiments, consisted of a decrease in axon- and fibre diameter in both types of injury. Additionally, changes in myelin sheath thickness, as well as a 5-7% decrease in numbers of axons have been reported after transection and reconstruction.<sup>1,3,5,6</sup>

Compound action potential amplitudes, measured using electroneurography (ENG), did decrease to 50-60% of the control nerves, and did not reach control values at 150 days after injury. Conduction velocity (CV) decreased in the first weeks after injury, but returned to normal<sup>8,9,11</sup> or remains around 80% of the contralateral nerve, after longer regeneration periods<sup>1</sup>.

Using MNG to study the effect of a crush injury, only a 30% decrease in peak-peak amplitude was demonstrated in the proximal segment (See Chapter 5). Experiments using magnetoneurography (MNG) to evaluate peripheral nerve regeneration in a transection and reconstruction model of the common peroneal nerve in rabbits, have shown a very consistent decrease in peak-peak amplitude 55-65% in the proximal stump following injury<sup>7-9,11,12</sup>. We demonstrated in an histological study that this decrease correlated well to a decrease in number of axons larger than 10 $\mu$ m.<sup>19</sup>

Studies evaluating the influence of different types of repair after nerve transection, i.e. direct suture, cable - and muscle graft, on the number and distribution of motorneurons in the rat spinal cord and of muscle afferents in the rat dorsal root ganglion found no significant differences<sup>4,14</sup>. Gilmour et al<sup>4</sup> demonstrated that survival of motorneurons was influenced by the type of injury. A crush injury showed a lesser degree of cell loss than a transection and reconstruction. Furthermore, in a transection and reconstruction model, a primary nerve repair did better than a nerve graft. Most interestingly, a difference could be demonstrated between a nerve graft and a muscle graft, bridging the same gap.

The aim of this study is to investigate whether the method of repair, i.e. direct repair using microsutures or fibrin glue versus delayed repair using microsutures, which are the most common repair techniques used at this moment, influences electrophysiological parameters of the proximal segment.

## Methods and Materials

71 New Zealand White rabbits, weighing between 2500 and 3000 grams received general anaesthesia (Hypnorm, 0.8ml IM for induction, Ethrane, 3% maximally, as anaesthetic). Fentanyl IV was used as analgesic, 0.5ml before operation, and 0.8ml before transection of the nerve. A 3 or 3.5mm tube was used for ventilation. No muscle relaxants were given. A standardised, microsurgical transection of the left common peroneal nerve was performed, approximately 1,5 cm proximal from were

the nerve passes underneath the tibialis anterior muscle. The nerve was partially mobilised but the vascular pedicle arising from the popliteal artery was left intact. The ventral surface of the nerve was marked with two 11-0 epineurial sutures, in order to obtain correct coaptation. The nerve was transected with a pair of straight microscissors and reconstructed in the following ways:

- Group a, immediate reconstruction group (n= 13 animals): immediate reconstruction using 4-6 epineurial 10/0 microsutures,
- Group b, 24 hour delay group (n= 12 animals): 24 hour delayed reconstruction using 4-6 epineurial 10/0 microsutures,
- Group c, 14 day delay group (n= 10 animals): 14 days delayed reconstruction using 4-6 epineurial 10/0 microsutures,
- Group d, fibrin glue group, NS (n= 16 animals): immediate reconstruction using a fibrin glue sleeve,
- Group e fibrin glue group, S (n= 8 animals): immediate reconstruction using 2 epineurial 10/0 microsutures and a fibrin glue sleeve,
- Group f, no reconstruction group (n= 12 animals): no reconstruction, serving as negative control group.

The operated limbs were not immobilised postoperatively, nor was there need for antibiotics. All surgical procedures were performed, by the same surgeon under sterile conditions and with the aid of an operating microscope. After reconstruction, the nerves were left to regenerate for 12 weeks following which the animals were re-operated and the nerves evaluated by MNG.

**Toe-Spread Reflex (TSR)** After a regeneration time of 12 weeks the Toe-Spread-Reflex (TSR) test was performed, prior to the anaesthesia for the evaluation. The rabbit (held by the skin of its neck) was dropped over a distance of 40 cm. Reflexively, the rabbit spreads its toes and dorsiflexes its foot. The response was graded 0 to ++, with 0 for no response, ++ for a normal TSR response and + for every response in between.

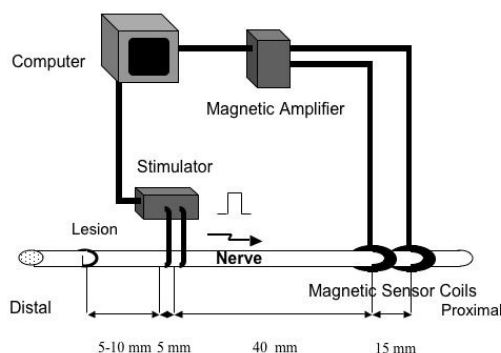


Figure 4.1: *Proximal measurement set-up. Stimulation is performed 10 mm proximal to the lesion. Recording at 40 and 55 mm proximal to the stimulator.*

Magnetoneurography-measurements (as described from Kuypers et al, Walbeehm et al<sup>9,19</sup>) All MNG-measurements were performed as described in earlier reports<sup>7-9,11,12</sup>. The rabbits received a general anaesthetic after which the common peroneal nerve was mobilised from the lumbar plexus to where it passes underneath the peroneus longus muscle and then threaded through the two magnetic sensors. The stimulator was adjusted and the sensors were placed 4 cm proximal to the sensor. The nerve was stimulated with a  $50 \mu\text{s}$  rectangular pulse and the changes in magnetic field were recorded (see fig. 4.1). During the entire procedure, the nerve was kept submerged in normal saline at  $36^\circ\text{C} \pm 0.5^\circ\text{C}$ . The same procedure was performed on the contralateral control nerve. All procedures were conducted according to the rules and regulations of the Animal Experimental Committee of the Erasmus University Rotterdam.

**Signal evaluation** All data were recorded in a custom written data acquisition programme (written in VBA, Microsoft, USA). Signals were then calibrated, by means of the  $1\mu\text{A}$  calibration signal that was recorded prior to every stimulus. The final signal is an average of 1024 measurements (consisting of 4 batches of 256 measurements). Further analyses were performed using MatLab<sup>®</sup> (The MathWorks, Inc. Natick, Mass. USA)

First, the baseline drift in a 1.6 ms window containing the MNG response was estimated using a piecewise cubic Hermite interpolation, based on the signal samples immediately preceding and following this window. After correction for this drift, the nerve compound action current (NCAC) peak-peak amplitude could be determined as the difference between NCAC maximum and minimum. The CV was estimated by cross-correlating the signal of the second toroidal sensor coil with that of the first. If the maximum value of the cross-correlation function exceeded 0.75, the signals were assumed to be sufficiently similar to allow reliable CV calculation. The position of the maximum was used as indication of the time shift  $\Delta t$  between the two signals. The CV was then calculated as  $\Delta x/\Delta t$ , with  $\Delta x$  the intertoroidal distance of 15mm. Finally, the area below the signal was determined between the signal onset latency (determined semi-automatically) and the end of the second phase of the MNG signal (as marked by the first zero-crossing of the signal after its minimum). The results were stored and statistically analysed in Excel X<sup>®</sup> (Microsoft Corp, Redmond, Wash., USA). Unless otherwise indicated, a two-sample Student t-test was used to test for significance (*p* values) of intergroup differences.

## Results

At 12 weeks regeneration the rabbits showed no signs of infection or contractures in the operated limbs. Two animals from group d, fibrin glue group, NS demonstrated autophagy of the operated limbs and were excluded from the study. The TSR showed a ++ for all control limbs, a + for all reconstructed limbs and 0 for all animals in Group f, no reconstruction group.

**NCAC amplitude** As expected, a statistically significant decrease in peak-peak amplitude between the reconstructed and control nerves was observed (Average Proximal/Control ratio  $36.95\% \pm 15.9\%$ ,  $n=71$ ). When comparing the different types of reconstruction, a statistically significant difference can be demonstrated between the signal amplitude after standard acute transection and reconstruction (Group a, immediate reconstruction group) compared to the reconstruction after 24 hours (Group b, 24 hour delay group) ( $36.33\% \pm 6.4\%$  vs  $43.01\% \pm 8.8$ ,  $p < 0.05$ ).

Furthermore, the group that was not reconstructed (Group f, no reconstruction group) showed a significantly lower peak-peak amplitude than the acute standard transection and reconstruction (Group a, immediate reconstruction group) ( $24.65\% \pm 7.9\%$  vs  $36.33\% \pm 6.4\%$ ,  $p < 0.001$ ). The amplitude in the reconstruction at 14 days (Group c, 14 day delay group) increased compared to the standard transection and reconstruction (Group a, immediate reconstruction group), but this trend did not reach statistical significance. There was no significant difference between the acute standard transection and reconstruction (Group a, immediate reconstruction group) and both fibrin glue groups (with or without microsutures, Groups d and e) (see fig 4.2, table 4.1).

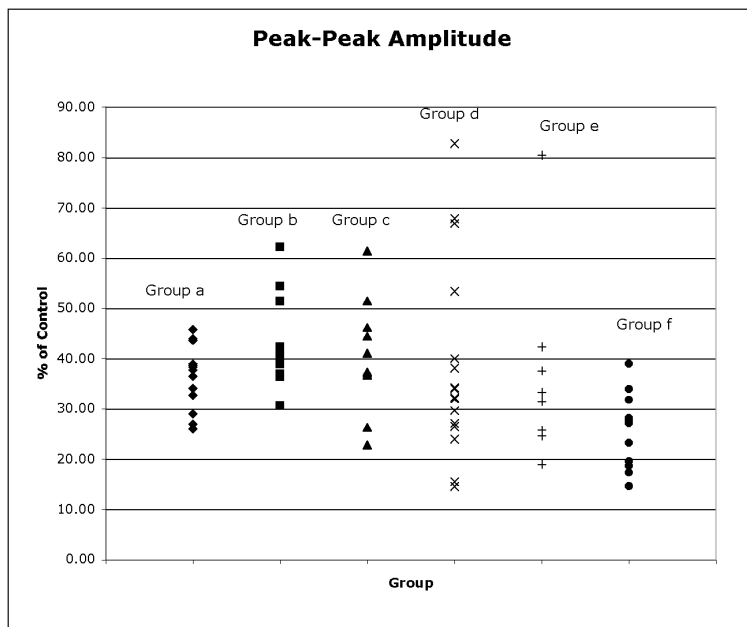


Figure 4.2: Graphic representation of the distribution of the different groups.

Conduction Velocity and Onset Latency Table 4.2 shows a statistically significant decrease in CV after reconstruction from 99.02 m/s to 81.76 m/s (t-student,  $p < 0.001$ ). The onset latency of the control nerves and the reconstructed nerves ( $0.35 \mu\text{s}$  vs  $0.38 \mu\text{s}$ , t-student,  $p < 0.02$ ) has changed accordingly. Again no statistically significant changes can be found between the different reconstructions with regards to the conduction velocities as well as the onset latencies.

	Group a	Group b	Group c	Group d	Group e	Group f
P-P Amp.(%)	36.33%	43.0%	40.4%	38.6%	36.7%	24.6%
SD	6.4	8.8	11.3	19.4	19.2	7.9

Table 4.1: TABLE 4.1The average peak-peak amplitudes and their standard deviation. Values are measured as the percentage of the contralateral control nerve.

	Group a	Group b	Group c	Group d	Group e	Group f
Average CV %	0.84	0.84	0.85	0.76	0.76	0.77
SD	0.08	0.12	0.16	0.18	0.12	0.10
Average OL %	1.09	1.26	0.92	1.07	1.27	1.22
SD	0.21	0.66	0.33	0.54	0.77	0.31

Table 4.2: *Conduction velocities (CV) and onset latencies OL for the different groups, presented as percentages of the contralateral control*

## Discussion

Following injury to a peripheral nerve, the proximal nerve segment demonstrated significant morphological and electrophysiological changes, as have been described in earlier reports<sup>7-10,12</sup>. For both MNG as well as ENG an average decrease of amplitude of approximately 55-65% of the control nerves was found in the proximal segment at 12 weeks. In the unreconstructed nerve the amplitude in the proximal segment reached similar values at 12 weeks stabilizing at 25% of the control nerves, at longer regeneration times<sup>1,2,6</sup>. A decrease in larger diameter axons appears to be the cause for the decrease in peak-peak amplitude, because the amplitude of a single fibre action current varies with the square of the diameter<sup>16,17</sup>. Conduction velocity changes proportionally with fiber diameter, and with the square root of amplitude<sup>3</sup>. Therefore comparatively small changes in conduction velocity are observed in this and other studies<sup>8,9,12,19</sup>. Using MNG, we demonstrated a strong correlation between the reduction in peak-peak amplitude in the proximal segment and a histological decrease in larger myelinated axons<sup>19</sup>.

The acute repairs (Groups a, d and e) in our experiments all showed similar results for peak-peak amplitude, onset latency and conduction velocity. There was no additional effect of the fibrin glue on the electrophysiological properties of the proximal segment, compared to the standard transection and reconstruction. Fibrin supposedly serves as a temporary supporting framework for growth cones. Furthermore, the fibrin glue is thought to create a regeneration chamber around the repair site, containing all essential neurotrophic factors. This is supposed to establish an optimal environment for axons to survive, resulting in an increased number of axons<sup>13,15</sup>. However, the results of this experiment do not substantiate these ideas.

Not reconstructing the nerve decreased peak-peak amplitude significantly more than repairing it acutely. Delaying the repair for 24 hours (Group b, 24 hour delay group), however, resulted in a significant increase in peak-peak amplitude in the proximal segment, compared to the acute, standard reconstruction (Group a, immediate reconstruction group). The 14 days delayed repair (Group c, 14 day delay group) showed a non-significant increase in peak-peak amplitude, compared to

the standard reconstruction (Group a, immediate reconstruction group). Conduction velocity, however, did not increase for both groups. This is suggestive of an increased number of axons surviving the injury, rather than an increase in larger diameter axons. This result is substantiated by Brown et al, who found an increased muscle mass and muscle force after a 24 hour delayed repair, compared to acutely and 4 weeks delay.

Theoretically, differences in peak-peak amplitude in the proximal segment can occur due to a) an increase in larger diameter axons, or b) an increased number of axons in the proximal segment. An increase in larger diameter axons could be induced by an increased rate of outgrowth of the axons. This is influenced by the decrease of neurofilaments in the proximal segment. If the concentration of neurofilaments decreases more, more tubulin can be transported distally, increasing the rate of outgrowth of the axons. Subsequently, contact with the peripheral target organs is reconstituted earlier. This reinitiates neurofilament synthesis, restoring axonal diameter earlier. Since the amplitude of a single fibre action current varies with the square of the diameter, an increase in diameter would also result in a strong increase in amplitude. However, larger diameter axons would also result in an increased conduction velocity.

Another possibility is that after injury, cell death in the motoneuron pool and the dorsal root ganglion can reach up to 30-40%. Gilmour et al<sup>4</sup> showed that the type of injury as well as the type of repair (transection, muscle graft or nerve graft) influences the amount of cell death in the motoneuron pool. If an increased number of neurons survived the injury, in theory, more axons will be present in the proximal segment. A loss of 5-7% of myelinated axons is described in the proximal segment. If more axons are present in the proximal segment, more axons contribute to the compound action current. Both processes result in a higher peak-peak amplitude, but only larger axons increase conduction velocity.

Based on these results it is only possible to speculate about the underlying mechanisms but that needs further clarification. However, that was not the aim of this study. It was only designed to investigate the influence of the repair method on the proximal segment. Therefore, on the basis of the electrophysiological properties at 12 weeks of regeneration time, it is possible to conclude that the peak-peak amplitude is influenced by means of the repair. In our study timing of nerve repair appears more important than the type of repair used.

#### Acknowledgements

The authors are indebted to Mrs Ineke Hekking for her invaluable assistance, Lourens van Briemen for the measurement sessions, and Enno Collij for anaesthesia. Baxter Healthcare corporation for providing Fibrin Glue (Sealagen).

## References

1. Cragg B, Thomas P. Changes in conduction velocity and fibre size proximal to nerve lesions. *J Physiol* 1961;157:315-327.
2. Davis L, Gordon T, Hoffer J, Jhamandas J, Stein R. Compound action potentials recorded from mammalian peripheral nerves following ligation or resuturing. *J Physiol (Lond)* 1978;285:543-559.
3. Gillespie M, Stein R. The relationship between axon diameter, myelin thickness and conduction velocity during atrophy of mammalian peripheral nerves. *Brain Res* 1983;259:41-56.
4. Gilmour J, Myles L, Glasby M. The fate of motoneurons in the spinal cord after peripheral nerve repair: a quantitative study using the neural tracer horseradish peroxidase. *J Neurosurg* 1995;82:623-629.
5. Gutman E, Sanders F. Recovery of fibre numbers and diameters in the regeneration of peripheral nerves. *J Physiol* 1943;101:489-518.
6. Horch K, Lisney S. On the number and nature of regenerating myelinated axons after lesions of cutaneous nerves in the cat. *J Physiol (Lond)* 1981;313:275-286.
7. Kuypers PD, Gielen FL, Wai RT, Hovius SE, Godschalk M, van Egeraat JM. A comparison of electric and magnetic compound action signals as quantitative assays of peripheral nerve regeneration. *Muscle Nerve* 1993;16:634-641.
8. Kuypers PD, van Egeraat JM, Dudok v Heel M, van Briemen LJ, Godschalk M, Hovius SE. A magnetic evaluation of peripheral nerve regeneration: I. The discrepancy between magnetic and histologic data from the proximal segment. *Muscle Nerve* 1998;21:739-749.
9. Kuypers PD, van Egeraat JM, Godschalk M, Hovius SE. Loss of viable neuronal units in the proximal stump as possible cause for poor function recovery following nerve reconstructions. *Exp Neurol* 1995;132:77-81.
10. Kuypers PD, van Egeraat JM, Godschalk M, Hovius SE. Loss of viable neuronal units in the proximal stump as possible cause for poor function recovery following nerve reconstructions. *Experimental Neurology* 1995;132:77-81.
11. Kuypers PD, van Egeraat JM, van Briemen LJ, Godschalk M, Hovius SE. A magnetic evaluation of peripheral nerve regeneration: II. The signal amplitude in the distal segment in relation to functional recovery. *Muscle Nerve* 1998;21:750-755.
12. Kuypers PD, Walbeehm ET, Heel MD, Godschalk M, Hovius SE. Changes in the compound action current amplitudes in relation to the conduction velocity and functional recovery in the reconstructed peripheral nerve. *Muscle Nerve* 1999;22:1087-1093.
13. Menovsky T, Beek JF. Laser, fibrin glue, or suture repair of peripheral nerves: a comparative functional, histological, and morphometric study in the rat sciatic nerve. *J Neurosurg* 2001;95:694-699.
14. Myles L, Gilmour J, Glasby M. Effects of different methods of peripheral nerve repair on the number and distribution of muscle afferent neurons in rat dorsal root ganglion. *J Neurosurg* 1992;77:457-462.

15. Palazzi S, Vila-Torres J, Lorenzo JC. Fibrin glue is a sealant and not a nerve barrier. *Journal Of Reconstructive Microsurgery* 1995;11:135-139.
16. Peyronnard J, Charron L, Lavoie J, Messier J, Bergouignan F. A comparative study of the effects of chronic axotomy, crush lesion and re-anastomosis of the rat sural nerve on horseradish peroxidase labelling of primary sensory neurons. *Brain Res* 1988;443:295-309.
17. Peyronnard J, Charron L, Messier J, Lavoie J. Differential effects of distal and proximal nerve lesions on carbonic anhydrase activity in rat primary sensory neurons, ventral and dorsal root axons. *Exp Brain Res* 1988;70:550-560.
18. Ramon y Cajal S. *Cajal's Degeneration & Regeneration of the Nervous System*. May R, translator. May R, editor. Oxford: Oxford University Press; 1991.
19. Walbeehm ET, Michiel Dudok Van Heel EB, Kuypers PD, Terenghi G, Hovius SE. Nerve compound action current (NCAC) measurements and morphometric analysis in the proximal segment after nerve transection and repair in a rabbit model. *J Peripher Nerv Syst* 2003;8:108-115.



# Chapter 5

## **The Distal/Proximal Peak-to-peak Amplitude Ratio as a Measure of Regeneration across a Nerve Repair**

*(submitted to Muscle and Nerve)*

Erik T. Walbeehm  
Stefan de Kool  
Joleen H. Blok  
Johan W. van Neck  
Steven E.R. Hovius

A Preliminary form of this work was presented at the IXth IFSSH, Budapest, 13th - 17th June, 2004.

### Abstract

By stimulating the nerve distal and subsequently proximal to a lesion, and recording exclusively from the proximal segment, the distal and proximal peak-to-peak response amplitude can be compared. Theoretically, calculating the ratio of the distal to the proximal peak-to-peak amplitude, only axons that regenerated into the distal segment are assessed. The hypothesis is that this reflects a measure of the quality of the repair. To test this, two well-studied types of injury i.e. crush and transection and reconstruction, were compared by magnetoneurography. This technique measures changes in magnetic field from nerve compound action currents and is less influenced by the tissues surrounding the nerve than conventional electroneurography. This increases reproducibility and allows for more accurate evaluation of nerve regeneration. After 12 weeks of regeneration, the peak-to-peak response amplitude in the proximal segment decreased significantly more for transection and reconstruction compared to crush ( $71.2\% \pm 15.7\%$  vs  $39.5\% \pm 11.6\%$ ). The crush group showed a significantly higher distal/proximal ratio than the reconstruction group ( $82.7\% \pm 10.8$  vs  $65.1\% \pm 6.1\%$ ). Muscle weight returned to normal after crush, but remained at 60% of the contralateral control after reconstruction. These results indicate that the quality of a nerve repair can be measured by the distal/proximal peak-to-peak amplitude ratio.

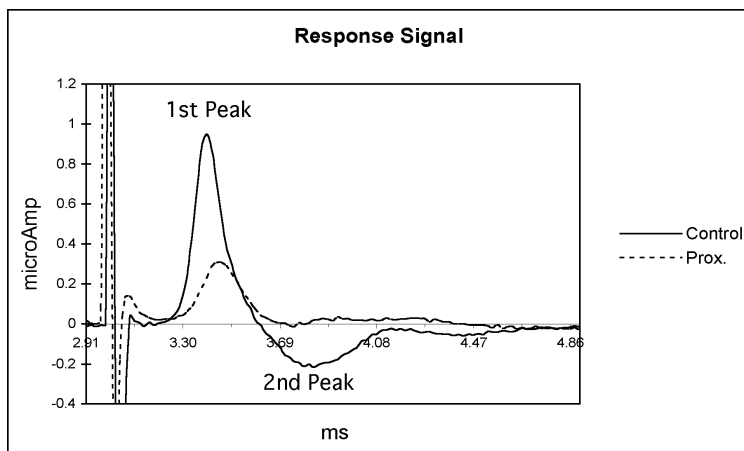


Figure 5.1: This shows an example of a response of the distal toroid (closest to the stimulator) of a control nerve and a proximal segment of a transected and reconstructed nerve. The calibration signal is not shown. Signal evaluation is based on peak-peak amplitude, onset latency and conduction velocity. Peak-peak amplitude is measured as the difference between maximum of the first peak and minimum of the second peak. For explanation of onset latency and conduction velocity see text.

## Introduction

In order to compare different surgical strategies for repairing transected peripheral nerves, regeneration across a site of repair, can be measured by electroneurography (ENG). However, this technique is influenced by the electric impedances of the surrounding tissues, and stimulator and recording-electrode placement vary too much to allow accurate evaluation. Magnetoneurography (MNG) is preferred because magnetic fields, in contrast to electrical potentials, are not significantly influenced by the composition of the biological tissue surrounding the nerve, or by the distance between nerve and sensor. MNG is based on the recording of nerve compound action currents (NCACs) by induction in two magnetic sensor coils (toroids). It has been validated extensively<sup>8,9,14-21</sup> and provides increased reproducibility of the response signal compared to ENG<sup>17-19</sup>. Another advantage of MNG is better separation of stimulus artifact and signal over short conduction distances. This allows for evaluation of electrophysiological parameters proximal and distal to a nerve lesion in a rabbit model.

MNG has been used to study a model of regeneration using the common peroneal nerve in rabbits<sup>8-12</sup>. In those experiments, assessing a standardized transection and reconstruction model, a consistent decrease of 50-60% in peak-to-peak

amplitude (see fig. 5.1) of the NCAC was found, measured 4 cms proximal to the lesion and compared to the normal contralateral control nerve<sup>8-12</sup>. A 75% decrease in peak-to-peak amplitude was shown in the distal segment, compared to the contralateral side. Theoretically, comparing results from distal- to proximal segment provides a measure for the number of axons that have crossed the site of repair from proximal to distal, excluding those present in the proximal stump that have not grown distally. An increased number of fibers distally, will increase the distal to proximal peak-to-peak amplitude ratio.

The aim of this study was to assess whether the peak-to-peak amplitude ratio of the distal-to-proximal segment provides an indication of regeneration across the repair site. To test our hypothesis that a higher distal/proximal peak-to-peak amplitude ratio is indicative of better regeneration across a repair site, the crush lesion model, not before evaluated by MNG, is compared to a transection and reconstruction. Both types of injury also are well studied electrophysiologically, and have a predictable outcome.

#### Materials and Methods

10 New Zealand White rabbits (2.5-3.0 kg) were anaesthetised (Hypnorm, IM induction, Ethrane, 3% maximally, as anaesthetic; Fentanyl IV as pre-medication and analgesic; pre-operation, and before nerve transection, no muscle relaxants). A 3 or 3.5 mm tube was used for ventilation. The left common peroneal nerve was dissected, approximately 1.5 cm proximal to where the nerve passes underneath the tibialis anterior muscle. The ventral surface of the nerve was marked with two, opposing, 11-0 epineurial sutures. The rabbits were divided in two groups. In the first group (reconstruction), the nerve was transected, and the nerve ends were approximated by two 10/0 microsutures. Subsequently, Human Fibrin glue (Sealagen, Baxter HealthCare Corp.) was applied to the repair site in a small rubber sleeve. After 7 minutes, the two 10/0 microsutures and the sleeve were removed. For the second group (crush), the nerves were prepared similarly, but crushed for 30 seconds with micro-forceps at the same level as the transection in the previous group. The operated limbs were not immobilised and no antibiotics were given (same surgeon for all procedures). Nerves were left to regenerate for 12 weeks.

**Toe-Spread Reflex (TSR)** After the regeneration time of 12 weeks the Toe-Spread-Reflex (TSR) test was performed, prior to the anaesthesia for the evaluation. The rabbit (held by the skin of its neck) was dropped for a height of 40 cm. Reflexively, the rabbit spreads its toes and dorsiflexes its foot. The response was graded 0 to ++, with 0 for no response, ++ for a normal TSR response and + for every response in between.

Magnetoneurography (MNG)-measurements (modified from Kuypers et al<sup>8,10</sup>) Subsequently, the animals were re-anaesthetized as above and the nerve was dissected between the biceps femoris- and vastus lateralis muscles. The nerve was mobilised from the knee to the lumbar plexus, and transected proximal to the femoral head. The nerve was guided through two toroidal sensor coils (ferrite core surrounded by an insulated 50  $\mu\text{m}$  copper wire) that were 15 mm apart. A bipolar stimulator was adjusted around the nerve. The distance between the distal toroid and the stimulator was kept at 40 mm. Supramaximal stimulation (i.e. 3 times maximal stimulation, 50  $\mu\text{s}$ , rectangular, monophasic pulse) was used in order to be certain that all fibres were stimulated (see fig 5.2a & b). The moving NCAC passes through the sensors in which it magnetically induces a current, which is then boosted by a magnetic amplifier. During the recording procedure the nerve was kept submerged in heated ( $36\text{ }^{\circ}\text{C} \pm 0.5\text{ }^{\circ}\text{C}$ ), counter-flow normal saline (0.9% NaCl). This entire procedure was repeated on the right side; the unoperated nerve served as control value. All procedures were conducted according to the regulations of the Animal Experimental Committee.

**Signal evaluation** All data were recorded using NDA and averaged with Datacorr 3.0, which are a custom-written data acquisition and correction programme, respectively. Each signal was calibrated by means of an accompanying  $1\mu\text{A}$  calibration signal, which was recorded prior to every stimulus. The final signal is an average of 1024 measurements (consisting of 4 batches of 256 measurements). Further analyses were performed using MatLab<sup>®</sup> (The MathWorks, Inc. Natick, Mass. US

First, the baseline drift in a 1.6 ms window containing the MNG response was estimated using a piecewise cubic Hermite interpolation, based on the signal samples immediately preceding and following this window. After correction for this drift, the NCAC peak-to-peak amplitude could be easily determined as the difference between NCAC maximum and minimum. Onset latency was determined semi-automatically, as the value at 5% increase of the first peak, outside the noise to signal ratio. This was visually checked for each signal.

The NCV was estimated by cross-correlating the signal of the second toroidal sensor coil with that of the first. If the maximum value of the cross-correlation function exceeded 0.75, the signals were assumed to be sufficiently similar to allow reliable NCV calculation. The position of the maximum was used as indication of the time shift  $\Delta t$  between the two signals. The NCV was then calculated as  $\Delta x/\Delta t$ , with  $\Delta x$  the intertoroidal distance of 15 mm. Finally, the area below the signal was determined between the signal onset (determined semi-automatically) and the end of the second phase of the MNG signal (as marked by the first zero-crossing of the signal after its minimum).

The results were stored and statistically analysed in Excel X<sup>®</sup> (Microsoft Corp, Redmond, Wash., USA). Unless otherwise indicated, a two-sample Student t-test was used to test for significance (p values) of intergroup differences.

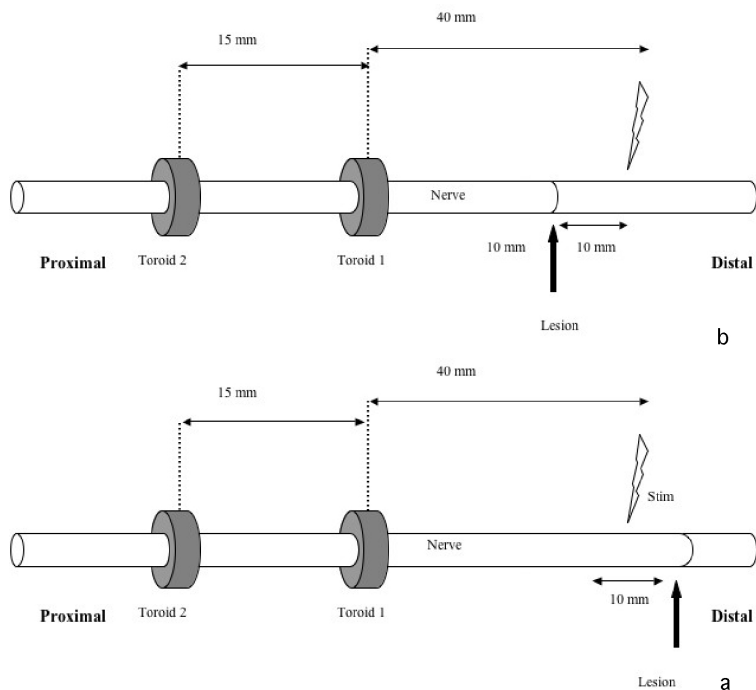


Figure 5.2: The MNG measurement set-up. Figure 5.2a is the first set of measurements with the stimulator stimulating distal to the lesion and recording proximally. Subsequently, both stimulator and toroids are moved to the position as described in figure 5.2b where stimulation and recording are performed proximal to the lesion.

**Muscle Weight** The tibialis anterior muscle was carefully dissected and excised from the tendinous origin to just distal of the distal musculo-tendinous junction on both legs. This muscle is exclusively innervated by the common peroneal nerve. Muscle weight was recorded within minutes after terminating the animal with barbiturates.

## Results

At twelve weeks regeneration, the rabbits showed no signs of infection, autophagy or contractures in the operated limbs. The TSR was performed after 12 weeks as an indication of regeneration, prior to anaesthesia. The crush group all scored ++, with the left leg responding equal to the right. However, the reconstruction group still showed a marked difference (all scoring + in the operated leg).

**Magnetoneurography** Compared to the control signal of the contralateral nerve, the peak-to-peak amplitude of the NCAC in the proximal segment decreased significantly for both groups (table 5.1), but the decrease in the crush group was significantly less than in the reconstructed nerves ( $71.2\% \pm 15.7\%$  of control vs  $39.5\% \pm 11.6\%$ ,  $p < 0.005$ ). Comparing the area under the proximal and control signals, a similar result was found ( $85.8\% \pm 18.9\%$  vs  $58.3\% \pm 10.9\%$ ,  $p < 0.005$ ) (table 5.1).

Table 5.1

Peak-peak Amplitude	Proximal/Control ratio	Distal/Control ratio	Distal/Proximal ratio
Crush	$71.2\% \pm 15.7\%$	$59.7\% \pm 19.0\%$	$82.7\% \pm 10.8\%$
Reconstruction	$39.51\% \pm 11.6\%$	$29.3\% \pm 6.9\%$	$65.1\% \pm 6.1\%$
two sample t-test	$p < 0.005$	$p < 0.005$	$p < 0.01$
Area ( $\mu\text{Amp} \times \text{ms}$ )	Proximal/Control ratio	Distal/Control ratio	Distal/Proximal ratio
Crush	$85.8\% \pm 18.9\%$	$73.9\% \pm 23.0\%$	$86.1\% \pm 20.4\%$
Reconstruction	$58.3\% \pm 12.4\%$	$44.1\% \pm 10.8\%$	$67.6\% \pm 13.5\%$
two sample t-test	$p < 0.005$	$p < 0.05$	no significance

Table 5.1: Table 5.1 shows the average ratios for peak-peak amplitudes and the ratios for Area under the Signal, for both the Crush group and the Transection and Reconstruction group. The calculated ratios are the Proximal Segment versus Control nerve (Ratio Proximal/Control), the Distal Segment versus the Control nerve (Ratio Distal/Control) and the Distal Segment versus Proximal Segment. Two-sample t-test assuming Equal Variances is used (confirmed by f-test).

CV (m/s)	Control	Proximal	Distal
Crush	77.0 m/s $\pm$ 10.8	63.4 m/s $\pm$ 7.6	66.3 m/s $\pm$ 6.2
Reconstruction	85.0 m/s $\pm$ 9.5	68.3 m/s $\pm$ 11.4	74.4 m/s $\pm$ 12.8
two sample t-test	No significance	No significance	No significance
Latencies (ms)	Control	Proximal Segment	Distal Segment
Crush	0.32 $\pm$ 0.03 ms	0.37 $\pm$ 0.09 ms	0.57 $\pm$ 0.16 ms
Reconstruction	0.32 $\pm$ 0,07 ms	0.37 $\pm$ 0.11 ms	0.57 $\pm$ 0.24 ms
two sample t-test	No significance	No significance	No significance

Table 5.2: Conduction velocities (CV) and onset latencies (OL) in the different segments if the nerve. No significant differences could be calculated.

In order to compare the signals in the distal segments, two ratios were calculated: a) the ratio of the peak-to-peak amplitude in the distal segment of the operated nerve to that of the control nerve (distal/control ratio), b) the ratio of the peak-to-peak amplitude of the distal segment to that of the proximal segment, both of the operated nerve (distal/proximal ratio).

The distal/control ratio for the crush group was significantly higher than for the reconstruction group (59.7%  $\pm$  19.0% vs 29.3%  $\pm$  6.9%,  $p < 0.005$ ). The intergroup difference for the distal/proximal ratio was also significant with the crush group showing the highest ratio (82.7%  $\pm$  10.8 vs 65.1%  $\pm$  6.1%,  $p < 0.01$ ). Similar results were found for the area measurements (table 5.1), without reaching statistical significance for the distal/proximal ratio.

Nerve conduction velocity (CV) showed a significant difference between the control and proximal segments, but no significant difference between the crush and reconstruction groups (table 5.2). Latencies showed no intergroup differences for the control nerves or for the proximal and distal segments (table 5.2). In the reconstruction group, one nerve showed no trans-lesional outgrowth of axons, due to dehiscence of the fibrin glue, and a technical failure prohibited measuring the distal segment of another nerve. The data from these nerves were excluded from the analyses.

**Muscle weight** At twelve weeks, the average weight of the tibialis anterior muscle for the reconstructed nerve in the transection and reconstruction group was 63% of the control (5.1 gr  $\pm$  1.3 gr vs 8.1 gr  $\pm$  0.9 gr). The average muscle weight in the crush group was the same as that of the contralateral control muscle, i.e. 100% (7.9 gr  $\pm$  0.7 gr vs 7.9 gr  $\pm$  0,8 gr). This intergroup difference was statistically significant ( $p < 0.001$ ). There was no statistically significant difference between the weights of the right control tibialis anterior muscle of both groups ( $p = 0.7$ ).

## Discussion

To test the hypothesis that the distal/proximal peak-to-peak amplitude ratio is a measure of regeneration across a nerve, repair two types of injury, crush and transection and reconstruction, were compared and evaluated by MNG.

However, in the evaluation of this ratio, changes following injury in the proximal- as well as the distal segment also have to be considered.

**Proximal Segment** The peak-to-peak amplitude in the proximal segment, after 12 weeks of regeneration, was smaller than that in the contralateral control nerve. In the crush lesion group, this decrease was only half of that in the transection and reconstruction group. The area under the signal showed similar results (table 5.1). Previous MNG measurements in a transection and reconstruction model in a rabbit, have demonstrated this decrease in peak-to-peak amplitude of the proximal segment before<sup>9,10,12</sup>. Using more conventional electroneurography (ENG), a 40-50% decrease in compound action potential, as opposed to current, was described for transection and reconstruction<sup>2</sup>. For the crush lesion the decrease in compound action potential was less marked. Changes in conduction velocity (CV) were present during the first 8 weeks post transection and reconstruction, but returned to normal after 12 weeks<sup>9,10,12</sup>.

Previous histological studies have demonstrated a 5-7% loss in axon numbers in the proximal segment, as well as a decrease in axon diameter distribution<sup>1,5</sup>. In a comparison between NCACs and histological axon counts, a correlation was found between the decrease in peak-to-peak amplitude and the decrease in axon diameter. This process has been described, for both crush as well as transection and reconstruction, as somatofugal atrophy<sup>16</sup>. After injury, the neurofilament synthesis is downregulated. Since neurofilaments control axonal diameter, this diameter decreases as neurofilaments synthesis decreases<sup>6</sup>. After distal reconnection neurofilament synthesis is upregulated again, and diameters increase<sup>7,13</sup>. In this experiment, the crush group has a significantly higher peak-to-peak amplitude in the proximal stump compared to the reconstruction group. This is consistent with a minimal loss of axons and, or, a lesser decrease in axon diameter.

**Distal Segment** When the distal peak-to-peak amplitude is compared to the contralateral side, a 40% decrease is found for the crush group, whereas the reconstruction group reveals a 75% decrease. Previous experiments using MNG to evaluate the distal segment after transection and reconstruction demonstrated the same decrease of 75% of the peak-to-peak amplitude of the contralateral control nerve, 8 weeks after reconstruction<sup>11,12</sup>. These experiments also showed a correlation between functional recovery, as evaluated by TSR, and the return of peak-to-peak amplitude in the distal segment. ENG studies showed similar results for transection and reconstruction in cats, with peak-to-peak amplitude decrease of 70% of the control value.

In the same experiment applying a crush lesion of crush, the signals in the distal segment showed a very similar result at twelve weeks, and returned almost to normal after 150 - 200 days<sup>3,4</sup>. The normalization of the muscle weight at 12 weeks as well as the recovery of the TSR in the crush group are a very strong indication that all axons have reached their target organs and that regeneration is (almost) complete. In comparison, the muscle weight of the transected and reconstructed nerve group has only reached 60%, at 12 weeks regeneration time.

**Distal/Proximal Peak-to-peak Amplitude Ratio** In the most optimal form of regeneration, the axon distribution of the distal segment is identical to the proximal segment, and the distal/proximal ratio should be 100%. The value of the distal/proximal peak-to-peak amplitude ratio can then be used as an indicator of regeneration across the repair site. A distal/proximal peak-to-peak amplitude ratio less than 100% represents a loss of signal across the repair. This loss may be explained by a decrease in number of axons in the distal segment compared to proximally. Alternatively, since the amplitude of a single axon varies with the square of the diameter, a decrease in the distal/proximal ratio could also mean a relatively lower overall diameter of axons, regenerating from the proximal part of the nerve. Both imply that a lower distal/proximal peak-to-peak amplitude ratio indicates less favourable regeneration across the repair. The return of muscle weight and the TSR in this experiment, substantiate this idea.

Differences in distal/proximal ratio between two groups could theoretically also be explained by changes in peak-to-peak amplitude in the proximal segment. The higher amplitude ratio in the crush group could then be the result of a lower amplitude on proximal stimulation. This experiment shows that the crush group has a higher average peak-to-peak amplitude in the proximal segment. Nevertheless, the distal/proximal ratio of the crush group has increased in comparison to the distal/proximal ratio of the transection and reconstruction.

The changes in the proximal segment are subject to the type of injury sustained to the nerve. Consequently, a higher proximal/control peak-to-peak amplitude ratio is possibly an indicator of the regenerative potential. Therefore, different types of reconstruction after transection are currently being investigated by the same method.

On conclusion, the hypothesis that a higher distal/proximal ratio is indicative of better regeneration across a repair site is supported by the comparison of the crush lesion and the transection and reconstruction model, used in this experiment. However, in the overall assessment of a repair, the proximal/control peak-to-peak amplitude ratio has an additional role, and should be evaluated separately.

**Acknowledgements** The authors are indebted to Ineke Hekking, for her assistance and her role as a microsurgical mentor and Enno Collij for the anaesthesia and, Rachel Evans for carefully reading the document.

## Acronyms

DRG: Dorsal Root Ganglion

ENG: Electro-Neurography

MNG: Magnetoneurography

NCAC: Nerve Compound Action Currents

NCV: Nerve Conduction Velocity

TSR: Toe-Spread-Reflex

## References

1. Cragg B, Thomas P. Changes in conduction velocity and fibre size proximal to nerve lesions. *J Physiol* 1961;157:315-327.
2. Davis L, Gordon T, Hoffer J, Jhamandas J, Stein R. Compound action potentials recorded from mammalian peripheral nerves following ligation or resuturing. *J Physiol (Lond)* 1978;285:543-559.
3. Fugleholm K, Schmalbruch H, Krarup C. Early peripheral nerve regeneration after crushing, sectioning, and freeze studied by implanted electrodes in the cat. *J Neurosci* 1994;14:2659-2673.
4. Fugleholm K, Schmalbruch H, Krarup C. Post reinnervation maturation of myelinated nerve fibers in the cat tibial nerve: chronic electrophysiological and morphometric studies. *J Peripher Nerv Syst* 2000;5:82-95.
5. Gutman E, Sanders F. Recovery of fibre numbers and diameters in the regeneration of peripheral nerves. *J Physiol* 1943;101:489-518.
6. Hoffman P, Griffin J, Price D. Control of axonal caliber by neurofilament transport. *J Cell Biol* 1984;99:705-714.
7. Hoffman P, Thompson G, Griffin J, Price D. Changes in neurofilament transport coincide temporally with alterations in the caliber of axons in regenerating motor fibers. *J Cell Biol* 1985;101:1332-1340.
8. Kuypers PD, Gielen FL, Wai RT, Hovius SE, Godschalk M, van Egeraat JM. A comparison of electric and magnetic compound action signals as quantitative assays of peripheral nerve regeneration. *Muscle Nerve* 1993;16:634-641.
9. Kuypers PD, van Egeraat JM, Dudok v Heel M, van Briemen LJ, Godschalk M, Hovius SE. A magnetic evaluation of peripheral nerve regeneration: I. The discrepancy between magnetic and histologic data from the proximal segment. *Muscle Nerve* 1998;21:739-749.
10. Kuypers PD, van Egeraat JM, Godschalk M, Hovius SE. Loss of viable neuronal units in the proximal stump as possible cause for poor function recovery following nerve reconstructions. *Exp Neurol* 1995;132:77-81.
11. Kuypers PD, van Egeraat JM, van Briemen LJ, Godschalk M, Hovius SE. A magnetic evaluation of peripheral nerve regeneration: II. The signal amplitude in the distal segment in relation to functional recovery. *Muscle Nerve* 1998;21:750-755.
12. Kuypers PD, Walbeehm ET, Heel MD, Godschalk M, Hovius SE. Changes in the compound action current amplitudes in relation to the conduction velocity and functional recovery in the reconstructed peripheral nerve. *Muscle Nerve* 1999;22:1087-1093.
13. Titmus MJ, Faber DS. Axotomy-induced alterations in the electrophysiological characteristics of neurons. *Prog Neurobiol* 1990;35:1-51.
14. van Egeraat J, Stasaski R, Barach J, Friedman R, Wikswow JP J. The biomagnetic signature of a crushed axon. A comparison of theory and experiment. *Biophys J* 1993;64:1299-1305.
15. van Egeraat J, Wikswow JP J. A model for axonal propagation incorporating both

radial and axial ionic transport. *Biophys J* 1993;64:1287-1298.

16. Walbeehm ET, Michiel Dudok Van Heel EB, Kuypers PD, Terenghi G, Hovius SE. Nerve compound action current (NCAC) measurements and morphometric analysis in the proximal segment after nerve transection and repair in a rabbit model. *J Peripher Nerv Syst* 2003;8:108-115.

17. Wijesinghe R, Gielen F, Wikswo JP J. A model for compound action potentials and currents in a nerve bundle. I: The forward calculation. *Ann Biomed Eng* 1991;19:43-72.

18. Wijesinghe R, Gielen F, Wikswo JP J. A model for compound action potentials and currents in a nerve bundle. III: A comparison of the conduction velocity distributions calculated from compound action currents and potentials. *Ann Biomed Eng* 1991;19:97-121.

19. Wijesinghe R, Wikswo JP J. A model for compound action potentials and currents in a nerve bundle. II: A sensitivity analysis of model parameters for the forward and inverse calculations [published erratum appears in *Ann Biomed Eng* 1991;19(3):339]. *Ann Biomed Eng* 1991;19:73-96.

20. Wikswo J, Barach J, Freeman J. Magnetic field of a nerve impulse: first measurements. *Science* 1980;208:53-55. 21. Wikswo JP Jr., van Egeraat JM. Cellular magnetic fields: fundamental and applied measurements on nerve axons, peripheral nerve bundles, and skeletal muscle. *J Clin Neurophysiol* 1991;8:170-188.

# Chapter 6

## **Primary- versus Delayed-primary Nerve Repair Evaluated by Magnetoneurography**

*(Submitted to PRS)*

Erik T. Walbeehm  
Joleen H. Blok  
Paul D.L. Kuypers  
Johan W. van Neck  
Steven E.R. Hovius

Part of these results have been presented at the IXth IFSSH, Budapest, 13th-17th  
June 2004

## Abstract

The consensus on timing of peripheral nerve repair after transection is that early repair is superior to late. Until recently, there was no indication that there would be a difference in outcome between acute and 24 hour delayed repairs. Nonetheless, it has been postulated in a recent study that, in a rat model, muscle weight and muscle contraction increased significantly following nerve reconstruction after 24 hours when compared to acute repairs in a rat model. This study is investigating the electrophysiological differences between acute repairs, after 24-hours and after 2 weeks delayed repairs by means of Magneto-neurography (MNG). With MNG the electrophysiological properties of the proximal- and distal segment are evaluated separately and a measure of the electrophysiological properties of the anastomosis can be calculated. Results show a significantly higher peak-peak amplitude of the nerve compound action signal in the proximal stump after a 24 hour delay, compared to the acute repair ( $43.01\% \pm 8.8$  vs.  $36.3\% \pm 6.4\%$ ,  $p < 0.05$ ) as well as the 2 weeks delayed repair. Similar results were found for the distal segment, without reaching statistical significance. On conclusion these results demonstrate that delaying a nerve repair for 24 hours in a rodent model gives a significant increase in peak-peak amplitude in the proximal segment compared to an acute- or a 2-week delayed repair, suggesting improved parameters of nerve regeneration.

## Introduction

The consensus on timing of peripheral nerve reconstruction after transection is that early repair will give superior results to a late repair<sup>1, 5, 17, 28, 31</sup>. The definition of “early”, however, is not very concise, although most authors agree that a repair for a clean, sharp injury should be carried out within 24 hrs after the initial trauma. Problems with small patient groups, the diversity of injuries and inaccuracy of clinical evaluation of nerve regeneration make this hypothesis difficult to test.

Nonetheless, clinically this question remains important, because of the implications of performing operations in the middle of the night. Experimentally, early versus delayed repairs have been validated in rabbit- and rat models, using electrophysiological and histological techniques. Most reports compared acute reconstructions with reconstructions after 1 week or more (with or without additional neurotrophic factors), finding that acute repairs provided superior results<sup>11,22,26,29</sup>.

A recent report by Brown et al showed that nerve reconstruction, in a rat model using muscle weight and muscle contraction as parameters, was superior if performed after 24 hrs, compared to acutely or at 4 weeks<sup>4</sup>. These results raised the interest to conduct an investigation into the electrophysiological properties of nerve after acute and delayed repairs, and, more specifically, whether a difference could be elicited after a delay of only 24 hours.

Magneto-neurography (MNG) is a valuable tool in the evaluation of electrophysiological properties. MNG measures the changes in magnetic field around a nerve, induced by a moving nerve compound action current (NCAC). The advantage of this technique, compared to conventional electrophysiological techniques, such as electro-neurography (ENG), is that it is highly reproducible because the magnetic field is less influenced by the impedance of the surrounding perineurial tissues<sup>12,14</sup>. MNG has shown a good correlation with functional recovery when compared to the toe-spread reflex and with the histological parameters of larger axons<sup>13,15,32</sup>. In addition, MNG allows evaluation of the proximal segment and the distal segment separately, from which, specifically, the electrophysiological properties across the anastomosis of the reconstructed nerve can be calculated (Walbeehm et al, Chapter 5).

The aim of this study was to compare the electrophysiological properties of a nerve after an acute repair, a 24 hour- delayed repair and a 2 weeks delayed repair, in a rabbit model.

## Methods and Materials

47 New Zealand White rabbits, weighing between 2500 and 3000 grams received general anaesthesia (Hypnorm, 0.8ml IM for induction, Ethrane, 3% maximally, as anaesthetic). Fentanyl IV was used as analgesic, 0.5 ml before operation, and 0.8 ml before transection of the nerve. A 3 or 3.5 mm tube was used for ventilation. No muscle relaxants were given. A standardised, microsurgical transection of the left

common peroneal nerve was performed, approximately 1,5 cm proximal from where the nerve passes underneath the tibialis anterior muscle. The nerve was partially mobilised but the vascular pedicle arising from the popliteal artery was left intact. The ventral surface of the nerve was marked with two 11-0 epineurial sutures, in order to obtain correct coaptation. Subsequently, the nerve was transected with a pair of straight microscissors and reconstructed in the following ways:

- Group DA: (n= 13 animals) acute reconstruction using 4-6 epineurial 10/0 microsutures,
- Group D1: (n= 12 animals) 24 hour delayed reconstruction using 4-6 epineurial 10/0 microsutures,
- Group D14: (n= 10 animals) 14 days delayed reconstruction using 4-6 epineurial 10/0 microsutures,
- Group DN: (n= 12 animals) no reconstruction.

The operated limbs were not immobilised postoperatively, nor was there need for antibiotics. All surgical procedures were performed by the same surgeon, under sterile conditions and with the aid of an operating microscope. After reconstruction, the nerves were left to regenerate for 12 weeks following which the animals were re-operated and the nerves evaluated by MNG.

**Toe-Spread Reflex (TSR)** After a regeneration time of 12 weeks the Toe-Spread-Reflex (TSR) test was performed, prior to the anaesthesia for the second operative procedure. The rabbit (held by the skin of its neck) was dropped over a distance of 40 cm. Reflexively, the rabbit spreads its toes and dorsiflexes its foot. The response was graded 0 to ++, with 0 for no response, ++ for a normal TSR response and + for every response in between.

**MNG measurements** MNG-measurements were performed as described in earlier reports<sup>12-16,32</sup>. In summary, the rabbits received a general anaesthetic after which the common peroneal nerve was mobilised from the lumbar plexus to where it passes underneath the peroneus longus muscle and then threaded through the two magnetic sensors. The stimulator was first adjusted 8-10 mm distal to the lesion and subsequently 8-10 mm proximal to the lesion. The sensors were placed 4 cm to the stimulator. The nerve was stimulated with a 50  $\mu$ s rectangular pulse and the changes in magnetic field were recorded (see fig. 6.1). During the entire procedure,

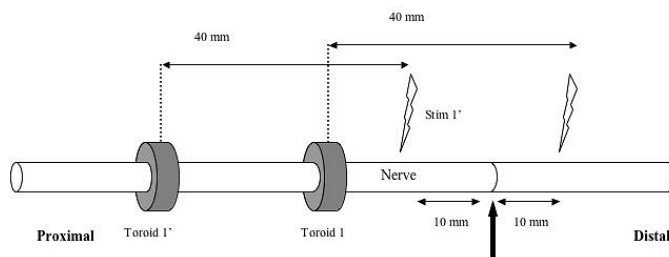


Figure 6.1: This shows the MNG set-up as used to evaluate nerve repairs. Stimulation is done by a stimulator (stim 1 & stim 1'), 4cm distal to the most distal toroid (Tor 1 & Tor 1'). Measuring proximal and distal to the lesion involves re-adjusting the stimulator as well as the toroids. Distances are shown in the figure. The calibration signal is a pulse sent through a wire, which is threaded through the toroids, parallel to the nerve. The signals are then recorded and processed in a custom written data acquisition programme.

the nerve was kept submerged in normal saline at  $36\text{ }^{\circ}\text{C} \pm 0.5^{\circ}$ . The same procedure was performed on the contralateral control nerve. All procedures were conducted according to the rules and regulations of the Animal Experimental Committee of the Erasmus University Rotterdam.

**Signal evaluation** All data were recorded in a custom written data acquisition programme. All signals were then calibrated, by means of the  $1\mu\text{A}$  calibration signal that was recorded prior to every stimulus. The final signal is an average of 1024 measurements (consisting of 4 batches of 256 measurements). Further analyses were performed using MatLab<sup>®</sup> (The MathWorks, Inc. Natick, Mass. USA). First, the baseline drift in a 1.6 ms window containing the MNG response was estimated using a piecewise cubic Hermite interpolation, based on the signal samples immediately preceding and following this window. After correction for this drift, the nerve compound action current (NCAC) peak-peak amplitude could easily be determined

as the difference between NCAC maximum and minimum. The CV was estimated by cross-correlating the signal of the second toroidal sensor coil with that of the first. If the maximum value of the cross-correlation function exceeded 0.75, the signals were assumed to be sufficiently similar to allow reliable CV calculation. The position of the maximum was used as indication of the time shift  $\Delta t$  between the two signals. The CV was then calculated as  $\Delta x/\Delta t$ , with  $\Delta x$  the intertoroidal distance of 15mm. Finally, the area below the signal was determined between the signal onset latency (determined semi-automatically) and the end of the second phase of the MNG signal (as marked by the first zero-crossing of the signal after its minimum). Subsequently, the proximal/control, the distal/control and the distal/proximal ratios for peak-peak amplitude were calculated. The distal/proximal ratio is used as a measure of regeneration across the repair site. This is possible due to the retrograde set-up: i.e. the current is directed from distal to proximal. Because recording is always performed in the proximal segment of the nerve, the ratio of the distal- and proximal signal is a measure of the axons that have crossed the repair.

## Results

At 12 weeks regeneration none of the rabbits had shown signs of infection or contractures in the operated limbs. Two animals in the DN group (not reconstructed) demonstrated autophagy of the operated limbs and were excluded from the study. The TSR showed a ++ for all control limbs, a + for all reconstructed limbs and 0 for all animals in Group DN (not reconstructed).

Peak-peak amplitude of the NCAC MNG evaluation of the proximal segments compared to the reconstructed nerves of the combined groups to their contralateral control nerves, demonstrated a statistically significant decrease in peak-peak amplitude was observed (average proximal/control ratio  $37.58\% \pm 13.8\%$ ,  $n=47$ ), as expected and described in earlier reports<sup>12-16,32</sup>.

When comparing the peak-peak amplitude for the different groups in the proximal segment, the D1 group had a significantly higher amplitude than the DA group ( $43.01\% \pm 8.8$  vs.  $36.33\% \pm 6.4\%$ ,  $p < 0.05$ ). The amplitude in the D14 group increased compared to the DA group, but this did not reach statistical significance. Furthermore, the DN group showed a significantly lower peak-peak amplitude than the DA group ( $24.65\% \pm 7.9\%$  vs.  $36.33\% \pm 6.4\%$ ,  $p < 0.001$ ) and the D1 Group ( $24.65\% \pm 7.9\%$  vs.  $43.01\% \pm 8.8\%$ ,  $p < 0.001$ ). (see fig 6.2).

For the distal segment, the D1 group showed a higher average peak-peak amplitude than the DA group ( $32.62\% \pm 11.5\%$  vs  $26.26\% \pm 6.9\%$ ), for the distal/control ratio, but failed to reach significance. The D1 group showed no difference in peak-peak amplitude with the D14 group ( $32.62\% \pm 11.5\%$  vs  $31.54\% \pm 8.9\%$ ) (see fig 6.3).

Similarly for the distal/proximal ratio, evaluating the anastomosis, the D1 group

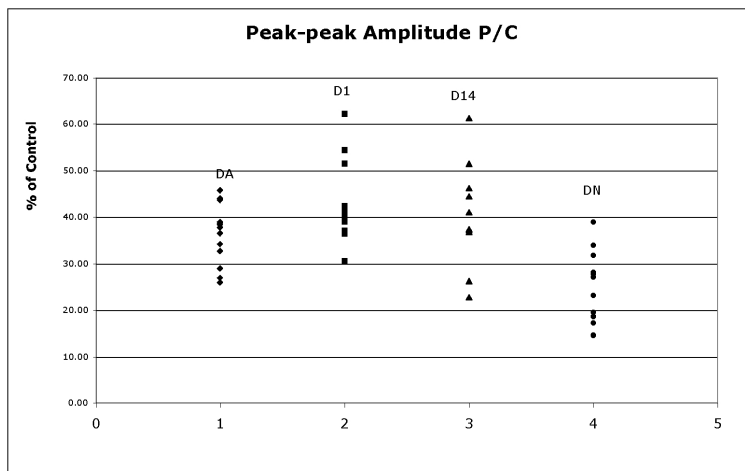


Figure 6.2: is a graphical representation of the results of the proximal/control ratio of the peak-peak amplitude for the different groups.

had a higher average peak-peak amplitude than the DA group, but again failed to reach statistical significance ( $74.74\% \pm 17.1\%$  vs  $68.59\% \pm 20.7\%$ ) (see fig 6.4). For the area below the signal measurements no statistically significant differences could be found in the proximal or distal segment (table 6.1)

Conduction Velocity (CV) and Onset Latency (OL). For the combined groups, there was a significant difference between the control nerves and the reconstructed nerves for CV as well as OL. However, no statistically significant difference between the different groups was found for CV or OL. (table 6.2)

## Discussion

The results show a significant increase in peak-peak amplitude of the proximal segment for a 24 hour delayed repair, compared to the acute repair and the 14-day delay. For the distal segment, a non-significant increase for the distal/control ratio, as well as the distal/proximal ratio is shown for the 24 hr delay, compared to the acute repair. The positive TSR does not show an improved result, but is only a very crude functional indication of regeneration. However, Brown et al<sup>4</sup> found a significant increase in muscle weight and -contraction, demonstrating an improved functional result. The DN group (not reconstructed), showing a decreased peak-peak amplitude in the proximal segment three months after transection, serves as a negative

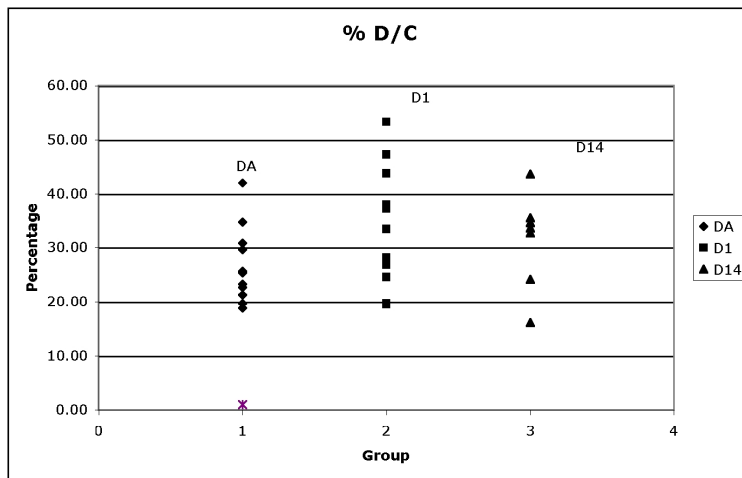


Figure 6.3: demonstrates results of the distal/control ratio of the peak-peak amplitude.

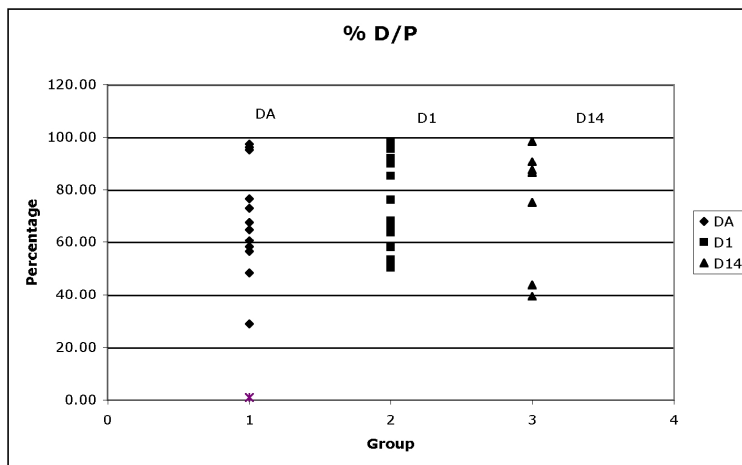


Figure 6.4: shows results of the distal/proximal ratio of the peak-peak amplitude.

Table 6.1 Area below the signal measurements				
Area	DA	D1	D14	DN
% P/C	52.24 ± 12.5	48.94 ± 9.3	52.14 ± 10.3	46.90 ± 23.7
% D/C	36.76 ± 6.9	44.71 ± 13.0	36.79 ± 6.9	n.a.
% D/P	73.77 ± 15.3	78.01 ± 22.9	67.60 ± 11.9	n.a.

Table 6.1: Table 6.1 shows the area below the signal measurements for the proximal/control ratio (%P/C), distal/control ratio (%D/C) and the distal/proximal ratio (%D/P). N.a. is not applicable, because no measurements were performed in the distal segment of the unreconstructed nerve (DN group).

Table 6.2 Conduction Velocity (CV)				
CV	DA	D1	D14	DN
Prox	83.62 ± 8.16	82.64 ± 12.1	85.25 ± 15.6	76.78 ± 10.36
Dist	90.06 ± 12.0	86.15 ± 8.24	84.24 ± 2.8	n.a.

Table 6.2: Table 6.2 shows the conduction velocity in the proximal and distal segments for the different groups.

control group, as the effects of chronic denervation on the proximal segment have been described as decrease in axon numbers and axon diameter<sup>6,7,9,23,24,27,29</sup>.

These results suggest either an earlier increase in axon diameter, or a lesser degree of loss of numbers of axons in the proximal segment after a 24 hour delay in nerve repair, consistent with the results of Brown et al<sup>4</sup>.

An earlier increase in axon diameter results in an increase in amplitude because the amplitude is related to the square of the diameter of the axon. An increase in numbers of axons increases the peak-peak amplitude by superposition of more signals to the compound signal. Because the distal/proximal ratio has not changed, the peak-peak amplitude in the distal segment has changed in proportion to the increase in the proximal segment, suggesting that the changes are mainly in the proximal segment, and not at the level of the nerve repair.

Although the improvement is strongest in the proximal segment, the origin could still lie in the distal segment, the proximal segment or more centrally, the dorsal root ganglion (DRG) or motor neuron pool. Centrally, the influence could be found in inhibition of apoptosis or of cell death in the DRG or motor neuron pool, as suggested by Brown et al<sup>4</sup>. Hart et al<sup>18</sup> showed that primary sensory neuronal cell death commenced 24 hrs after sciatic nerve transection in rats, demonstrated by TUNEL. However, a significant loss of cells was only found almost 6 days later. This

discrepancy occurs because TUNEL is a marker of DNA fragmentation, detecting the onset of cell death, whereas it takes a number of days for the cell to actually break down<sup>18</sup>. There is evidence that cell-death continues for as long as 6 months after axonotmesis. Nerve repair reduced the number of TUNEL-positive neurons as well as the numbers of cells lost, with greater reduction after immediate repair compared to a 1 week delayed repair<sup>8,18</sup>. Brown et al did not find a difference whether or not LIF (leukaemia inhibitory factor) was applied or not, with the 24 hour delayed reconstruction, and proposed that LIF is a central inhibitor of apoptosis, with local concentrations reaching peak values 24 hours after injury<sup>4</sup>. This, however, does not explain why an acutely repaired nerve, which is also in contact with the distal segment at 24 hours, does not achieve the same result. Another possibility is a conditioning lesion effect, considering the initial trauma to be the conditioning lesion. The repair subsequently applies sufficient subsequent trauma to accelerate regeneration and decrease initial delay. However, most studies find that the optimal timing for a conditioning lesion is around 4 to 7 days, prior to the final lesion<sup>2,3,10,19–21,25,30,33</sup>.

It is possible that both mechanisms are co-existing. Nonetheless, the increased peak-peak amplitude in the proximal segment is to be seen as an increase in regenerative potential of axons regenerating into the distal segment. As a final possibility, it is conceivable that the early phase of wallerian degeneration of the distal segment forms noxious substances that are removed in the first 24 hours post injury. But this hypothesis needs further investigation. Most papers investigating results of delayed repairs applied longer delays, starting at a 1-week delay, up to delays of six months<sup>1,5,17,28,31</sup>. This is mostly given by surgical tradition rather than scientific arguments, where the philosophy is either to repair a nerve acutely, or to postpone to a logistically convenient time of operation.

The conclusion, however, that every nerve repair should be delayed for 24 hours, based on Brown et al<sup>4</sup> and the results of this paper is premature, because both papers use a rodent model and directly extrapolating results to a human setting is precarious. Furthermore, long term functional outcome has not been established, since both evaluations have been at 3 months post-repair. However, the practice of not operating during the night, but postponing surgery to the next day, might not only be of benefit to the surgeon, but also to the patient.

#### Acknowledgements

The authors are indebted to Mrs Ineke Hekking for her invaluable assistance, Lourens van Briemen for the measurement sessions, and Enno Collij for anaesthesia.

## References

1. Birch R, Raji A. Repair of median and ulnar nerves. Primary suture is best. *J Bone Joint Surg [Br]* 1991;73:154-157.
2. Bondoux-Jahan M, Sebille A. Electrophysiological study of conditioning lesion effect on rat sciatic nerve regeneration following either prior section or freeze. I. Intensity and time course. *Brain Res* 1986;382:39-45.
3. Bondoux-Jahan M, Sebille A. Electrophysiological study of conditioning lesion effects on rat sciatic nerve regeneration following either prior section or freeze. II. Blocking by prior tenotomy. *Brain Res* 1988;449:150-156.
4. Brown DL, Bennett TM, Dowsing BJ, Hayes A, Abate M, Morrison WA. Immediate and delayed nerve repair: improved muscle mass and function with leukemia inhibitory factor. *J Hand Surg [Am]* 2002;27:1048-1055.
5. Dumont CE, Alnot JY. [Proximal median and ulnar resections. Results of primary and secondary repairs]. *Rev Chir Orthop Reparatrice Appar Mot* 1998;84:590-599.
6. Fu S, Gordon T. Contributing factors to poor functional recovery after delayed nerve repair: prolonged axotomy. *J Neurosci* 1995;15:3876-3885.
7. Fu S, Gordon T. Contributing factors to poor functional recovery after delayed nerve repair: prolonged denervation. *J Neurosci* 1995;15:3886-3895.
8. Groves MJ, Christopherson T, Giometto B, Scaravilli F. Axotomy-induced apoptosis in adult rat primary sensory neurons. *J Neurocytol* 1997;26:615-624.
9. Hoke A, Sun HS, Gordon T, Zochodne DW. Do denervated peripheral nerve trunks become ischemic? The impact of chronic denervation on vasa nervorum. *Exp Neurol* 2001;172:398-406.
10. Jenq CB, Jenq LL, Bear HM, Coggeshall RE. Conditioning lesions of peripheral nerves change regenerated axon numbers. *Brain Res* 1988;457:63-69.
11. Jergovic D, Stal P, Lidman D, Lindvall B, Hildebrand C. Changes in a rat facial muscle after facial nerve injury and repair. *Muscle Nerve* 2001;24:1202-1212.
12. Kuypers PD, Gielen FL, Wai RT, Hovius SE, Godschalk M, van Egeraat JM. A comparison of electric and magnetic compound action signals as quantitative assays of peripheral nerve regeneration. *Muscle Nerve* 1993;16:634-641.
13. Kuypers PD, van Egeraat JM, Dudok v Heel M, van Briemen LJ, Godschalk M, Hovius SE. A magnetic evaluation of peripheral nerve regeneration: I. The discrepancy between magnetic and histologic data from the proximal segment. *Muscle Nerve* 1998;21:739-749.
14. Kuypers PD, van Egeraat JM, Godschalk M, Hovius SE. Loss of viable neuronal units in the proximal stump as possible cause for poor function recovery following nerve reconstructions. *Exp Neurol* 1995;132:77-81.
15. Kuypers PD, van Egeraat JM, van Briemen LJ, Godschalk M, Hovius SE. A magnetic evaluation of peripheral nerve regeneration: II. The signal amplitude in the distal segment in relation to functional recovery. *Muscle Nerve* 1998;21:750-755.
16. Kuypers PD, Walbeehm ET, Heel MD, Godschalk M, Hovius SE. Changes in the compound action current amplitudes in relation to the conduction velocity and func-

- tional recovery in the reconstructed peripheral nerve. *Muscle Nerve* 1999;22:1087-1093.
17. Mackinnon SE, Dellon AL. *Surgery of the Peripheral Nerve*. New York: Thieme; 1988.
  18. McKay Hart A, Brannstrom T, Wiberg M, Terenghi G. Primary sensory neurons and satellite cells after peripheral axotomy in the adult rat: timecourse of cell death and elimination. *Exp Brain Res* 2002;142:308-318.
  19. McQuarrie I, Jacob J. Conditioning nerve crush accelerates cytoskeletal protein transport in sprouts that form after a subsequent crush. *J Comp Neurol* 1991;305:139-147.
  20. McQuarrie IG. The effect of a conditioning lesion on the regeneration of motor axons. *Brain Res* 1978;152:597-602.
  21. McQuarrie IG. Structural protein transport in elongating motor axons after sciatic nerve crush. Effect of a conditioning lesion. *Neurochem Pathol* 1986;5:153-164.
  22. Moir MS, Wang MZ, To M, Lum J, Terris DJ. Delayed repair of transected nerves: effect of brain-derived neurotrophic factor. *Arch Otolaryngol Head Neck Surg* 2000;126:501-505.
  23. Peyronnard J, Charron L. Decreased horseradish peroxidase labeling in deafferented spinal motoneurons of the rat. *Brain Res* 1983;275:203-214.
  24. Peyronnard J, Charron L, Lavoie J, Messier J. Differences in horseradish peroxidase labeling of sensory, motor and sympathetic neurons following chronic axotomy of the rat sural nerve. *Brain Res* 1986;364:137-150.
  25. Sjoberg J, Kanje M. Effects of repetitive conditioning crush lesions on regeneration of the rat sciatic nerve. *Brain Res* 1990;530:167-169.
  26. Sobol JB, Lowe IJ, Yang RK, Sen SK, Hunter DA, Mackinnon SE. Effects of delaying FK506 administration on neuroregeneration in a rodent model. *J Reconstr Microsurg* 2003;19:113-118.
  27. Sulaiman OA, Midha R, Munro CA, Matsuyama T, Al-Majed A, Gordon T. Chronic Schwann cell denervation and the presence of a sensory nerve reduce motor axonal regeneration. *Exp Neurol* 2002;176:342-354.
  28. Sunderland S. *Nerve Injuries and their Repair. A Critical Appraisal*. Melbourne: Churchill Livingstone; 1991. 418-420 p.
  29. Terenghi G, Calder JS, Birch R, Hall SM. A morphological study of Schwann cells and axonal regeneration in chronically transected human peripheral nerves. *Journal Of Hand Surgery British Volume* 1998;23:583-587.
  30. Torigoe K, Hashimoto K, Lundborg G. A role of migratory Schwann cells in a conditioning effect of peripheral nerve regeneration. *Exp Neurol* 1999;160:99-108.
  31. Trumble TE, McCallister WV. Repair of peripheral nerve defects in the upper extremity. *Hand Clin* 2000;16:37-52.
  32. Walbeehm ET, Michiel Dudok Van Heel EB, Kuypers PD, Terenghi G, Hovius SE. Nerve compound action current (NCAC) measurements and morphometric analysis in the proximal segment after nerve transection and repair in a rabbit model. *J Pe-*

ripher Nerv Syst 2003;8:108-115.

33. Widerberg A, Lundborg G, Dahlin LB. Nerve regeneration enhancement by tourniquet. *J Hand Surg [Br]* 2001;26:347-351.



# Chapter 7

## **Mechanical Functioning of Peripheral Nerves: Linkage with the “Mushrooming” Effect**

*(Cell Tissue Research 2004;316(1):115-121)*

Erik T. Walbeehm  
Andrew Afoke  
Thijs de Wit  
Fabian Holman  
Steven E.R. Hovius  
Robert A. Brown

Preliminary forms of this project were presented at the 1st. UK Tissue & Cell Engineering Society meeting, Hammersmith Hospital, RPMS, London, 5th July 1999, and at the 7th FESSH, Barcelona, Spain, 22nd June 2000

**Abstract** Biomechanical properties of nerve have been studied extensively. All neural matrix tissues have been suggested to be the main load-bearing component.

Based on the ultrastructure it has been proposed that the architecture of the epineurium allows some degree of extensibility of the nerve. A role of the perineurium could be to withstand the positive endoneurial pressure.

The hypothesis is that the mechanical behaviour of nerves is dependent on an interaction between the core swelling pressure and restraint by the outer sheath. Loss of this balance will alter that behaviour.

To test this rat sciatic nerves were subjected to mechanical loading at in vivo- and ex vivo tension. Retraction of nerve segments were measured after excision and after incubation at 37°C or freezing. Swelling properties of the nerve were measured by immersion in water or PBS (phosphate buffer solution), with intact or opened epineurium. Results showed a significant decrease in strength and stiffness with an increase in strain of the nerve after excision, compared to in vivo. Retraction was on average 11%. Freezing or incubation at 37°C did not alter retraction. The swelling properties of the nerve demonstrated a significant difference between intact and opened epineurium and similar results for water and PBS indicating that epineurium is a constraint and that the nerves are underhydrated.

The proposed model for the intact nerve is a continuous connective tissue tube surrounding and constraining an inner swelling pressure of the neural core. Loss of integrity of the nerve has detrimental effects on its biomechanical properties.

## Introduction

The mechanical and connective tissue functions (normal or pathological) of peripheral nerves are rarely considered as important areas for research because of the overwhelming specialisation of the neural (conductive) elements. Nonetheless, examination of the mechanical parallels with forearm tendon function indicates that tension- and shear forces will predominate on the peripheral nerve. It is striking to consider, given the delicacy and extreme cytoplasmic elongation of peripheral nerve axons, that innervation of the fingertips can routinely survive during locomotion or extreme exercise.

Biomechanical properties of the whole nerve, like stress, strain and hysteresis phenomena have been described in detailed studies<sup>1,3,8,10,14,15</sup>. In these studies, all the matrix elements of the nerve, epineurium, perineurium, and endoneurium, have in turn been reported to be the main load-bearing component. There is a consensus, however, that the conductive tissues have little capacity to withstand any longitudinal forces.

Ultrastructural studies of the collagen scaffolding of rat sciatic nerve have shown that the epineurium consists of interwoven, thick, flat, tape-like collagen bundles. The perineurium comprises a lacework of smaller collagen fibres orientated longitudinally and obliquely spiralling, also containing the perineurial cell layer and basement membrane<sup>11,13</sup>. Based on this ultrastructure it has been suggested that the architecture of the epineurium might allow some degree of extensibility of the nerve, and that the perineurium is set up to withstand the positive endoneurial pressure<sup>5,7,11,13</sup>. A clinical observation of this endoneurial pressure is a phenomenon called mushrooming. After injury the nerve ends retract, seemingly due to tension, and bulging out of the nerve ends occurs (see fig. 7.1).

Though it is simple to postulate which type of forces are most important and potentially damaging to nerve function, there is in fact too little known of how perineurial connective tissues operate to construct a detailed, well argued hypotheses.

The hypothesis under test in this study is that the mechanical behaviour of nerves is dependent on a fine interaction between the core swelling pressure and restraint by the outer sheath. The loss of this balance will alter that behaviour. This test consisted of 3 experiments: 1. Tensile testing of the entire nerve structure (assessment of the idea that a 'toe' region provides mechanical protection; Kwan et al. 1992<sup>3</sup>). 2. Assessment of mechanisms of retraction (Rydevik et al. 1990<sup>10</sup>). 3. Investigation of the nature of 'mushrooming' and the swelling/water uptake characteristics of the core material.

## Materials and Methods

1) Tensile Experiments Sprague Dawley rats (300 - 350 grams, male and female) were killed and placed in a standard position, on a side, limbs free to assume a neutral position of tension in hip and knee joint. The sciatic nerve was exposed from

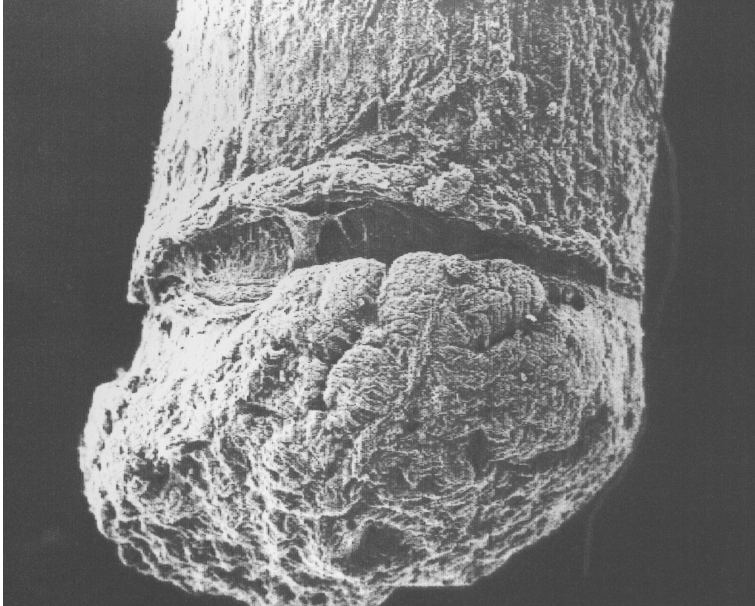


Figure 7.1: A SEM picture of a proximal end of a rat sciatic nerve, approximately one hour after transection. The “mushrooming” of the contents extruding further to the cut end of the epineurium is shown.

the lumbar spine to the trifurcation at the knee level. After exposure, 25 mm nerve segments were clamped using a purpose designed clamp to preserve the in-situ internal organisation, tension, length and diameter of the nerve. The clamped nerve was transected outside the clamp and clamp containing nerve was removed from the animal. Immediately after excision, the nerve diameter was measured using a profile projector with x50 magnification (Nikon 6C-2, Nippon Kogaku, Japan).

Two sets of tensile experiments were carried out.

Tensile experiment 1: (n=9, left nerves) the nerve segments were released from the clamp and allowed to retract in normal saline at room temperature for 1 hour before they were tested for tensile properties. Tensile experiment 2: (n=9, right nerves) were transferred to the test rig, without removal from the clamp, preserving the in-situ properties. The tensile tests were performed using a tensile testing machine (Testometric 220M, Testometric Co. Ltd. Lancashire, UK). Figure 7.2 shows the experimental set-up for clamping the nerve in the testing machine. Force was measured using a load cell (0 - 10 N) and extension was monitored with a linear voltage differential transformer (LVDT). Using a gauge length of 10 mm, the specimens were loaded at an extension rate of 2 mm/minute and an X-Y plotter recorded

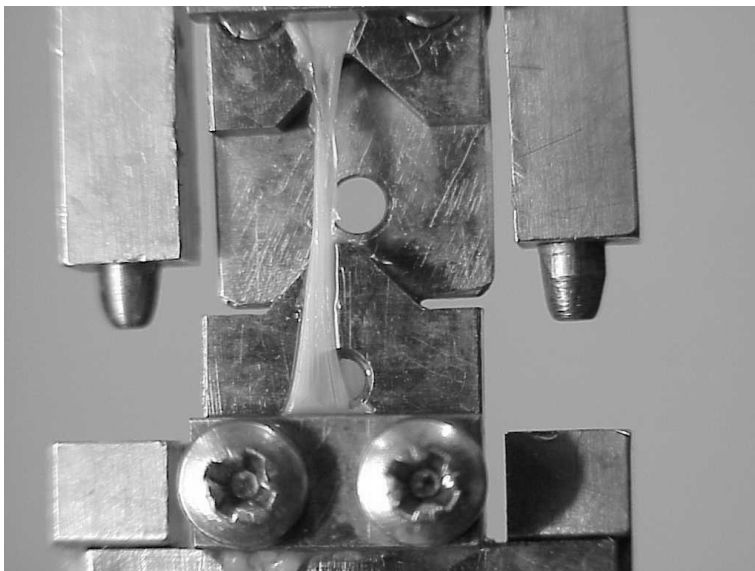


Figure 7.2: *Clamping-Extension device used for the tensile experiments.*

the force-extension curves. The following parameters were calculated:

1. Stiffness modulus =  $(L_0 \times dF / A_0 \times dL)$  in:  $N/mm^2$
2. Maximum Strength =  $F_{max} / A_0$  in:  $N/mm^2$
3. Maximum Strain =  $L_{Fmax} / L_0$  in: %

F is force in Newtons,  $F_{max}$  is maximum force measured, L is length in mm,  $L_0$  is length of the nerve at  $t=0$ ,  $L_{Fmax}$  is the length of the nerve at maximum force,  $A_0$  is cross-sectional area of the nerve at  $t=0$ .

2) Retraction Experiments. Nerve segments ( $n=18$ ), approximately 15mm (bilateral sciatic nerve, 9 Sprague Dawley rats, 300 - 350 grams, male and female), were exposed as described above, and ligated at both ends using 6/0 Nylon. The ligatures served as markers and prevented loss of neural material after excision. The exact distance between the sutures was measured using a digital vernier caliper with a resolution of 0.01 mm. The nerve segments were placed in DMEM culture medium, and allowed for 30 minutes at room temperature. The retracted length and diameters measured using a travelling microscope with a resolution of 2 microns. The nerves were then extended to their original length and kept in that position in specially designed dishes containing DMEM culture medium and their “in-situ”

diameters measured. Eight nerves (four rats) were divided into two groups: Retraction experiment 1, the nerves were incubated for 24 hours at 37°C and 5% CO<sub>2</sub> and Retraction experiment 2, the nerves were frozen in their dishes at -200°C for 24 hours. After 24 hours, the nerves were thawed. Measurements of length and diameters before and after the clamps holding the nerve were released were made on all the nerves in both groups

3) Mushrooming or Swelling experiments Four groups of five rat sciatic nerve segments were used. In two groups, the nerves were left intact while in the other two groups, the nerves were stripped of their outer connective tissue tube. The nerves were weighed and then allowed to swell unrestrained in a) distilled water or b) PBS (phosphate buffer solution). The nerves were removed from the fluid at regular intervals of 15 minutes and any free water was removed with blotting paper before they were weighed again. This procedure was repeated up to 24 hours.

## Results

**Tensile Experiments.** Initial measurements in this study began with the relatively simple assessment of the mechanical properties of the rat sciatic nerve, using two distinct methods. In the first tensile experiment, the nerves were clamped in their retracted state and therefore the extension of the force-extension curve will include the amount of stretch required to bring the specimen to its in-situ length. The stress-strain curve in figure 7.3 show a reproducible toe-region with an average load carriage point at a strain value of 8.3%. The toe-region persisted to an average strain of 27.6%, corresponding to an applied load of 1.5 N. This was followed by a near linear extension until the point of rupture. The average maximum strength was 6.15 N/mm<sup>2</sup> (SEM= 0.6) and the average strain to maximum strength was 41.4% (SEM = 3.0). The stiffness modulus was 24.24 N/mm<sup>2</sup> (SEM = 2.4, n = 9). (Table 7.1)

The second tensile experiment was designed to eliminate any possible effects of loss of structure and tension during excision and surprisingly this produced a different stress-strain pattern. This experimental protocol produced stress-strain curves with no toe region (see fig 7.4). The average maximum strength was 7.2 N/mm<sup>2</sup> (SEM = 0.5) with an average strain to maximum strength of 29.8 % (SEM = 2.0). Thus, the nerve tested in the in-situ condition showed a significant increase of 18% in maximum strength ( $p = 0.001$ ) and a significant decrease of nearly 30% in strain to maximum strength ( $p = 0.001$ ). The stiffness modulus increased significantly by 21% to 29.3 N/mm<sup>2</sup> (SEM = 3.2,  $p < 0.02$ ). (Table 7.1)

The implication that the structural integrity of the nerve governed its mechanical properties, prompted the need to investigate the interaction of the nerve components.

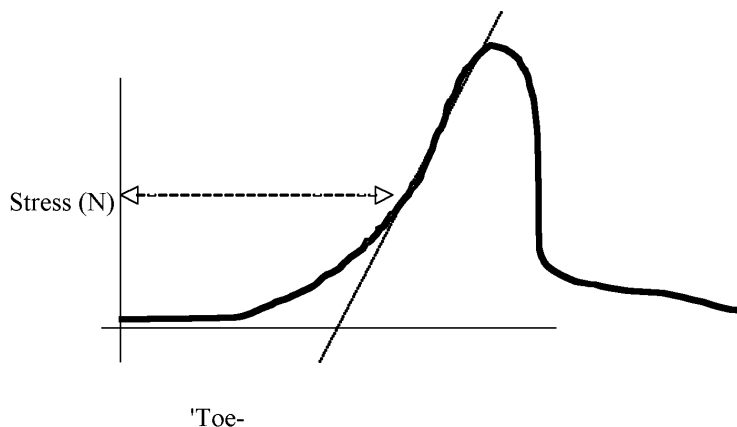


Figure 7.3: *Schematic representation of a typical force-extension curve, indicating the nature of the toe-region and the point of load carriage ( 8.3% strain) for series 1 nerves.*

**Retraction experiments** The question asked is whether retraction was cell mediated or due to material properties. Since the rate of retraction was slow (as is the mushrooming phenomenon itself, which typically continues for a number of hours after cutting) it was considered unlikely that this was an elastic recoil due to inherent material properties of the sheath matrix. Shortening of the outer sheath is shown in table 7.2 at an average of 11.6% (SEM = 1.2%), with an average increase in diameter of 14.9% (SEM = 5.2). After treatment nerves retracted to the same extent, whether pre-incubated for 24 hrs or freeze/thawed for 24 hrs. In neither case was the retraction significantly altered. This effectively eliminated the possibility that the process is driven by cells of the sheath and suggests that swelling (or “mushrooming”) of the core is primarily responsible. (table 7.3)

**Mushrooming or Swelling experiments** To test this hypothesis a series of swelling experiments were carried out to determine the pattern of water uptake, particularly by the inner core, and how this might be affected by mechanical constraint of the outer collagenous lattice sheath. These were designed to distinguish between two plausible mechanisms for the observed expulsion of core material, during mushrooming; i.e. the sheath retracts or the inner core protrudes. Figure 7.5 shows that the core material of the nerve core alone (i.e. unrestrained) demonstrated a 5.7-fold increase in weight compared to 2.3- fold for the intact, sheath & core composite in water. The smooth increase in mass over time, for core only, contrasted with the temporal pattern of swelling, where the sheath is in place, with its repeating cycles of increasing and decreasing rates of swelling (stepwise swelling). Similar results

N=9	Max. Strength (N/mm <sup>2</sup> )	Av. Strain at Max. Strength (%)	Stiffness Modulus (N/mm <sup>2</sup> )
Ex Vivo av.	6.15	41.4	24.4
SEM	0.6	3.0	2.4
In Situ av.	7.2	29.8	29.3
SEM	0.5	2.0	3.2
p-value	p=0.001	p= 0.001	p < 0.02

Table 7.1: Table 7.1 summarises the results from the loading experiment in the ex-vivo set-up where the nerve segment was excised, allowed to retract, restretched to its original length and loaded. It also shows the in situ experiments where the nerve segment was excised at its original tension and loaded from there. Breaking strength (Max. Strength) and elongation at breaking strength (Average Strain at Max. Strength) were recorded. The stiffness modulus was calculated.

	Immediate retraction (n=18)	Diameter increase (n=9)
Average	11.6%	14.9%
SEM	1.2%	5.2%
Range	2.2-22%	0-41.0%

Table 7.2: Table 7.2 shows the immediate retraction, measured in all 18 nerves. Diameter increase was measured in nine.

	Immediate retraction (n=8)	Incubation At 37 ° C (n=4)	Incubation At -20 ° C (n=4)
Average	10.8%	13.4%	10.5%
SEM	1.4%	2.5%	1.9%
Range	4.6-14.5%	8.5-17.7%	8.5-11.2%

Table 7.3: Table 7.3 summarises the immediate retraction in eight nerves. four were frozen and thawed. Four nerves were incubated at 37°C. No significant differences could be elicited.

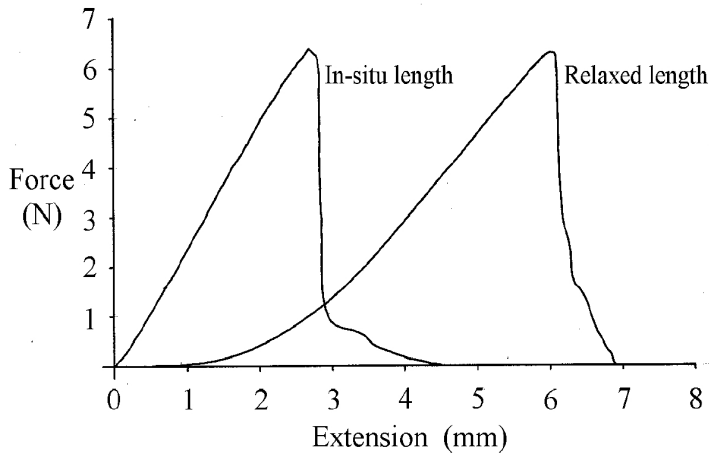


Figure 7.4: This graph shows a typical stress-strain curves for nerves that have been allowed to retract before testing (ie with toe region) and a typical stress-strain curve for nerves tested with their in-situ conditions intact (ie without toe-region).

were obtained in PBS with a 3.5-fold increase in weight without and 2.3-fold with epineurium (sheath).

#### Discussion

The model proposed for connective tissue function during loading of the rat sciatic nerve consists of a neural tissue core and a surrounding “connective tissue” tube. Ushiki and Ide<sup>13</sup> described the tube, the epineurium, as a woven mesh of thick collagen fibres, with a basket-like organisation. The core consists of peri- and endoneurium and the axons. The separation between the layers appears to be at the level of the perineurial cells. (see fig. 7.6)

The hypothesis is that the inner “conductive”, neural elements are mechanically different from the outer connective tissue “sheath”, and that the interface between these two, insulates the neural elements from surrounding tensional loading, converting this into modest compressive loads against the swelling pressure of the core (see fig. 7.7). The mechanical properties of whole nerves have been described previously and the finding of a “toe-region” is consistent with earlier publications<sup>3,10,12</sup>. Rydevik et al<sup>10</sup> reported a similar region up to approximately 15% strain, and linear stiffness was reached around 27%. However, excised nerves were used and based on their histological results they concluded that the perineurium was the main load-bearing compartment.

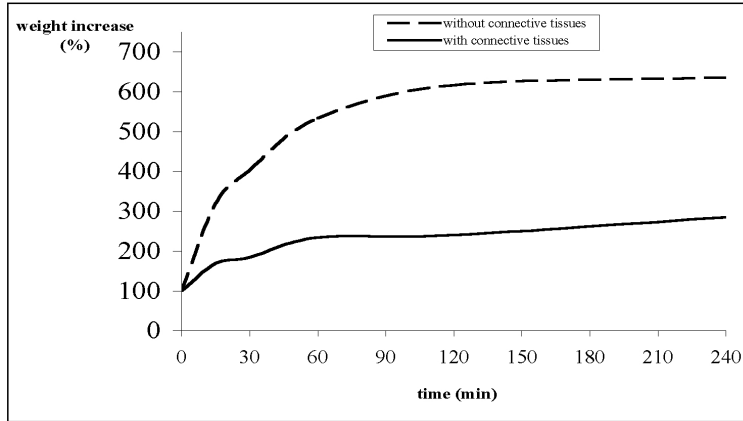


Figure 7.5: : Swelling of whole- and core nerve sections in distilled water as function of increasing mass over time. Swelling in distilled water indicates the gross tendency for fluid uptake and the effects of the restraining outer layer. Swelling in PBS was designed to identify tissues which are underhydrated. The entry of PBS to the nerve core implies that it was unable to become fully hydrated in the intact nerve - when constrained by the nerve sheath. In turn this supports the idea that the core is mechanically constrained (from swelling) by presence of the sheath.

Interestingly, uniaxial stretch of squid giant axon, (a single, unmyelinated fibre, diameter between 400 - 600 nm, little extracellular matrix) has also shown a similar load deflection curve with a turning point at approximately 10% stretch <sup>2</sup>. Functional irreversible impairment started from 19% stretch. This implies that the intact neural tissue is able to cope with elongation. However, the forces necessary to elongate the axon are considerably smaller than those for the connective tissues. This indicates the need for a protective system, but no detailed mechanical model has been proposed until now. Rydevik et al <sup>10</sup> described how the toe-region of slow force might protect the axons. The idea, though, that a system based on minimal initial stiffness and load-bearing capacity (i.e. “slack”) might represent an effective protection against loading damage, is mechanically counter intuitive. In contrast, it is assumed that the mechanical behaviour of nerves clamped in their in situ position is a more realistic reflection of the in vivo response to stretch, and that no “toe-region” is present in vitro.

The conclusion that the ‘toe region’ is an artefact induced by excision, is a key finding. Furthermore, correlation of these post-sectioning changes in mechanical properties with the change in geometry, extrusion and swelling of the core suggests that the mechanical behaviour of nerves is a cooperative mechanism involving the

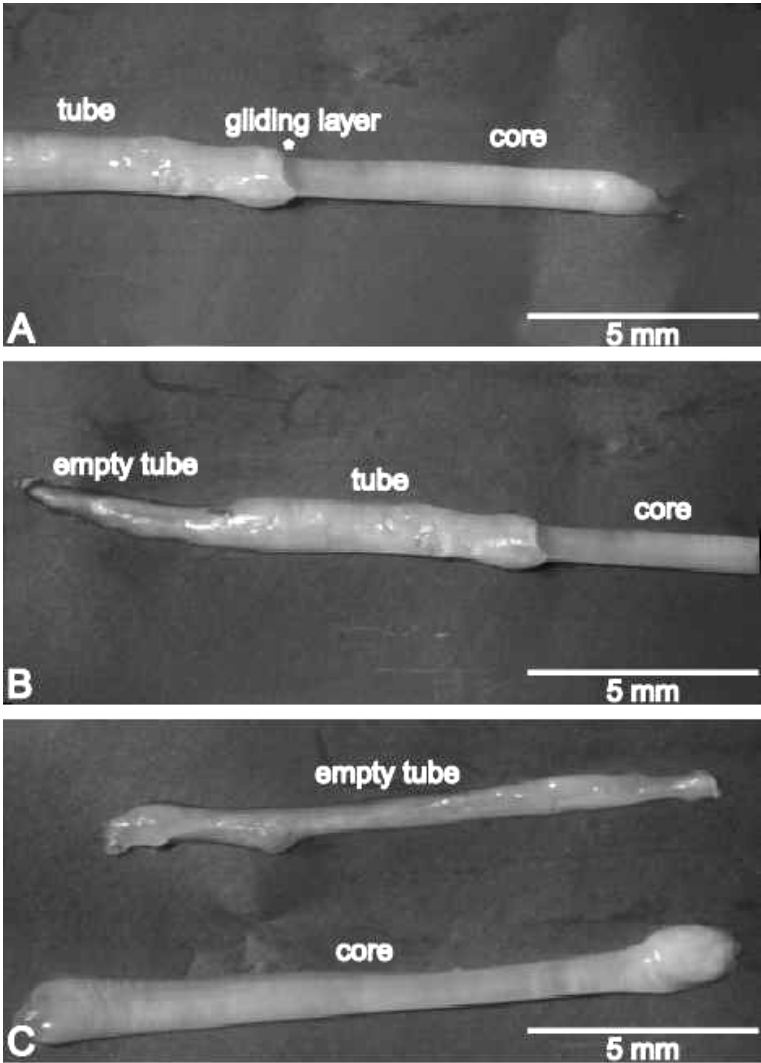


Figure 7.6: The separation between “tube” and “core” shown in detail.

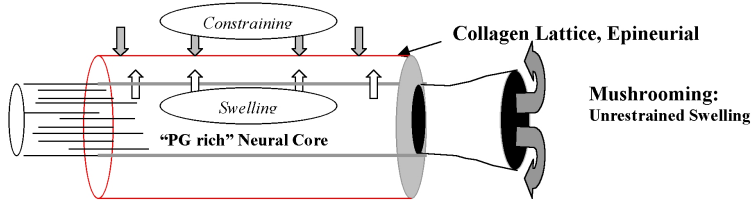


Figure 7.7: Postulated model for the mechanical function of peripheral nerve. In the intact tissue a continuous connective tissue (collagen lattice) tube surrounds and constrains an inner swelling neural core. Between the two is an interface at which core and sheath separate. The two surfaces are kept together in part by the modest swelling and reactive restraint of the core and sheath and in part by weak tensile elements. By analogy with other connective tissues (eg. cartilage) application of tension to the outer sheath will apply a compressive force onto the core but this will be rapidly equalised and negated by expression of water from the inner core: ie the core will shrink. Cutting of the ends of this structure will allow expansion of the core and force the sheath to increase in diameter at its cut margins, leading to shortening and further exposure of the core material -ie mushrooming.

outer sheath and the inner core materials. The phenomenon of 'mushrooming' is consistent with the proposed model. It is observed as exudation of core material following incision of the epineurium or transection of a nerve. It has been causally linked with the endoneurial fluid pressure<sup>5,6</sup>, first measured (at 2.5 cm H<sub>2</sub>O) by implanting a small polyethylene matrix capsule in the nerve<sup>4</sup> and postulated to be the result of a hypertonic fluid composition<sup>9</sup>. However, if direct fluid pressure was responsible, then cutting would be expected to elicit an immediate rather than slow, long term extrusion.

Mushrooming occurs over a period of minutes to hours as seen in figure 4 with the swelling of nerve sections, with the concomitant slow increase of weight. Direct observation of the mushrooming response established that movement of the sheath was involved, though it was unclear whether this was a primary contraction of the sheath (e.g. cell mediated) or expansion of the core pushing back the sheath into a shorter wider tube. The indirect studies of swelling properties of the nerve in distilled water and PBS indicate that some form of proteoglycans are responsible for the positive endoneurial pressure. Such swelling behaviour is common in connective tissues, mediated by localised deposition of proteoglycans in particular layers which are incompletely hydrated, often through mechanical constraints of other layers. For instance, the nucleus pulposus, of the intervertebral disc, is largely composed of proteoglycans representing a stressed, underhydrated gel, constrained by the surrounding annulus. Loss of mechanical integrity of the annulus will inevitably

allow gradual swelling of the stressed gel element. The rate of swelling is related to the relative under-hydration of the stressed gel. Direct analysis of the proteoglycan content in the nerve core is the subject of a separate, current study. Importantly, the epineurium acts as a constraint of this positive pressure, as indicated by the 5.3-fold increase in weight of the nerve segments when the epineurial sheath was removed. This is consistent with a dynamic balance between core expansion and sheath restraint. For core-only swelling, expansion was more or less continuous to a high plateau level after only 1-2 hours. This showed clearly that the core (non-cell mediated) swelling is mechanically limited and restrained by the sheath.

The mushrooming phenomenon can therefore be explained by a combination of extrusion of the contents by swelling and retraction of the sheath, which loses its integrity and continuity when cut. This allows the nerve to retract in length and to expand in diameter under the remaining endoneurial pressure. In order to increase in diameter, the sheath shortens because of the basket-weave architecture of the epineurium<sup>13</sup>.

It is axiomatic, then, that the reverse is true. If the nerve is increased in length by stretching, the epineurial sheath must decrease in diameter. However, any disturbance to the two-component composite system in the nerve will result in drastic changes to its mechanical properties as shown in this study by transecting the nerve. Although the lattice network allows the sheath to stretch or to contract considerably when empty (manuscript in preparation), it is limited in-vivo by the content of the core. The nerve then behaves as a pressurised system during stretching, by virtue of the incompressibility of the core content and the impermeability of the perineurium, analogous to a reinforced water hose. In this way, the weaker core material is protected from stretch injuries. For example a stress of 1.6MPa is required to produce a 6% strain whereas a stress of 3.6MPa is needed to produce a 12% strain. In the rabbit, nerves stretched to 6% strain fully recover to normal level whereas incomplete recovery to only 50% is reached for those stretched to 12% strain<sup>3</sup>. Furthermore, the geometry of this system also protects the nerve around joints, minimising any stress concentrations.

On conclusion peripheral nerves behave mechanically as a two component composite system and disturbing the balancing forces of this system changes mechanical behaviour of the nerve. And, the model explains the common problems of retraction and mushrooming of nerve ends after traumatic transection in peripheral nerve surgery.

#### Acknowledgements

We are grateful to Ms R. Porter, Dr T. Luijsterburg and Mr I. Khan for their 'graphical' help. Support was partly given by EU-grant QLK3-CT-1999-00625: NEURO-TEC

## References

1. Brown R, Pedowitz R, Rydevik B, Woo S, Hargens A, Massie J, Kwan M, Garfin SR. Effects of acute graded strain on efferent conduction properties in the rabbit tibial nerve. *Clin Orthop* 1993;288-294.
2. Galbraith JA, Thibault LE, Matteson DR. Mechanical and electrical responses of the squid giant axon to simple elongation. *J Biomech Eng* 1993;115:13-22.
3. Kwan MK, Wall EJ, Massie J, Garfin SR. Strain, stress and stretch of peripheral nerve. Rabbit experiments in vitro and in vivo. *Acta Orthopaedica Scandinavica* 1992;63:267-272.
4. Low P, Marchand G, Knox F, Dyck PJ. Measurement of endoneurial fluid pressure with polyethylene matrix capsules. *Brain Res* 1977;122:373-377.
5. Lundborg G. Intraneural microcirculation. *Orthop Clin North Am* 1988;19:1-12.
6. Lundborg G. *Nerve Injury and Repair*. Edinburgh London Melbourne and New York: Churchill Livingstone; 1988.
7. Lundborg G, Myers R, Powell H. Nerve compression injury and increased endoneurial fluid pressure: a "miniature compartment syndrome". *J Neurol Neurosurg Psychiatry* 1983;46:1119-1124.
8. Lundborg G, Rydevik B. Effects of stretching the tibial nerve of the rabbit. A preliminary study of the intraneural circulation and the barrier function of the perineurium. *Journal Of Bone And Joint Surgery British Volume* 1973;55:390-401.
9. Myers RR, Powell HC, Costello ML, Lampert PW, Zweifach BW. Endoneurial fluid pressure: direct measurement with micropipettes. *Brain Res* 1978;148:510-515.
10. Rydevik BL, Kwan MK, Myers RR, Brown RA, Triggs KJ, Woo SL, Garfin SR. An in vitro mechanical and histological study of acute stretching on rabbit tibial nerve. *Journal Of Orthopaedic Research* 1990;8:694-701.
11. Stolinski C. Structure and composition of the outer connective tissue sheaths of peripheral nerve. *Journal Of Anatomy* 1995;186 ( Pt 1):123-130.
12. Sunderland S. Stretch-compression neuropathy. *Clin Exp Neurol* 1981;18:1-13.
13. Ushiki T, Ide C. Three-dimensional organization of the collagen fibrils in the rat sciatic nerve as revealed by transmission- and scanning electron microscopy. *Cell And Tissue Research* 1990;260:175-184.
14. Wall EJ, Kwan MK, Rydevik BL, Woo SL, Garfin SR. Stress relaxation of a peripheral nerve. *Journal Of Hand Surgery American Volume* 1991;16:859-863.
15. Wall EJ, Massie JB, Kwan MK, Rydevik BL, Myers RR, Garfin SR. Experimental stretch neuropathy. Changes in nerve conduction under tension. *Journal Of Bone And Joint Surgery British Volume* 1992;74:126-129.

# Chapter 8

## **Investigating the Mechanical Shear-plane between Core and Sheath Elements of Peripheral Nerves**

*(Submitted to Cell and Tissue Research)*

G. A. Georgeu  
E. T. Walbeehm  
R. Tillett  
A. Afoke  
R. A. Brown  
J. B. Phillips

Preliminary forms of this study were presented at the British Matrix Biology Society meeting, Manchester, March 2001, and the Tissue and Cell Engineering Society meeting, Keele, United Kingdom, September 2001

## Abstract

The mechanical architecture of rat sciatic nerve has been described as a central core surrounded by a sheath, though how these contribute to the overall mechanical properties is unknown. Here the retraction responses of core and sheath following transection were studied, along with the tensile properties of each and the interface between them. Nerves were harvested and maintained at their in situ tension, then each was either transected entirely, through the sheath only, or through an exposed section of the core. The retraction distance of each component was measured within 5 min and again after 45 min. Post mortem loss of retraction was tested by measuring 0 or 60 min after excision. For fresh nerves, immediate retraction was 12.68% (whole nerve), 5.35% (sheath) and 4% (core), with a total retraction of 15%, 7.21 and 5.26 respectively. For stored nerves, immediate retraction was 5.33% (whole nerve), 5.87% (sheath) and an extension of 0.78% for core, with a total retraction of 6.71, 7.87 and an extension of 1.74 respectively. Tensile extension and pullout force profiles were obtained for the sheath, the core, and the interface between them. These showed a consistent hierarchy of break strengths which would, under increasing load, result in failure of interface then core then sheath. These data reflect the contributions of material tension from the sheath and fluid swelling pressure from the core to the total retraction, and the involvement of an energy dependent process that runs down rapidly post mortem.

## Introduction

Peripheral nerves exhibit an intriguing structure comprising distinct layers of connective and neural tissue. The cross-sectional morphology has been thoroughly characterised using histological and electron-microscopic techniques. The nerve fibres (myelinated or non-myelinated axons of motor and sensory neurones) are packed into fascicles with Schwann cells and longitudinally aligned collagen to form the endoneurium. This is surrounded by the perineurium, consisting of dense layers of specialised cells that form a diffusion barrier. These are interlaced with bundles of collagen running obliquely to the longitudinal axis. Outside the perineurium is the epineurium, a connective tissue layer containing undulating collagen fibres aligned predominantly axially.<sup>10</sup>

The structure and ultrastructure of the collagen within this layered architecture suggests that these distinct concentric layers within the nerve trunk may have specific mechanical properties. Based on other connective tissues it seems likely that these layers work in concert to provide peripheral nerves with their remarkable mechanical properties. In particular they are able to withstand major changes in tensile load before conductive function is altered.<sup>8,12</sup> The overall tensile properties of nerves have been measured in many animal and human studies, but little is known about the contribution made by each element within the nerve.

The importance of movement between the fascicular elements within a nerve has been suggested, and intraneural fibrosis is known to be a factor that can compromise nerve function after surgical repair.<sup>7</sup> Some groups have shown that perineurium integrity is the critical factor which is compromised when a nerve is stretched to failure<sup>2,9</sup>, although others believe that epineurium is the first tissue to rupture.<sup>1</sup> Recent work has demonstrated that the rat sciatic nerve displays the mechanical features of a two layered composite material comprising a distinct core and sheath.<sup>11</sup> This core and sheath arrangement is commonly described in protocols for preparation of primary cultures of Schwann cells where discarding the sheath reduces fibroblast contamination. It also helps to explain the “mushrooming” effect that occurs when a nerve is severed, resulting in characteristic protrusion of the endoneurial tissue. Fluid pressure within the nerve is thought to be important in maintaining the structural integrity, and has been implicated as contributing to mushrooming.<sup>3</sup> When a nerve is transected, the severed ends both retract to leave a gap, suggesting the presence of some resting tension. The mechanism of this retraction is likely to depend on the mechanical properties of the different layers within the nerve, in conjunction with the fluid pressure. Here we have exploited this retraction feature as a probe to investigate subtle differences in the mechanical behaviour of intraneural layers. The core and sheath showed different retraction responses after transection, indicating the existence of a distinct interface between them. The strength of this interface was measured, along with the tensile strengths of the core and sheath in isolation.



Figure 8.1: *Nerve clamped in situ prior to excision for use in retraction experiment.*

#### Methods and Materials

Harvesting of sciatic nerve Wistar rats (400 - 450 g) were sacrificed by CO<sub>2</sub> asphyxiation followed by dislocation of the cervical spine. Dissection and removal of the sciatic nerve occurred in all rats within 10 min post mortem. Each animal was placed in a lateral position and an initial skin incision made along the line from hip to knee joint. Deep dissection reflected the biceps femoris muscle off the femur and away from the underlying sciatic nerve. Using an operating microscope, the sciatic nerve was mobilised for approximately 15-20 mm, from below the first branch in the upper thigh to just above the division into its terminal branches, usually just above the knee. Care was taken to minimise stretch or trauma to the nerve and continuous topical application of normal saline prevented drying.

#### Mechanical Tests

**Retraction Experiment** A 15mm length of sciatic nerve was clamped at its in situ tension then dissected free (see fig 8.1).

Nerves were divided into three experimental groups where either the retraction of the whole nerve (group 1), the outer sheath (group 2) or the inner core (group 3) was measured. Retraction was measured at two time points; as soon as the respective layers were divided (within 25min), and after 45 min (to allow full retraction). Between these time points nerves were kept in saline at room temperature. All

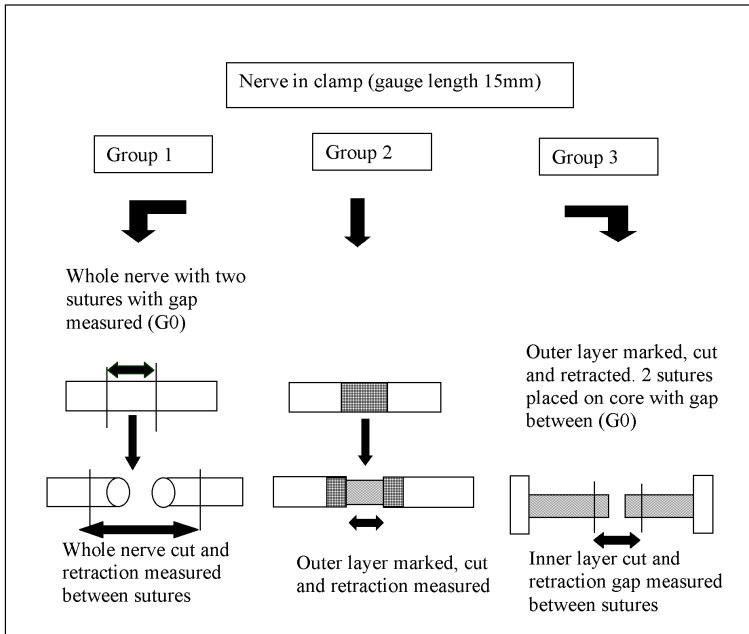


Figure 8.2: Schematic representation of the retraction experiment for the whole nerve (Group 1), outer sheath (Group 2) and inner core (Group 3). Inner core represented by wavy pattern, sutures by single black lines and outer layer marker is shown hatched..

retraction experiments were performed under microscopic control, with measurements obtained using a travelling microscope, resolution of  $2 \mu\text{m}$  (Beck, London, U.K.). Figure 8.2 shows a schematic representation of the retraction experiment for the three groups.

**Group 1 -Whole nerve:** Two epineurial marking sutures (8/0 Prolene) were placed near the middle of the nerve trunk to serve as reference points. The gap between the sutures ( $G_0$ ), which was kept to a minimum (approximately 1 mm), was measured prior to transection of the nerve between the two sutures. The immediate retraction of the two cut ends was measured within 2-5 min and the final retraction was measured after 45 min.

**Group 2 - Outer layer:** The centre of the excised nerve was stained with Bonney's Blue (Eastbourne DGH Pharmaceuticals, UK), then a circumferential incision was made through the sheath only. The blue dye stained only the sheath, the core remaining white, which allowed the depth of the cut to be gauged. The immediate retraction gap ( $G_1$ ) was measured as the sheath retracted back along the core, after which the clamped nerve was placed in saline for 45 min until measurement of final

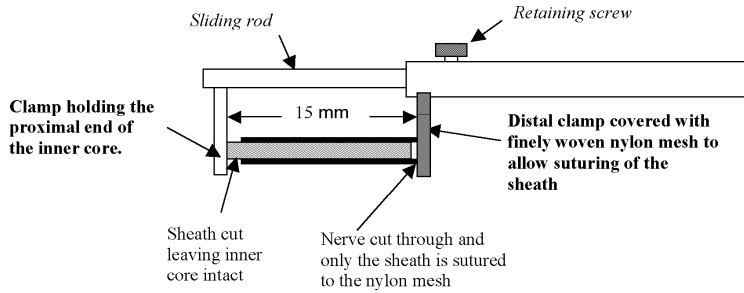


Figure 8.3: Schematic representation of the clamping jig used for the pullout experiment.

retraction (GF).

Group 3 - Inner core: The same initial procedure was carried out on the clamped nerve as for Group 2, and then the centrally divided outer layer was pulled back towards both clamp ends. Care was taken to not stretch the inner core. The exposed core was then sutured and transected as for the nerve trunk in group 1, and the initial and final retraction measured.

**Pullout force.** This experiment was designed to investigate the resistance to movement at the interface between the inner core and the outer layer. A purpose built clamping jig was designed which allowed the outer layer of the nerve to be sutured to the clamp at one end and the inner core clamped at the other. By undoing the retaining screw, the clamped inner core could be pulled away from the outer layer (see fig. 8.3).

The sciatic nerve was exposed and clamped as before with a gauge length of 15 mm, then carefully excised. Under microscopic control, the outer layer was dissected off the inner core at the proximal end of the nerve. At the distal end, the nerve was completely transected and two diametrically opposed sutures were placed through the outer sheath and the distal clamp, which was covered with a fine nylon mesh. The jig was placed in a tensile testing machine (Testometric 220M, Testometric Co Ltd, Rochdale, Lancs, UK), which applied traction to the nerve. Force was measured using a 10N load cell (TEDEA-Huntleigh Ltd, Cardiff, UK) and extension was monitored using a linear voltage differential transformer. Using an extension rate of 10 mm/min, a force/extension curve was obtained for each nerve tested.

**Measurement of inner core and outer sheath strength.** Although the strength of the whole nerve has been investigated, little is known about the strength of the

core and the sheath independently. The procedure used for the pullout experiment was adapted to measure the core strength. With the nerve clamped in the jig, the sheath at both the proximal and distal ends was cut circumferentially, taking care not to damage the core. The clamping jig was placed in the tensile testing machine and the core was extended at the rate of 10 mm/minute until it failed. To obtain the load characteristics of the sheath, the core was pulled out of a length of nerve 20 mm in length. The empty outer sheath was then secured in the clamping jig, which allowed the sheath to be pulled under tension until it failed. The clamping jig provided a gauge length of 10 mm for the sheath and the same extension rate of 10 mm/min was used. Force/extension curves for both the inner core and the empty outer sheath were recorded.

## Results

**Retraction Experiments** Since both the left and the right sciatic nerves were used, there was an inevitable time difference of 30 to 60 min between the dissections of the two nerves from each animal. The results from the “early” dissection (those obtained immediately after the animal was sacrificed) were separated from those obtained during the “late” dissection. Table 8.1 on 124 shows the mean percentage retraction for the early and late dissections for the three groups tested. For groups 1 and 3, the length  $G_0$  between the marking sutures was subtracted from the 15 mm gauge length for the calculation of the percentage retraction.

Table 8.1		Group 1	Group 2	Group 3	Group 3
		Whole nerve, (early dissection)	Sheath (early dissection)	Sheath dissection)	Core (late dissection)
Mean Percentage Immediate Retraction (SEM)		12.78 (0.73) n=10 p=0.0001	5.35 (0.74) n = 11 p = 0.59	5.87 (0.59) n = 9	4.0 (0.44) - n = 13 p = 0.0003
Mean Percentage Total Retraction (SEM)		15.13 (0.60) p = 0.0001	7.21 (0.86) p = 0.55	7.87(0.64)	5.26 (0.73) p = 0.0003
Ratio of immediate over total retraction		0.84	0.74	0.74	0.76
					-0.87 (1.51) n = 5
					-1.74 (1.28)
					0.50

Table 8.1: Table 8.1. The results of immediate and final retraction, for the whole nerve, the sheath and the core respectively. Retraction was measured as a percentage of available nerve retracted. Final retraction was measured after incubation in saline for 45 min. Dissected nerves divided into those operated upon early and late. The statistical significance (using Student t-test) between the 'early' and 'late' results is represented by the 'p' value.

In group 1, the whole nerve in the early dissection showed an immediate retraction of 12.68%, representing 84% of the total retraction of 15.13%. In contrast, the immediate retraction for the whole nerve in the late dissection was only 5.33%, representing 79% of the total retraction of 6.71%. When the early and late dissection results were compared, immediate and total retraction were both significantly lower in the late dissection samples (58% lower for immediate, 56% lower for final,  $p < 0.0001$ ).

In group 2 (sheath only), for both the early and the late dissections, the outer layer showed an immediate retraction of 5.35% and 5.87% representing 74% of the total retraction of 7.21% and 7.87% respectively. This represents less than half of the retraction levels for whole nerve. In contrast to the whole nerve group, the outer layer in the late dissections retracted by only 10% more than that for mean early dissections and this was not statistically significant ( $p > 0.5$ ).

In group 3 (core only), the inner core in the early dissections retracted 4% representing 76% of the total retraction of 5.26%. In the late dissections, instead of retracting, the inner core extended immediately on cutting by 0.87%, representing 50% of the total extension of 1.74%. These differences between early and late dissection were statistically significant ( $p = 0.0003$ ).

It is also interesting to note that in the early dissections, the sum of the retraction for sheath plus core was 26% and 18% less than that of the whole nerve for the immediate and total retraction respectively. By comparison, for the late dissections, the sum of the outer layer and the inner core were within the range of the values obtained for the whole nerve. Comparisons of core and sheath strengths with core-sheath pullout response Fifteen fresh nerves were tested during the pullout experiments. The inner core of all 15 specimens pulled out cleanly from their outer sheath with an average pullout force of 0.41 N (SEM  $\pm$  0.03) over a gauge length of 15 mm. Figure 8.4 shows a typical force/extension curve for the separation of core from sheath along with the force/extension curve for the core in isolation. The pullout curve is characterised by three distinct regions: Initially as traction was applied the core together with its surrounding sheath stretched in an elastic manner up to point A, representing about 6% strain. At point A, the slope of the curve became less steep until a peak force was reached at point B, equivalent to 12% strain. Further traction caused a sharp fall in force until point C was reached, equivalent to 22% strain.

From thereon, the core slid away from the sheath with minimal force. In contrast the force-extension curve for the core strength shows that after the toe region (representing 5% strain) was taken up, the force increased rapidly until a peak was reached at around 27% strain. Ten inner cores were tested giving an average breaking force of 0.65 N (SEM  $\pm$  0.03), more than 5% greater than the force required for core/sheath separation. Figure 8.5 shows a typical force/strain profile for the

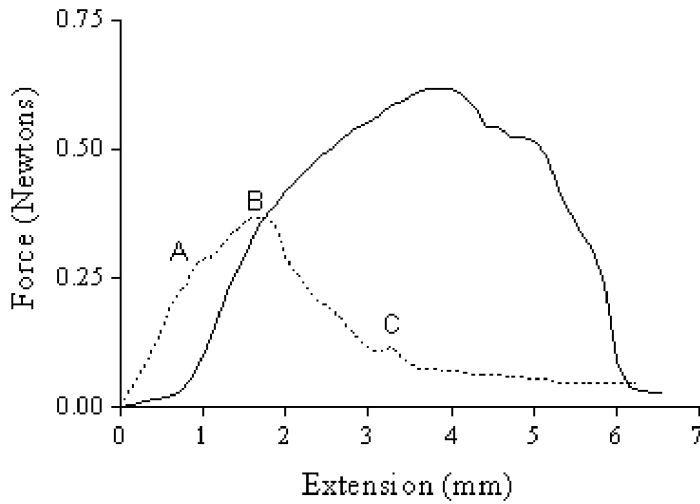


Figure 8.4: Typical curves showing force against extension of the core being pulled out of its sheath (dotted line) and of the core being pulled to failure (solid line) respectively. The 3 phases of the pullout profile are shown; (A) elastic extension, (B) yield, (C) free gliding.

“empty” sheath, compared with that for the inner core (gauge length 10 mm). The curve for the empty sheath shows that it can extend up to 30% strain before any force transmission can be measured (i.e. it has an extensive elastic toe region). From thereon, the force increased steeply with increasing strain followed by a sudden and complete failure once the maximum force was reached at 60% strain.

#### Discussion

From the results it is clear that the different structural elements within the rat sciatic nerve behave as distinct mechanical entities when separated, but apparently in a cooperative manner when together as an intact nerve. The presence of a core and a sheath defined in mechanical terms rather than by their histological appearance has been described recently by Walbeehm et al.<sup>11</sup> and the presence of intraneural regions which retract to different extents relative to each other has long been of interest to surgeons (reviewed by Millesi<sup>7</sup>). This contributes to the effect whereby core elements of a severed nerve fascicle protrude (known as “mushrooming”).

However for this to occur, different layers of the nerve with distinct material

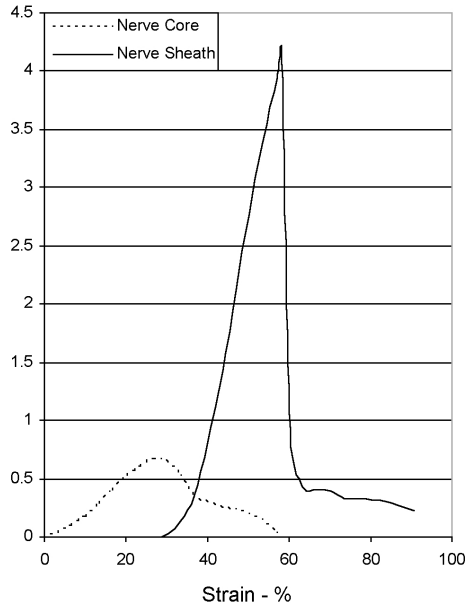


Figure 8.5: Force/strain curves for the nerve core (dashed line) and the outer sheath.

properties appear to respond differently to the changed mechanical environment following cutting. The present study was undertaken to quantify how these differing material features translate into the mechanical properties of the whole rat sciatic nerve. The relatively simple, principally monofascicular structure of this common experimental model is a particular advantage in trying to understand the relationship between tissue architecture and mechanical properties. Clearly similar mechanisms are likely to operate in the multifascicular nerves more common in clinical surgery.

The retraction experiments shown here demonstrated that the basal tension within excised nerves (held at their physiological length) was alone sufficient to produce the immediate retraction seen after transection, consistent with the previous study of Walbeehm et al.<sup>11</sup>. This showed that intraneural (core) elements of the rat sciatic nerve have the capacity to move independently of the outer sheath both after cutting and under pullout mechanical load. The aim of the retraction ex-

periments was to quantify the contribution of each element to this movement using independent transection of each layer.

A key observation here was that nerves used immediately after dissection from the animal (i.e. minimal post mortem changes) retracted twice as much as late dissected nerves from contra-lateral limbs of the same animals. This is consistent with the idea that part of the resident tension is produced by an active energy-dependent process which runs down rapidly post mortem. Previous studies<sup>3,4,11</sup> have identified a modest internal swelling pressure in the core elements that contributes to nerve tension and retraction. Such a swelling pressure, within a restraining connective tissue sheath, is a common material composite in mammalian tissues. Such constrained tissue swelling can be produced through localised water uptake due to accumulation of proteoglycans (an extreme example being inter-vertebral disc) or active ion pumping, leading to osmotic gradients. Rapid disappearance of tension, 60 min post mortem, (together with our inability to identify glycosaminoglycan staining in the core region; data not shown) is consistent with the ion pumping mechanism. The presence of some residual retraction even 60 min post mortem however suggests that at least a proportion of the tension is a result of background, material (elastic) tension probably within the outer sheath (note the elastic properties of isolated sheath between 0 and 30% strain seen in fig 8.5).

Further support for this dual mechanism is seen in the remarkable retraction profile of isolated core, with complete contraction loss by 60 min post mortem. Hence, the putative fluid pressure swelling tension disappeared with great rapidity (expected for an energy-dependent osmotic gradient). At the same time the force/extension profile shows that the core contributes no significant tension by material elasticity.

Interestingly, an estimate of the relative contributions of these two tensile components may be derived from mean retraction levels of the “early” core (5.26%; swelling element) plus the “late” sheath retraction element (7.87%; material tension). The sum of these two isolated elements (i.e. 13.14% retraction) approaches that of native whole nerve retraction of 15.13%, suggesting that the total retraction of the (composite) model nerve can be explained as the sum of the two mechanisms.

The pullout experiment was designed to determine the nature of the core-sheath interface. This interface has been described as a potential gliding layer<sup>11</sup> potentially allowing the independent movement of intraneural elements as discussed for multifascicular nerves.<sup>7</sup> However, it is equally possible that it is a non-physiological shear plane resulting from nerve structure. Interestingly, pullout occurred in a highly consistent manner in all nerves tested. The interface mean break-force in this study of 0.41 N was again a consistent value, though relatively high if it is to act as a physiological functional gliding layer. Interestingly the interface break strength was considerably (50%) less than the break strength of the inner core element, and the core in turn broke at a much lower force than the sheath. This means that a hierarchy of mechanical break strengths exists which would, under increasing ten-

sile loading, produce (1) interface gliding, (2) core rupture, (3) sheath rupture, respectively. This rupture sequence could suggest a potential protective role of the interface on the core elements, allowing dissipation of applied strain by rupture of the shear plane at forces below that where the core ruptures. However, it is now established that the interface comprises a physical material adhesion between core and sheath. Since this will allow transmission of loads from sheath to core its protective role, if any, must be questioned. Studies are currently underway to investigate this.

In summary, this study has shown that the rat sciatic nerve can behave as a composite material in which the layers have distinct mechanical properties. There is a central core that is relatively weak in terms of break-strength compared to the sheath. Retraction of the nerve after cutting can now be explained in terms of this composite structure and the two distinct sources of intrinsic nerve tension present prior to cutting (material elasticity and an opposing swelling pressure, see also Walbeehm et al.<sup>11</sup>). The latter swelling pressure element disappears rapidly post mortem suggesting that it is metabolically maintained. This may have important implications for post injury structural changes if the same holds true for the proximal nerve stump following nerve sectioning. Previous work has identified endoneurial pressure as being an essential factor in maintaining peripheral nerve integrity.<sup>3,4,11</sup> Endoneurial pressure seems likely to be maintained through a combination of perineurium impermeability and energy dependent ion gradients.

The interface between the two opposing layers comprises a physical adhesion material such that its separation needs significant force. This makes the interface a structural shear plane, not a freely gliding layer. It seems more likely to be an incidental consequence of an essential structural feature associated with the various structural layers. This is a key element in understanding how nerves function at a mechanical level and which elements need to be restored during nerve regeneration or tissue engineering. In addition, these mechanical (pullout) characteristics provide novel monitoring points of nerve regeneration, in particular for signs of intraneural fibrosis, often associated with poor functional outcome following surgery.

#### Acknowledgements

Financial support was from the EU framework 5 programme in neural tissue engineering (QLK3-CT-1999-00625).

## References

1. Haftek J (1970) Stretch injury of peripheral nerve. Acute effects of stretching on rabbit nerve. *Bone Joint Surg Br* 52:354-365
2. Kwan MK, Wall EJ, Massie J, Garfin SR (1992) Strain, stress and stretch of peripheral nerve. Rabbit experiments in vitro and in vivo. *Acta Orthop Scand* 63:267-272
3. Low P, Marchand G, Knox F, Dyck PJ (1977) Measurement of endoneurial fluid pressure with polyethylene matrix capsules. *Brain Res* 122:373-377
4. Lundborg G, Myers R, Powell H (1983) Nerve compression injury and increased endoneurial fluid pressure: a "miniature compartment syndrome". *J Neurol Neurosurg Psychiatry* 46:1119-1124
5. Millesi H (1993) Forty-two years of peripheral nerve surgery. *Microsurgery* 14:228-233
6. Millesi H, Zoch G, Reihnsner R (1995) Mechanical properties of peripheral nerves. *Clinical Orthopaedics and Related Research* 314:76-83
7. Millesi H, Zoch G, Rath T (1990) The gliding apparatus of peripheral nerve and its clinical significance. *Ann Hand Surg* 9:87-9
8. Ochs S, Pourmand R, Si K, Friedman RN (2000) Stretch of mammalian nerve in vitro: Effect on compound action potentials. *J Peripher Nerv Syst* 5:227-235.
9. Rydevik BL, Kwan MK, Myers RR, Brown RA, Triggs KJ, Woo SL, Garfin SR (1990) An in vitro mechanical and histological study of acute stretching on rabbit tibial nerve. *J Orthop Res* 8:694-701
10. Ushiki T, Ide C (1990) Three-dimensional organization of the collagen fibrils in the rat sciatic nerve as revealed by transmission- and scanning electron microscopy. *Cell Tissue Res* 260:175-184
11. Walbeehm ET, Afoke A, de Wit T, Holman F, Hovius SER, Brown RA (2004) Mechanical functioning of peripheral nerves: linkage with the "mushrooming" effect. *Cell Tissue Res* 316:115-121
12. Wall EJ, Massie JB, Kwan MK, Rydevik BL, Myers RR, Garfin SR (1992) Experimental stretch neuropathy. Changes in nerve conduction under tension. *J Bone Joint Surg* 74:126-129

# Chapter 9

## General Discussion

The general aim of this thesis was to describe the role of the proximal segment in peripheral nerve regeneration. Early studies have described the morphological changes in the proximal nerve segment that occur after nerve transection and nerve crush, and demonstrated that axonotmesis and neurotmesis had different effects. However, it was unclear what the influence of the proximal segment was on functional recovery of peripheral nerve injury.

Magnetoneurography (MNG) provides a novel method of evaluating the electrophysiological properties of a nerve. It is highly reproducible compared to electroneurography (ENG), and it is less susceptible to the electrical impedances of the surrounding tissues (i.e. differences in dissection of the nerve) than ENG. Using MNG to evaluate the proximal segment after transection and reconstruction of the common peroneal nerve in a rabbit model, we found a very consistent decrease of 55-65% in peak-peak amplitude in the proximal segment, 4 cm proximal to the lesion. A series of experiments was performed in order to further evaluate this decrease in peak-peak amplitude, and to evaluate whether this decrease could be influenced.

Signal Amplitude versus Conduction Velocity in the proximal segment. In chapter 2 the changes in peak-peak amplitude in the proximal segment after nerve transection and reconstruction are related to the changes in conduction velocity that occurred during the first 8 weeks after the surgical reconstruction, and to functional recovery. It is important to realise that the conduction velocity is measured between two toroidal sensors in the proximal segment, 1.5 cm apart, and not across a nerve repair. That is part of the explanation of the differences in conduction velocities in literature. Chapter 2 further describes that after 8 weeks, conduction velocity had returned to normal, whereas the peak-peak amplitude remained at 45% the control nerve, and the toe spread reflex (TSR), a crude test of return of motor function in rabbits, remained only a +.

At twelve weeks conduction velocity returns to normal and, since amplitude and conduction velocity are linearly related, it can only be hypothesised that this is because a small number of axons will have reached their distal target organs and have started to mature. Those axons will then dictate the onset of the NCAC signal and hence conduction velocity returns to normal. Interestingly, when simply comparing the proximal segments and the control nerves of all animals used in chapter 4, not taking into account the experimental group, clear differences were demonstrated between conduction velocities in the proximal segments and the control nerves of all animals at 12 weeks reaching approximately 80% (99.02 m/s to 81.76 m/s), of the control nerves. Literature describes similar differences, with conduction velocities reaching 80% at 80-150 days and reaching normal values at 200-250 days. It is unclear why there is a difference between both experiments, but it could be biological variance, since Cragg et al also showed increases of conduction velocity in their groups at 80 days.

**Peak-peak Amplitude versus Myelinated Axon Counts.** The relationship between axon diameter and single fibre action currents (SFAC) has been studied extensively, and has been described as a square relationship. In order to explain the decrease in peak-peak amplitude in the proximal segment after transection and reconstruction, myelinated axon counts were correlated to peak-peak amplitude (chapter 3).

A decrease in number of fibres as well as a shift to smaller fibres in the proximal segment have been described in literature. After nerve transection and repair, the number of myelinated axons did not change (axons larger than 1  $\mu\text{m}$ ). However, axons larger than 10  $\mu\text{m}$  decreased significantly in numbers. Secondly, the largest axons found in the samples of the transected and repaired nerves, is considerably smaller than in the control nerves, although this could be chance, since only 5 areas (out of approximately 20) were counted.

An explanation was found in the control of axonal diameter by neurofilament synthesis. Neurofilament synthesis and gene expression are downregulated after nerve trauma. This results in a reduction of axonal diameter. This process has been described as somatofugal atrophy. As described in chapters 1.3.1 and 3, it was hypothesized in earlier publications that the 50% decrease in peak-peak amplitude was due to a 50% decrease in functional fibres. This hypothesis cannot be disproved, since it is impossible to test for non-functional fibres. However, it is very likely that, based on the observations by Dudok van Heel et al (unpublished results) and the results presented in chapter 3, that the decrease in larger fibers is mainly responsible for the decrease in peak-peak amplitude.

**Evaluation of the Proximal Nerve Segment as a Modulator of Regeneration.** To investigate whether different surgical reconstructions affected the changes in the proximal segment differently, a number of experiments were compared (chapter 4). This comparison was possible, since the experiment was carried out using the same experimental set-up, under the same circumstances and by the same surgeon.

Delaying a nerve repair for 24 hours demonstrated a significantly higher peak-peak amplitude in the proximal segment. This observation raises the question whether an increased peak-peak amplitude in the proximal segment is a sign of better regeneration. Without taking into consideration the results of the distal segment, it is better to refer to a better regenerative potential.

Chapter 5 adds argument to that discussion, since the comparison between transection and reconstruction and crush experiments (chapter 5) demonstrated an almost two-fold difference in peak-peak amplitude in the proximal segment after crush compared to transection and reconstruction, where crush did significantly better. These modes of injury were compared because earlier studies using ENG demonstrated similar results and the end result of crush is almost nearing a 100% return of function. Subsequently, the higher peak-peak amplitude in the proximal segment after crush underscores the hypothesis for increased regenerative potential. The results for the distal segment and muscle weight, presented in chapter 5,

acknowledged indirectly, that crush had better return of function.

The first cautious conclusion, based on these results, is that it is possible to influence the proximal segment, and that this improves the regenerative potential in a lesioned peripheral nerve. The second conclusion is that delaying a nerve repair for 24 hrs increases the regenerative potential of the proximal segment. However, the therapeutic consequences of both conclusions need further investigation.

The Distal/proximal ratio as a measure of regeneration across a nerve repair. The Distal/Proximal ratio has been shown to assess the anastomosis on theoretical as well as experimental grounds (chapter 5). However, when evaluating an evaluation method in nerve regeneration, a number of problems become apparent. First of all, there is no correlation between different methods of evaluation, as described by Kanaya et al. Secondly, there is no correlation between tests evaluating the nerve and functional tests in animals. This means that there is nothing to test a hypothesis against. Therefore, in the experiments presented in this thesis, two types of injury were tested with known but different outcome.

It was shown that the crush experiment had a higher D/P ratio than the transection and reconstruction group. An increase of the D/P ratio can be the result of an increase in peak-peak amplitude in the distal segment, or a decrease in the peak-peak amplitude in the proximal segment. If the D/P ratio remains the same with improved peak-peak amplitude in the proximal segment, the repair has influenced the regenerative potential in the proximal segment. This, in turn, has improved the number of fibers crossing the repair or the fraction of fibers in the proximal segment that have crossed the repair has larger diameters or both. All these parameters indicate improved regeneration.

Interestingly, the crush group showed an increased D/P ratio notwithstanding an increased peak-peak amplitude in the proximal segment. This meant not only a higher regenerative potential, but also better regeneration across the repair. Therefore, before concluding whether a nerve repair is performing superiorly, the peak-peak amplitude of the proximal segment needs to be evaluated separately, remaining the same or improving and the D/P ratio needs to improve.

In the evaluation of the delayed nerve repair (chapter 6), it became clear that delaying a nerve repair for 24 hrs showed better results in the proximal segment, and the D/P ratio remained the same. It could not demonstrate changes in the distal segment (see chapter 6 for explanation), Regrettably, no muscle weight was recorded during these experiments. However, the paper by Brown et al did show increased muscle weight and muscle contraction. This could be due to problems in the MNG set-up as will be discussed in the next paragraph.

Nonetheless, this was the first paper that actually demonstrated a difference in peak-peak amplitude after different surgical techniques of peripheral nerve repair. As described above, an unchanged D/P ratio, with an increased peak-peak amplitude in the proximal segment means that the regenerative potential has increased

and that regeneration across the repair has improved. This could tentatively mean that delaying a nerve repair provides better results.

**Problems with the MNG set-up** One of the drawbacks of the MNG set-up as used in these experiments was that the measurements are performed with the nerve in situ (still inside the animal). In the animal it was difficult to keep all circumstances the same. Distances between stimulator and lesion and stimulator and toroidal sensors could be subject to considerable, unmeasurable bias. Temperatures could vary considerably because the flow of the fluid was not equal in all areas due to depth differences of the wound bed. Tension on the nerve was uncontrolled. Especially difficult was control of the distances between stimulator and toroid, and only minor changes could influence the distal peak-peak amplitude and conduction velocity considerably.

Therefore, based on these experiences, an ex-vivo set-up has been created, where distances are fixed, temperatures are controlled and tension could be estimated by changes in stretching the nerve. Hopefully, this will reduce the signal-to-noise ratio, improving accuracy.

**The proximal segment and Stretch.** In order to overcome the problem of suturing a nerve under tension or using a nerve graft, it was necessary to examine the effect of longitudinal tension on peripheral nerves (chapter 7). Furthermore the relation between tension and mushrooming was examined.

Several important points are raised. First, on transection a 10-15% recoil is found in rat sciatic nerves. This was calculated by measuring a part of intact nerve, transecting it and re-measuring its length. Recoil appeared to be not only a material-, but essentially a structural property. Endoneurial fluid pressure pushed the epineurium outward, which then had to be followed by an increase in diameter and subsequent shortening of that epineurium, when the nerve was transected. This is normally constrained by the intact epineurium. The fluid pressure was also released on the sides, making the ends extrude (a clinical phenomenon called “mushrooming”). Furthermore it was found that the toe-region as presented in other papers was an artefact of transection. First it was thought that there was a gliding layer present between the sheath and the core, however, more accurate investigation of that layer (chapter 8) revealed very consistent pull-out strength of the core and cross-linking of collagen between the layers. The interface between the two opposing layers comprises a physical adhesion material such that its separation needs significant force. This makes the interface a structural shear plane, not a freely gliding layer. The central core was relatively weak in terms of break-strength compared to the sheath. The swelling pressure element disappeared rapidly post mortem suggesting that it was metabolically maintained. This may have important implications for post injury structural changes if the same holds true for the proximal nerve stump following nerve sectioning. Endoneurial pressure seems likely to

be maintained through a combination of perineurium impermeability and energy dependent ion gradients.

It seems more likely to be an incidental consequence of an essential structural feature associated with the various structural layers Chapter 7 and 8 also demonstrated that the epineurium is the strongest layer of the nerve and that the whole is stronger than the sum of its parts. Based on these findings a three layer composite model was postulated that demonstrated the effects of transection, but in reverse, also the effects of longitudinal loading on the nerve.

Conclusions. The conclusions of this thesis, derived from peripheral nerve regeneration experiments in rabbits, are:

- Nerve conduction velocity changes in the proximal segment but returns to normal at 8 weeks, whereas the peak-peak amplitude decreases by 60% and remains that way until 36 weeks.
- Peak-peak amplitude decreases in the proximal segment and correlates well with decreases in axon diameter of the larger axons.
- It is possible to modify NCAC peak-peak amplitude in the proximal segment surgically.
- The Distal/Proximal peak-peak amplitude ratio is a measure for regeneration across a repair, provided the Proximal/Control ratio is considered simultaneously.
- Delaying a nerve repair for 24 hours in a rabbit model seems to give better results.
- A nerve behaves as a three layer composite material when stretched.
- No obvious gliding layers are present in a nerve, but a weaker layer is present between epineurium and perineurial cells, behaving as a layer that takes the first damage.
- The intact nerve is stronger than the sum of epineurium, perineurium, endoneurium and axons.

For the future Several directions for future research can be highlighted from this thesis. First of all, described above and already applied, was changing the MNG set-up. The set-up needed to be more standardised and controlled and is shown in figure 9.1. This was possible by changing the toroids, and making a MNG chamber, where fluid flow and temperature are constantly monitored and kept constant more easily. Also, distances are more accurately controlled by applying two clamps and fixing the stimulator and the toroids. The idea was to minimise noise reduction and variability of the set-up, so that MNG became even more accurate. This made it also possible to decrease the distances between stimulator and toroids from 6 to 3.5 cm, with minimally compromising the interference of the stimulation artefact and the signal. The exact onset latency of the signal could not be measured anymore, but first peak latency provided a good alternative. With this improved method it was possible to measure smaller animals, such as rats.<sup>1</sup> The first results of experiments on rat sciatic nerves are being submitted for publication.

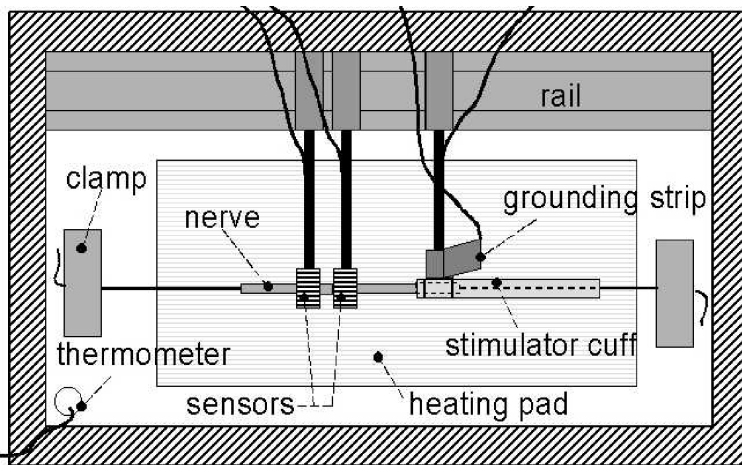


Figure 9.1: Schematics of the recording chamber.

The proximal segment remains elusive. The value of the changes in the proximal segment in relation to nerve repair remains difficult to interpret. So are the differences between cell death and the only minor decline in axon numbers. Timing of peripheral nerve surgery has taken a different impulse by the paper of Brown et al. It has not been conceptualised that there could actually be a difference in result between an acute and a 24 hour delayed repair in nerve surgery. However, the mechanism is still uncertain. Trying to elucidate the processes involved in timing of nerve repair might change the concept of nerve surgery considerably. Stretch of peripheral nerve is again the subject of much current research interest. Clinically ex-

ternal fixators are being applied and used to stretch nerve repairs with reasonable results. However, the mechanism through which the peripheral nerve deals with stretch are just being discovered and it is still unclear what the differences in mechanical behaviour between the rat sciatic and the human median and ulnar nerves are. Histological comparisons between layers, and good cooperation between scientists, surgeons and engineers are essential to solve this problem.

In short, the balance of research is not in providing all answers but in creating more questions.

## References

1. Smit X, Stefan de Kool B, Walbeehm ET, Dudok van Heel EB, van Neck JW, Hovius SE. Magnetoneurography: recording biomagnetic fields for quantitative evaluation of isolated rat sciatic nerves. *J Neurosci Methods* 2003;125:59-63.



# Chapter 10

**Summary, Samenvatting & Dankwoord**

*“Vi resta un ora.”*  
Tosca, Giacomo Puccini

## 10.1 Summary

The role of the proximal segment in peripheral nerve regeneration has been viewed as a membranous pipe, transporting building blocks from the cell body to the growth cone. Previous research demonstrated that there were undeniably changes in the proximal segment following nerve injury. These changes involved a decrease in number of axons from 5-7%, a decrease in axonal diameter, a decrease in peak-peak amplitude of compound action potentials, decreases in conduction velocity. Furthermore, crushing a nerve produced less dramatic changes than transection and subsequent reconstruction. When a transection and reconstruction model, utilising the common peroneal nerve in rabbits, was evaluated using magnetoneurography (MNG) a very consistent 55-65% decrease in peak-peak amplitude was found. This decrease was still measurable up to 36 weeks following the transection and reconstruction. A decrease in conduction velocity was measurable up to eight weeks post-reconstruction but normalised at twelve weeks.

For this thesis, the decrease in peak-peak amplitude was compared to conduction velocity and function recovery, demonstrating a significant decrease in signal amplitude and CV in the first 8 weeks after reconstruction. After 8 weeks of regeneration time, motor function and the CV of the recorded signals start to recover, but the signal amplitudes did not. This remained the same until 36 weeks. It was suggested that a number of the axons, not reaching a proper target organ lost their signal-conducting capability.

When comparing electrophysiological parameters to myelinated axon counts, a correlation was found between the decrease in peak-peak amplitude and the decrease in larger, myelinated axons. The larger the diameter of an axon, the higher its peak-peak amplitude and this implied that the decrease in peak-peak amplitude could be explained by the decrease in larger axons.

Comparing the results of 71 proximal segments in order to clarify whether the changes in the proximal segment could be influenced by the type of repair, demonstrated that delaying a repair for 24 hrs actually resulted in a lesser decrease in peak-peak amplitude. This could not be corroborated for the distal segment in a following chapter.

To determine the quality of a repair the distal/proximal ratio was calculated. This ratio is an indication of the fibres that have actually crossed a repair. This was tested by comparing two types of injury, a crush injury with a transection and reconstruction, with known different outcome. This showed a higher d/p ratio for the crush injury, even though the proximal segment also showed a higher peak-peak amplitude. It was concluded that the d/p ratio is a measure of regeneration across a repair, but to reach a conclusion the peak-peak amplitude of the proximal segment needs to be taken in consideration also.

After injury to a nerve, the nerve ends retract. Sometimes the ends cannot be sutured together without creating tension. Consequently a nerve graft is used, to

reduce that tension. A primary repair, however, produces better results than a nerve graft. To understand the effects of tension on a nerve repair, the mechanism of how a normal peripheral nerve deals with longitudinal tension needed clarification first. On excision, nerve segments shortened by 10-15%. That mechanism was structural-, rather than cell based. Stretching the nerve demonstrated that an intact nerve has different properties than an excised nerve. Furthermore, nerve segments absorbed more water without epineurium, than with intact epineurium. Based on these results a three layer composite model was hypothesised demonstrating how a nerve deals with longitudinal tension.

Following this paper an interest rose in the strength of the separate layers, gliding layers of the nerve and the endoneurial swelling pressure. Stretching the core showed this was the weakest structure of the nerve. It furthermore appeared that the interface between sheath and core was not a free gliding layer but demonstrated an interface break strength at about 50% of the core break strength, suggesting a rupture sequence of interface gliding, core rupture and sheath rupture. The endoneurial fluid pressure disappeared by 60 min post mortem. This contradicted the notion that the pressure was proteoglycan based but rather metabolically maintained, in combination with epineurial impermeability. Furthermore, based on the results of the last two papers, it appears that the whole nerve is stronger than the sum of its parts.

## 10.2 Samenvatting

De rol van het proximale segment in perifere zenuwregeneratie werd gezien als een membraneuze pijp die bouwstenen aanlevert van het cellichaam voor de growth cone. Eerder onderzoek toonde al aan dat er onweerlegbare veranderingen waren in het proximale segment, na zenuwletsel. Deze veranderingen omvatten een 5-7% afname van aantal vezels, een afname in piek-piek amplitude van de samengestelde actiepotentialen en een afname van de geleidingssnelheid van de zenuw. Een crush letsel gaf dezelfde veranderingen alleen in mindere mate. In eerder onderzoek waarin een transsectie en reconstructie model van de nervus peroneus longus bij konijnen werd gebruikt en ge-evalueerd middels magnetische neurografie (MNG), werd een consistente 55-65% afname gezien van piek-piek amplitude.

Voor dit proefschrift werd de afname in piek-piek amplitude vergeleken met geleidingssnelheid en functie herstel. Dit liet een afname van piek-piek amplitude zien en een afname van geleidingssnelheid tot 8 weken. Na 8 weken regeneratie tijd herstelden motor functie en geleidingssnelheid zich, maar piek-piek amplitude bleef verlaagd. Dit bleef hetzelfde tot 36 weken. De hypothese was dat een aantal axonen hun geleidingsvermogen verloren.

Vervolgens werden de elektrofysiologische parameters, in hetzelfde model, vergeleken met histologische tellingen van gemyeliniseerde axonen. Er werd een goede correlatie gevonden tussen de afname van piek-piek amplitude en afname van de grotere axonen (tussen 10 en 15  $\mu\text{m}$ ). Omdat de piek-piek amplitude quadratisch toeneemt met de diameter, werd geconcludeerd dat de afname in piek-piek amplitude met name lag aan de afname in grotere axonen.

In een vergelijking van 71 proximale segmenten na verschillende types herstel kon worden geconcludeerd dat het type herstel geen verschil gaf, maar een 24 uren uitstel gaf een mindere afname in piek-piek amplitude. Dit kon niet worden aangetoond voor het distale segment in een volgende studie.

Om de kwaliteit van een zenuwnaad te bepalen werd de distaal/proximaal ratio bepaald. Deze ratio geeft een indicatie van het aantal vezels dat over een naad heen is gegroeid. Om dit te testen werden twee types zenuwletsel, een crush en een transsectie en reconstructie, met bekende uitkomst met elkaar vergeleken. Het crush letsel toonde een hogere d/p ratio, ondanks dat de piek-piek amplitude in het proximale segment ook verhoogd was. Er werd geconcludeerd dat de d/p ratio een maat geeft voor regeneratie over een zenuwnaad, maar, om conclusies te kunnen trekken, moet de piek-piek amplitude in het proximale segment ook in ogenschouwen genomen worden

Na een doorsnijding van een zenuw trekken de zenuweinden terug. Dit kan spanning geven bij het weer aan elkaar hechten van de uiteinden, met name enkele dagen na het trauma. Als gevolg daarvan moet er een zenuwtransplantaat gebruikt worden om de spanning te neutraliseren. Het herstel van een primaire zenuwnaad is echter beter dan dat van een transplantaat. Om de effecten van spanning

op een zenuwnaad te kunnen doorgronden, moet eerst begrepen worden hoe een zenuw met longitudinale spanning omgaat. Een zenuwsegment verkleinde 10-15% na doorsnijding. Dat mechanisme bleek eerder op structurele eigenschappen te bestaan dan op celcontractie. Tevens werd gevonden dat een intacte zenuw anders met spanning omgaat dan een doorgesneden zenuw. Het epineurium bleek een barriere voor wateropname van de zenuw. Op basis van deze resultaten werd een drie lagig model gepostuleerd.

Hierop volgend werd de sterkte van de verschillende lagen onderzocht, de interfaces tussen de lagen geanalyseerd en gekeken naar het mechanisme van de endoneuriale vloeistof druk. De rekexperimenten toonden aan dat de kern (endoneurium met axonen) de zwakste structuur was. Tevens was er geen echte glijlaag tussen de kern en het epineurium, maar was er ongeveer 50% van de breeksterkte van de kern nodig om de lagen te scheiden. Dit suggereert een breekvolgorder van interface, kern, epineurium. De endoneuriale vloeistof druk verdween na 60 minuten post-mortem. Dit was in contradictie met een op proteoglycanen gebaseerd mechanisme en indiceert meer een metabool ondersteund proces, in combinatie met epineurale impermeabiliteit. Op basis van de trekresultaten van de laatste twee papers is de gehele zenuw sterker dan de som van de delen.

### 10.3 Dankwoord

Dit proefschrift is opgedragen aan allen die geholpen hebben.

Negen jaar is een lange tijd en mensen zijn gekomen en gegaan gedurende dit project. Een poging te doen hun namen op te schrijven leidt onoverkomelijk tot omissies.

Ik ben jullie allen ongelooflijk dankbaar.

*This thesis is dedicated to all those that helped. Nine years is a long time, and people have come and gone during this project. Trying to put their names down in writing will indubitably cause people to be omitted.*

*My gratitude is to you all.*

/ \

## 10.4 Curriculum vitae

The author was born in the Hague, 24 April 1964. Medical school started in Gent, Belgium, due the famous dutch Lottery system.

It was continued at the Erasmus University Rotterdam 2 years later. In 1990 he did his first research project with Dr J.N.A.L Leijnse and Prof S.E.R. Hovius. After medical school he went to Prof. Gus McGrouther and Prof. Robert Brown at University College London for 1 year, in 1993.

An AGNIO year followed at the Sophia's Children's Hospital. In 1995 this PhD-project started. Basic surgical training was done at the Department of General Surgery with Dr. J.A. Roukema at the Elisabeth Hospital Tilburg.

Currently, back in Rotterdam, the author is finishing his training in Plastic Surgery with Prof. S.E.R. Hovius at the Erasmus MC. Research continues.